# REVISTA DE LA REAL ACADEMIA DE CIENCIAS

# REVISTA DE LA REAL ACADEMIA DE CIENCIAS Exactas Físicas Químicas y Naturales DE ZARAGOZA

Serie 2.ª
Volumen 80

2025

REVISTA DE LA REAL ACADEMIA DE CIENCIAS
Exactas, Físicas, Químicas y Naturales
DE ZARAGOZA
Serie 2.ª. Volumen 80
2025

**Revista de la Real Academia de Ciencias Exactas, Físicas, Químicas y Naturales de Zaragoza** es una revista anual, editada por la Real Academia de Ciencias Exactas, Físicas, Químicas y Naturales de Zaragoza, y editada y distribuida a través de Prensas de la Universidad de Zaragoza. Calle Pedro Cerbuna, 12. 50009 Zaragoza (España). Tel +34 976761330 puz@unizar.es http://puz.unizar.es/

Este número se publica con la financiación del Vicerrectorado de Política Científica de la Universidad de Zaragoza. La Real Academia de Ciencias de Zaragoza agradece el apoyo de la Facultad de Ciencias de la Universidad de Zaragoza.



Depósito legal: Z 218-1960
ISSN: 0370-3207

Edita: Prensas de la Universidad de Zaragoza
Imprime: Servicio de Publicaciones. Universidad de Zaragoza

## ÍNDICE DE MATERIAS

*Rev. Real Academia de Ciencias. Zaragoza.* **80:** 7–46, (2025).
ISSN: 0370-3207

# Efficient numerical solution of a simple discretization of Biot's model

Carmen Rodrigo (carmenr@unizar.es)

Instituto Universitario de Matemáticas y Aplicaciones (IUMA), Departamento de Matemática Aplicada, Universidad de Zaragoza

*Premio a la Investigación de la Academia* 2025. *Sección de Exactas*

**Abstract**

This work presents a simple and efficient approach for the numerical solution of the single-phase flow problem in deformable porous media. To this end, Biot's model is derived from basic principles of fluid and solid mechanics, and the numerical challenges associated with its discretization and the solution of the resulting algebraic systems are discussed. Piecewise linear finite element methods are considered as one of the simplest discretization strategies for this problem, and a suitable stabilization technique is introduced to ensure uniform stability properties and a monotone discrete scheme. To solve the algebraic systems arising from the stabilized discretization, efficient decoupled solvers are reviewed and theoretically analyzed. In particular, we propose an iterative coupling method and a non-iterative sequential method for solving the resulting stabilized scheme. The efficiency and robustness of both the discretization and the solution approaches are demonstrated.

## 1 Introduction

The focus of this work is the efficient numerical simulation of multiphysics problems involving single phase flow in a deformable porous medium within the context of the Biot theory of poroelasticity. This continuum theory studies the behaviour of a porous media consisting of an elastic matrix containing interconnected pores filled by fluids and it is based on the fact that the

presence of a freely moving fluid within the pores modifies the mechanical response of the media. In particular, the theory postulates that when a porous material is subjected to stress, the resulting matrix deformation causes volumetric changes in the pores. Since the pores are filled by fluid, the presence of the fluid not only acts as a stiffener of the material, but also leads to the flow of the pore fluid between regions of higher and lower pore pressure.

The first work accounting for the interrelation of pore fluid and the quasi-static deformation of soils was by Terzaghi [78]. However, his work was based on experimental work and on a one-dimensional consolidation model. Further on, his theory was generalized by Biot, who established the general theory of poroelasticity through several pioneering papers [14, 15]. This theory originally was developed for soil mechanics especially for consolidation problems, since most rocks are porous materials which are generally saturated by different fluid phases. The mechanical behavior of porous rocks is affected by variations of fluid pressures, and, at the same time, the flow kinetics of each fluid phase is influenced by rock deformation. Thus, Biot's theory soon became crucial in geophysical applications related to enhanced oil recovery, injection/pumping operations into geological formations, oil and gas-hydrate exploration or seismic monitoring of CO2 storage, among others. Since then, many researchers have contributed to its further development, and new applications have benefited from the extensive development of the poroelastic theory. In particular, such a theory found its applications in biology, medicine and biomedical engineering for the description of different anatomical structures as vertebrate discs or cornea, biological tissues as cartilage, different organs as the brain or the heart, for example, becoming fundamental in important applications as the study of tumor growth, heart perfusion, brain mechanics, for instance. Nowadays, Biot's model is extensively studied, both theoretically and computationally, since it is essential in the understanding of a wide range of applications in different branches of science and engineering.

The existence, uniqueness, and regularity of the solutions of Biot's equations have been widely studied, see the works by Showalter [72], Zenisek [84] and Phillips and Wheeler [63], and the references therein. The mathematical models for flow in deformable porous media consist of coupled, and possibly nonlinear, partial differential equations, and therefore, analytical solutions of these poroelastic models in closed form are only possible for very particular and restricted cases. For example, some of these benchmark models with analytical solution are Terzaghi [78], Mandel [52, 1] and Barry and Mercer [9] problems. So, the numerical simulation of Biot's models are of great interest to scientists and engineers, since reliable numerical methods for solving poroelastic problems are needed for the accurate solution of multiphysics phenomena appearing in a great variety of fields. It is therefore necessary to develop discrete numerical

models suitable for computer solution. The discrete model arises from the discretization of the continuous model by different techniques, and gives rise to a large set of algebraic equations per time step. The main focus is then twofold: first, to choose appropriate discretization schemes that provide numerical solutions whose behavior resembles that of the real problems and, second, to design suitable large-scale computational algorithms for their efficient solution.

Discretization schemes for Biot's equations have been widely studied. Finite difference methods, which are simple and easy to implement have been analyzed for such a problem [33, 34]. Cell-centered finite volume methods are predominant in the numerical simulation of flow problems [8, 23], as in the industry standard simulation software Eclipse (by Schlumberger and Stars by CMG). These methods have been traditionally combined with finite element methods for dealing with the coupling between flow and mechanics, but recently, a compatible finite volume scheme for coupled hydromechanic flows in porous media was proposed by Jan Martin Nordbotten (MPSA) [58, 59, 60]. This approach is a generalization of the multi-point flux approximation (MPFA) for the scalar conservation equation to mechanical deformation, and has the advantage that the same data structures are used in both the flow problem and the mechanics part. The finite element method, however, provides flexibility to handle complex geometries and has a better developed convergence and stability theory, and thus, has been widely considered to approximate the solution of complex poromechanics problems. See for example the monograph by Lewis and Schrefler [50], where the authors provide an exhaustive compilation of their work on finite element schemes for poroelastic problems, the references therein and some other more recent works such as [46, 49, 70, 82].

One of the main challenges in the numerical simulation of poroelasticity problems is to avoid the appearance of numerical instabilities in the approximation of the pressure variable [5, 26, 28, 37, 66, 83]. Problems where the solution is smooth are satisfactorily solved by standard discretization schemes, but when strong pressure gradients appear, strong nonphysical oscillations can appear in the numerical approximation of the fluid pressure. Such instabilities occur in presence of low-permeability materials and/or when a small time step is used at the beginning of the consolidation process. The oscillations can be removed if considering very fine target grids, or when imposing stability restrictions between the space and time discretization parameters (see [5, 79]). Such techniques, however, can result in prohibitively expensive computational methods and therefore are not practical for real applications. There are different points of view about the nature of these instabilities in the literature. In a finite element framework, they are often attributed to the violation of the inf-sup condition, or the lack of monotonicity of the scheme, in general. These oscillations can be minimized (but not completely alleviated

without reducing the spatial mesh size) if inf-sup stable finite element methods are used. In several papers, Murad and Loula [55, 56, 57] analyzed the behavior of stable discretizations for the classical two-field formulation. The inf-sup condition, however, is not a sufficient requirement to guarantee numerical solutions free of oscillations, as seen in [5] and [69] where Taylor-Hood elements [76] (continuous piecewise quadratic functions for the approximation of the displacement and continuous piecewise linear functions for the pressure), and the so-called MINI element [7] (continuous piecewise linear functions for both variables, enriching the space for displacements with the element bubble functions) are considered, respectively. Other authors have proposed other techniques to avoid the appearance of non-physical oscillations as for example the use of least-squares mixed finite-element methods [45, 77], different combinations of continuous and discontinuous Galerkin methods and mixed finite-element methods [63, 64, 65], nonconforming finite-element methods [41], or a new formulation of the problem including the so-called total pressure variable [61]. These non-physical oscillations can be also eliminated by appropriate stabilization techniques, adding, in particular, certain stabilization terms to the Galerkin formulation of the problem, see for example [13] and [5, 69].

Following the numerical discretization of the problem, the other important aspect of computational schemes is the design of efficient solvers for the solution of the arising large-scale linear system of algebraic equations that has to be solved at each time step. Such linear systems are usually ill-conditioned and difficult to solve in practice. Incorporation of more detailed physics and geometry into the mathematical models requires the use of efficient numerical algorithms, becoming the design of these methods a crucial step to allow the numerical simulation of realistic problems. In particular, the solution of the large linear systems of equations arising from the discretization of Biot's model is the most time-consuming part when real simulations are performed, and often constitute a major bottleneck in coupled flow and geomechanics simulations. For this reason, during the last years, significant effort has been focused on designing efficient iterative solution methods for these problems. Poroelastic models are computationally complex to retain the characteristics of the underlying physical processes, and their numerical simulation becomes expensive, time consuming and difficult. In fact, up to our knowledge, there are no commercial packages readily available to solve these type of coupled problems. The classical approach is to consider separate software modules for mechanics and flow calculations, implemented in both a sequential or iterative setting. In the literature, there are mainly three different approaches for solving the coupling between geomechanics and flow in a porous media: the fully implicit schemes, the iterative coupling methods and the explicit approach.

On the one hand, the so-called monolithic, fully coupled or fully implicit methods solve

the coupled flow and geomechanics system simultaneously in a monolithic manner, that is, simultaneously for all the unknowns on each time level. This strategy allows to take larger time steps and enjoys excellent stability properties. Its main disadvantage, however, lies in their high computational cost due to the need of solving complex ill-conditioned linear systems. Also, it does not allow to use well tested robust versions of individual model components, and looses some flexibility since it does not permit to use larger time steps for the geomechanics than for the flow subproblem. Within this framework, Krylov-type iterative methods and/or multigrid algorithms are frequently used, due to their scalability and good parallel performance. In the case of Krylov iterative methods, an essential ingredient is to design an effective preconditioner which could address both the ill-conditioning and the strong coupling nature of the governing equations, and thus accelerate the convergence of Krylov subspace methods. Some examples can be found in [3, 2, 71, 12, 27, 18, 22, 36, 39, 67]. Multigrid methods are known to have optimal complexity for solving many numerical problems. However, in practice their performance in solving individual problems varies significantly. Multigrid methods for the transport of a fluid in porous media are well understood, but the black-box multigrid treatment of the poroelasticity equations is less common. Within the multigrid framework, the focus is on the design of appropriate smoothers to deal with the saddle point type character of the resulting system. Different smoothers have been proposed in the literature for dealing with Biot's problem within a multigrid framework. Coupled Vanka smoothers, decoupled distributive relaxations, Uzawa type smoothers and other decoupled relaxations based on iterative coupling methods have been successfully applied for such a problem [32, 31, 51, 35, 4].

An alternative to the monolithic methods is a sequential approach in which the fully coupled system is broken into subproblems (flow and mechanics problems) that are solved one after the other. This fully explicit coupling approach is a very simple scheme which allows much flexibility in the implementation and has a low computational cost, however it pays maybe the price of a less accurate numerical solution by using the same discretization parameters and might also only be conditionally stable. This approach has the advantage that established numerical methods and existing software and simulators can be used for each of the subproblems. In this way, it results quite attractive in practice since smaller linear systems need to be solved in order to obtain the solution for the whole coupled poroelastic system. Due to the appealing advantages of these methods, intensive research is currently being carried out in this direction. Some examples can be found in [48, 19, 85, 6, 21, 68].

A sequential approach may be iterated further at each time step until the solution converges within a specified tolerance. This is commonly known as an iteratively coupled approach, and

the solution obtained is, in principle, the same as the that obtained using a monolithic approach. Thus, for solving Biot's model, the iterative coupling schemes solve, on each time step, either the flow or the mechanic part, followed by the solution of the other subproblem, repeating this process until a converged solution within a prescribed tolerance is obtained [44]. This approach has the same advantages of the previous decoupling solution methods regarding their flexibility, since two different existing codes (one for the fluid flow and one for the geomechanics) can be used for solving the whole coupled poroelastic problem. Special care, however, is needed for their appropriate design, avoiding a slow convergence of the coupling schemes. In addition, these splitting techniques can be also considered as preconditioners for the fully implicit approach, see [29, 30]. The most commonly used iterative coupling methods are the drained and undrained splittings, which solve the mechanical problem first, and the fixed-strain and fixed-stress splittings, which solve the flow problem first [42, 43]. In particular, the fixed stress splitting is the most used in practice due to its unconditional convergence, and it has been widely analyzed [16, 17, 20, 35, 53, 74]. In this scheme, the flow problem is firstly solved fixing the volumetric mean total stress, and then the mechanics part is solved from the values obtained at the previous flow step. This method, however, requires the choice of a certain stabilization parameter which has to be sufficiently large in order to ensure the convergence of the iteration [17].

There is another important issue to take into account in the numerical simulation of poroelastic problems. The corresponding mathematical models involve a large number of physical parameters, and the values of some of such parameters may vary over orders of magnitude in different applications. For example, the value of the permeability can typically range from $10^{-9}$ to $10^{-21}$ $m^2$ in geophysical applications [47, 80], and from $10^{-14}$ to $10^{-16}$ $m^2$ in biophysical applications such as in the modeling of soft tissue or bone [11, 73, 75]. The Poisson ratio can take values varying from 0.1 to 0.5 depending on the degree of incompressibility of the media. Therefore, the large variation of values of these physical parameters makes important to consider discretizations that are uniformly stable, independently of the values of the physical parameters, and solution methods that perform well under such large variations of the parameters. When a numerical method satisfies such properties, it is called parameter-robust method and the design of such type of methods has been the focus of study of the scientific community for the past few years (see for example [2, 38, 47, 71, 70]).

In this work, we gather some numerical techniques that we proposed to deal with the issues raised above by using a very simple numerical scheme for poroelastic problems. More concretely, piecewise linear finite element methods are considered as the simplest discretization scheme for this problem, together with an appropriate stabilization to avoid non-physical oscillations, and

two different decoupled strategies for solving the resulting systems of algebraic equations are derived from the stabilized scheme and theoretically analyzed. Thus, the structure of the paper is as follows. In Section 2 we derive the governing equations for Biot's model, while in Section 3 we introduce the considered discretization together with the proposed stabilization technique and a discussion about the numerical issue arising with the appearance of non-physical oscillations. Section 4 is devoted to derive the decoupled solvers from the stabilized formulation of the discrete problem previously introduced. In particular, in Section 4.1 an iterative coupling approach is presented and in Section 4.2 a non-iterative sequential scheme is derived. Finally, in Section 5 some conclusions are drawn.

## 2 Biot's model. Mathematical formulation

Biot's model is built from the basic principles of fluid and solid mechanics. In particular it couples the governing equations for fluid flow and solid deformation in poroelastic media, taking into account the equilibrium and mass conservation principles, as well as Darcy's law.

We assume a linearly elastic, homogeneous and isotropic porous medium, saturated by a Newtonian fluid. The model is based on the interaction between a solid skeleton and a freely moving pore fluid, which dictates the choice of the main quantities to deal with: the solid displacement vector $\mathbf{u}$, which tracks the movement of the solid matrix, and the fluid velocity vector $\mathbf{q}$, denoting the rate of fluid volume that crosses a unit area of porous solid. This latter is related to the gradient of the pore pressure $p$ by the following linear relationship

$$\mathbf{q} = -\frac{\kappa}{\mu_f}\left(\nabla p - \rho_f \mathbf{g}\right) \tag{1}$$

which is known as Darcy's law, and where $\kappa$ is the permeability of the soil, $\mu_f$ is the viscosity of the fluid, $\rho_f$ is the density of the fluid and $\mathbf{g}$ is the gravitational acceleration vector. The strain tensor $\varepsilon(\mathbf{u})$ is introduced to follow the deformation of the solid skeleton by the following compatibility equation

$$\varepsilon(\mathbf{u}) = \frac{1}{2}(\nabla \mathbf{u} + \nabla^T \mathbf{u}). \tag{2}$$

For a stressed body to remain in equilibrium, all the forces acting on it must balance each other. This requirement leads to the equilibrium equation, given by

$$\operatorname{div} \boldsymbol{\sigma} + \mathbf{f} = 0, \tag{3}$$

where $\boldsymbol{\sigma}$ is the stress tensor, and $\mathbf{f}$ is the density of applied body forces. There are three reasons by which a change of volume of a porous medium can appear: due to compression of the fluid, due to compression of the grains or due to a rearrangement of the grains. The two first mechanisms are controlled by the fluid and solid compressibility, respectively. The latter one is related to the principle of effective stress. This notion was introduced by Terzaghi, who established that the total stress is carried in part by the fluid and in part by the soil structure. The part of the total stress that is not carried by the fluid is called the effective stress, and actually this is the stress applied to the grains of the porous medium. Thus, rearrangement of the soil grains is caused by changes in the effective stress and not by changes in the total stress. Therefore, the total stress $\boldsymbol{\sigma}$ can be split up into the sum of the effective stress, usually denoted by $\boldsymbol{\sigma}'$, and the pore pressure p, that is,

$$\boldsymbol{\sigma} = \boldsymbol{\sigma}' + \alpha p \mathbf{I}, \tag{4}$$

where parameter $\alpha$ is the Biot coefficient and depends on the compressibilities of the solid $c_s$ and porous medium $c_b$ such that $\alpha = 1 - \dfrac{c_s}{c_b}$. In continuum mechanics, the effective stress tensor and the strain tensor are fundamentally related through the material's constitutive equations, which characterize its mechanical behavior under loading. In the case of linear elasticity, as it is our case, this relationship is linear and is described by Hooke's law, which expresses the stress components as linear functions of the strain components via the material's elasticity tensor. For isotropic materials, this relation can be written as

$$\boldsymbol{\sigma}' = \lambda tr(\varepsilon(\mathbf{u}))I + 2\mu\varepsilon(\mathbf{u}), \tag{5}$$

where $\lambda$ and $\mu$ are the so-called Lamé coefficients, which can be computed in terms of the Young modulus, $E$, and the Poisson ratio, $\nu$, as follows:

$$\lambda = \frac{E\nu}{(1-2\nu)(1+\nu)} \quad \text{and} \quad \mu = \frac{E}{1+2\nu}.$$

In order to describe the amount of fluid in a deformable porous media, the so-called fluid content $\xi$ is defined as

$$\xi = \frac{p}{\beta} + \alpha \operatorname{div} \mathbf{u}, \tag{6}$$

where $\beta$ is known as the Biot modulus. Note that the first part in the right-hand side of this

equation measures the change in the amount of fluid as a result of the change in the pore pressure $p$ under constant volumetric strain $\nabla \cdot \mathbf{u}$. In turn, the second part $\alpha \nabla \cdot \mathbf{u}$ measures the amount of fluid content due to deformation of the porous medium. The fluid mass conservation equation is given by

$$\frac{\partial \xi}{\partial t} + \operatorname{div} \mathbf{q} = g, \tag{7}$$

where the source term $g$ represents a forced fluid extraction or injection process. Substituting (6) into (7), we obtain the

$$\frac{\partial}{\partial t}\left(\frac{1}{\beta} p + \alpha \operatorname{div} \mathbf{u}\right) + \operatorname{div} \mathbf{q} = g. \tag{8}$$

Thus, the system of equations governing the consolidation process is given by the equilibrium equation for the porous medium, obtained combining (3) and (4), and the continuity equation (8),

$$-\operatorname{div} \boldsymbol{\sigma}' + \alpha \nabla p = \mathbf{f}, \tag{9}$$

$$\frac{\partial}{\partial t}\left(\frac{1}{\beta} p + \alpha \operatorname{div} \mathbf{u}\right) + \operatorname{div} \mathbf{q} = g. \tag{10}$$

Finally, for linear isotropic materials the stress tensor $\sigma$ is given by Hooke's law (5) and the Darcy velocity $\mathbf{q}$ relates to the pressure through Darcy's law (1). Under these assumptions, this set of partial differential equations can be written as a coupled system in terms of the displacements of the solid matrix $\mathbf{u}$ and the pore pressure $p$, giving rise to the so-called displacement-pressure formulation or two-field formulation for Biot's model, which is given by the following system of partial differential equations (PDEs):

$$-\nabla \left(2\mu \varepsilon(\mathbf{u}) + \lambda \nabla \cdot \mathbf{u}\right) + \alpha \nabla p = \mathbf{f}, \tag{11}$$

$$\frac{1}{\beta}\frac{\partial p}{\partial t} + \alpha \nabla \cdot \frac{\partial \mathbf{u}}{\partial t} - \nabla \cdot \left(K(\nabla p - \rho_f \mathbf{g})\right) = g, \tag{12}$$

on a space-time domain $\Omega \times (0, T_f]$, where $\Omega \subset \mathbb{R}^d$, $d \leq 3$, $T_f > 0$, where $K$ denotes the hydraulic conductivity which is given by the quotient between the permeability $\kappa$ and the viscosity of the fluid $\mu_f$, i.e. $K = \dfrac{\kappa}{\mu_f}$.

To complete the formulation of a well-posed problem, we need to include appropriate boundary and initial conditions. For example, we can consider a part of the boundary which is free to drain and where a traction is applied, and other part that is assumed to be rigid and impermeable, that

is,

$$
\begin{aligned}
& p = 0, && \boldsymbol{\sigma}\mathbf{n} = \mathbf{t}, && \text{on } \Gamma_t, \\
& \mathbf{u} = \mathbf{0}, && K\left(\nabla p - \rho_f \mathbf{g}\right)\cdot \mathbf{n} = 0, && \text{on } \Gamma_c,
\end{aligned} \tag{13}
$$

where $\mathbf{n}$ is the unit outward normal to the boundary $\Gamma$, which is split into two disjoint subsets $\Gamma_t$ and $\Gamma_c$ with non null measure such that $\Gamma = \Gamma_t \cup \Gamma_c$.
For the initial time $t = 0$ the following condition is assumed,

$$
\left(\frac{1}{\beta} p + \alpha \nabla \cdot \mathbf{u}\right)(x, 0) = 0, \ x \in \Omega. \tag{14}
$$

## 3 Discrete scheme. Numerical issues

To present the variation formulation of problem (11)-(14), we first introduce appropriate function spaces. Let $L^2(\Omega)$ be the Hilbert space of square integrable scalar valued functions defined on $\Omega$, with inner product

$$
(p, q) = \int_\Omega p\, q \, \mathrm{d}x, \ p, q \in L^2(\Omega),
$$

and let us consider $H^1(\Omega)$ which denotes the subspace of $L^2(\Omega)$ of functions with weak first derivatives in $L^2(\Omega)$. Then, we define the following Sobolev spaces for displacements and pressure variables:

$$
\mathbf{V} = \left\{\mathbf{u} \in (H^1(\Omega))^d \mid \mathbf{u} = \mathbf{0} \text{ on } \Gamma_c\right\}, \tag{15}
$$

$$
Q = \left\{q \in H^1(\Omega) \mid q = 0 \text{ on } \Gamma_t\right\}. \tag{16}
$$

By considering the bilinear forms corresponding to the elasticity and the scaled Laplacian operators, that is,

$$
a(\boldsymbol{u}, \boldsymbol{v}) = 2\mu \int_\Omega \varepsilon(\boldsymbol{u}) : \varepsilon(\boldsymbol{v}) \, \mathrm{d}\Omega + \lambda \int_\Omega \operatorname{div} \boldsymbol{u} \operatorname{div} \boldsymbol{v} \, \mathrm{d}\Omega, \qquad a_p(p, q) = \int_\Omega K \nabla p \cdot \nabla q \, \mathrm{d}\Omega,
$$

we can write the variational formulation of the two-field formulation of Biot's problem as follows: Find $(\mathbf{u}(t), p(t)) \in C^1([0, T_f]; \mathbf{V}) \times C^1([0, T_f]; Q)$ such that

$$
a(\boldsymbol{u}, \boldsymbol{v}) - \alpha(p, \operatorname{div} \boldsymbol{v}) = (\boldsymbol{f}, \boldsymbol{v}), \quad \forall\, \boldsymbol{v} \in \boldsymbol{V}, \tag{17}
$$

$$
\frac{1}{\beta}(\partial_t p, q) + \alpha(\operatorname{div} \partial_t \boldsymbol{u}, q) + a_p(p, q) = (g, q) + (K \rho_f \mathbf{g}, \nabla q), \ \forall\, q \in Q. \tag{18}
$$

with the initial condition,

$$\left(\frac{1}{\beta}p(0) + \alpha\nabla\cdot\mathbf{u}(0), q\right) = 0,\ \forall q \in L^2(\Omega). \tag{19}$$

Notice that in (18) the time derivative is denoted by $\partial_t$ for compactness of notation.

Now, we consider the finite element approximation of problem (17)-(19) and, in particular, linear finite element methods are used to approximate both displacement and pressure unknowns, as previously commented. Let $\mathcal{T}_h$ be a partition of $\Omega \subset \mathbb{R}^d$ consisting of triangles ($d = 2$) or tetrahedrons ($d = 3$). Thus, we choose the following finite-element pair of spaces $\mathbf{V}_h \times Q_h$ to approximate the displacements and the pressure, respectively, where

$$\begin{aligned}
\mathbf{V}_h &= \{\boldsymbol{v}_h \in (H^1(\Omega))^d \mid \boldsymbol{v}_h|_T \in (P_1)^d,\ \forall T \in \mathcal{T}_h,\ \boldsymbol{v}_h|_{\Gamma_c} = \mathbf{0}\},\\
Q_h &= \{p_h \in H^1(\Omega) \mid p_h|_T \in P_1,\ \forall T \in \mathcal{T}_h,\ p_h|_{\Gamma_t} = 0\},
\end{aligned}$$

where $P_1$ denotes the space of scalar piecewise linear functions on $\mathcal{T}_h$. To discretize in time, we use the backward Euler method on a uniform partition of the time interval $(0, T_f]$, $t_j = j\tau$, $j = 0, \ldots, N$, with time-step $\tau = \frac{T_f}{N}$, leading to the following fully-discrete scheme:
For given initial values $(\mathbf{u}_h^0, p_h^0) \in \mathbf{V}_h \times Q_h$, for $n = 1, 2, \ldots, N$, find $(\mathbf{u}_h^n, p_h^n) \in \mathbf{V}_h \times Q_h$ such that

$$a(\boldsymbol{u}_h^n, \boldsymbol{v}_h) - \alpha(p_h^n, \operatorname{div}\boldsymbol{v}_h) = (\boldsymbol{f}_h^n, \boldsymbol{v}_h), \quad \forall\, \boldsymbol{v}_h \in \boldsymbol{V}_h, \tag{20}$$

$$\frac{1}{\beta}(\bar{\partial}_t p_h^n, q_h) + \alpha(\operatorname{div}\bar{\partial}_t \boldsymbol{u}_h^n, q_h) + a_p(p_h^n, q_h) = (g_h^n, q_h),\ \forall\, q_h \in Q_h, \tag{21}$$

where $\bar{\partial}_t p_h^n := (p_h^n - p_h^{n-1})/\tau$, $\bar{\partial}_t \boldsymbol{u}_h^n := (\boldsymbol{u}_h^n - \boldsymbol{u}_h^{n-1})/\tau$, and where $(g_h^n, q_h)$ includes the discrete counterpart of the right-hand side $(g, q) + (K\rho_f\mathbf{g}, \nabla q)$ of (18).

By introducing operators notation, and establishing the following correspondences among operators and the bilinear forms:

(22)

$$a(\boldsymbol{u}_h, \boldsymbol{v}_h) \to A,\ -\alpha(p_h, \operatorname{div}\boldsymbol{v}_h) \to G,\ \alpha(\operatorname{div}\mathbf{u}_h, q_h) \to D,\ a_p(p_h, q_h) \to A_p,\ (p_h, q_h) \to M.$$

we can rewrite the discrete problem (20)-(21) in the following block form:

$$\mathcal{A}\begin{pmatrix}\boldsymbol{u}\\ p\end{pmatrix} = \begin{pmatrix}f\\ g\end{pmatrix}, \quad \text{with} \quad \mathcal{A} = \begin{pmatrix}A & G\\ D & \tau A_p + \beta^{-1}M\end{pmatrix}. \tag{23}$$

Note that $D = -G^T$ by definition.

### *3.1 Numerical difficulties. Non-physical oscillations*

As previously commented in the introduction, the pressure field may exhibit non-physical oscillations when some standard combinations of finite elements are used to discretize the problem. This is the case, for example, when linear finite element methods are used to approximate both displacement and pressure unknowns. In particular, such an unstable behavior may occur when the porous material has a low permeability and/or when a small time step is used at the beginning of the consolidation process. To illustrate this behavior, below we present some examples. First, we consider a very simple one-dimensional problem: the Terzaghi's problem. After that, a modification of such a simple problem, in which we have included an intermediate layer with a very low permeability is considered. Finally, a two-dimensional benchmark problem is analyzed too.

#### 3.1.1 Example 1 - Terzaghi Problem

The Terzaghi problem models a column of a porous medium with height, $H$, saturated by an incompressible fluid, bounded by impermeable and rigid lateral walls and bottom, and supporting a load $\sigma_0$ on the top boundary which is free to drain (see Figure 1(a)). This results in the following one-dimensional version of model (11)-(12):

$$\begin{aligned} &-\frac{\partial}{\partial x}\left((\lambda+2\mu)\,\frac{\partial u}{\partial x}\right)+\frac{\partial p}{\partial x}=0,\\ &\frac{\partial}{\partial t}\left(\frac{\partial u}{\partial x}\right)-\frac{\partial}{\partial x}\left(K\,\frac{\partial p}{\partial x}\right)=0, \end{aligned} \qquad (x,t)\in(0,H)\times(0,T_f], \tag{24}$$

where for simplicity we have fixed $\alpha = 1$ and $1/\beta = 0$. This system is supplemented with the following boundary and initial conditions,

$$\begin{aligned} &(\lambda+2\mu)\,\frac{\partial u}{\partial x}(0,t)=\sigma_0, \quad p(0,t)=0,\ t\in(0,T_f],\\ &u(H,t)=0,\ K\frac{\partial p}{\partial x}(H,t)=0,\ t\in(0,T_f],\\ &\frac{\partial u}{\partial x}(x,0)=0,\ x\in[0,H]. \end{aligned}$$

A uniform partition of spatial domain $\Omega = (0, H)$ with mesh size $h$ is considered, and the backward Euler method is chosen for discretization in time, together with the spatial P1-P1 method.

When discretizing using linear finite elements for both displacement and pressure, non-

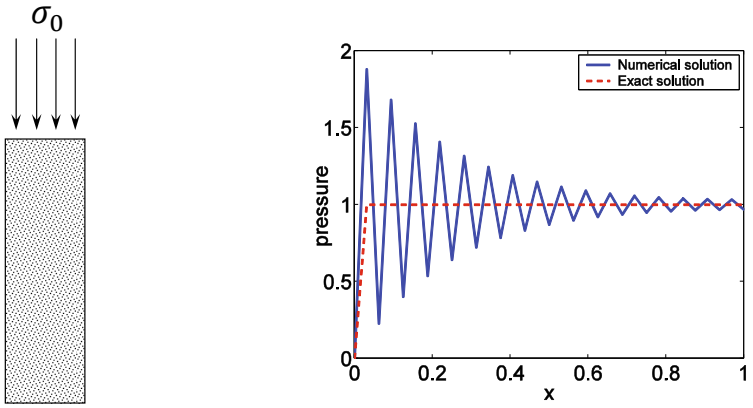


(a) (b)

Figure 1: (a) Domain for Terzaghi problem and (b) non-physical oscillations in the numerical solution of the pressure field for Terzaghi problem.

physical oscillations are observed in the numerical solution of the pressure even for this simple problem. This can be seen In Figure 1(b), where we display the numerical solution obtained for the pressure field at the final time $T_f = 0.1$, taking the hydraulic conductivity $K = 10^{-6}$, $\lambda + 2\mu = 1$, Biot coefficient $\alpha = 1$, and a mesh size $h = 1/32$.

### 3.1.2 Example 2 - Two-layer Problem

Non-physical oscillations in the pressure field may also appear when a low-permeability is assumed in a region of the domain. In order to illustrate this, we consider a porous material on which a low–permeable layer ($K = 10^{-8}$) is placed between two layers with unit permeability ($K = 1$), as shown in Figure 2(a). The boundary of the squared domain is split into two disjoint subsets $\Gamma_1$ and $\Gamma_2$ on which we assume the following boundary conditions: on the top, which is free to drain ($p = 0$), a uniform load is applied, that is, $\sigma' \mathbf{n} = \mathbf{g}$ with $\mathbf{g} = (0, -1)^t$, on $\Gamma_1$, whereas at the sides and bottom of the domain that are rigid ($\mathbf{u} = \mathbf{0}$) the boundary is impermeable, that is, $\nabla p \cdot \mathbf{n} = 0$ on $\Gamma_2$. This test can be reduced to a one-dimensional problem, and, therefore, it is enough to analyze the numerical solutions corresponding to one vertical line in the domain as displayed in Figure 2(a).

When linear finite elements for displacements and pressure are considered, the approximation for the pressure field that is obtained by using 32 elements in the grid is shown in Figure 2(b). There, we can observe that strong spurious oscillations appear in the part of the domain corresponding to the low-permeable layer.

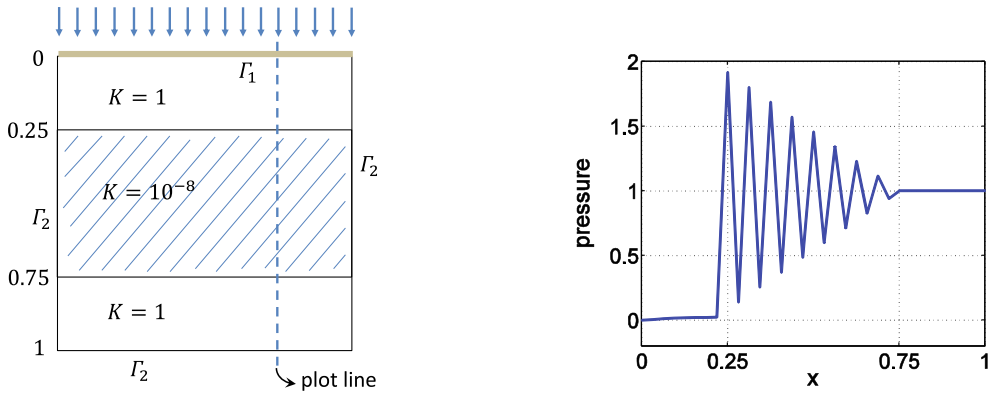


(a) (b)

Figure 2: (a) Domain for the two-layer problem and (b) non-physical oscillations in the numerical solution of the pressure for the two-layer problem.

#### 3.1.3 Example 3 - Barry & Mercer problem

As third example we consider a well-known poroelastic benchmark test on a finite two-dimensional domain which is called Barry & Mercer's problem [9]. It models the behavior of a rectangular uniform porous material $[0, a]\times[0, b]$ drained on all sides, and with zero tangential displacements assumed on the whole boundary, in which a pulsating point source is considered. Such a point-source corresponds to a sine wave and is given by $f(t) = 2\upsilon\,\delta_{(x_0,y_0)}\,\sin(\upsilon\,t)$, where $\upsilon = \dfrac{(\lambda+2\mu)K}{a\,b}$ and $\delta_{(x_0,y_0)}$ is the Dirac delta at the point $(x_0, y_0)$. In Figure 3(a), the computational domain and the boundary conditions of the problem are depicted.

In particular, we consider the unit square domain $(0, 1) \times (0, 1)$, and the following values of the material parameters: $E = 10^5$, $\nu = 0.1$, $\alpha = 1$, $\beta = 10^8$ and $K = 10^{-6}$. The source is positioned at the point $(1/4, 1/4)$, and a right triangular grid of mesh size $h = 2^{-6}$ is used for the simulations. Fluid pressure oscillations for the Barry and Mercer's problem can be observed by considering standard P1-P1 discretizations. In Figure 3(b), we show the numerical solutions obtained for the pressure field at a final time $T_f = 10^{-4}$, with only one time step. We observe that non-physical oscillations appear in the numerical pressure near the source-point.

### *3.2 Stabilization scheme*

In order to deal with the numerical issues presented above in the previous section, by using one of the simplest discretization that one can consider for the two-field formulation of Biot's model (linear finite elements for both displacements and pressure unknowns), we propose a way to

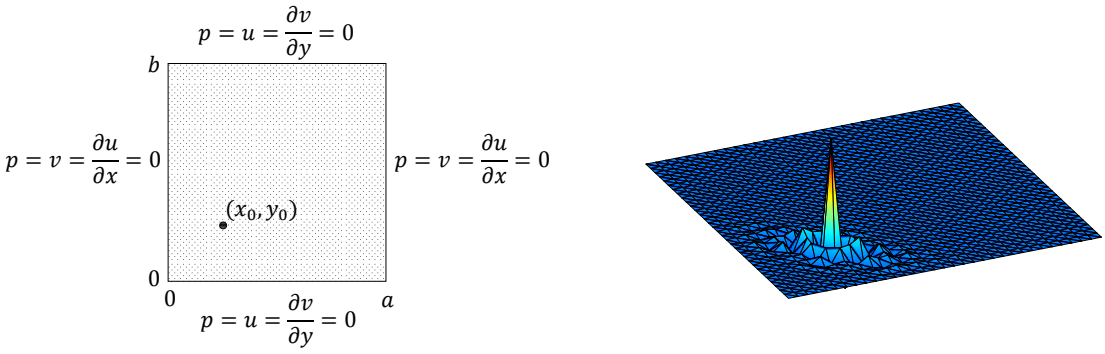


(a) (b)

Figure 3: (a) Computational domain and boundary conditions for the Barry and Mercer's source problem, and (b) numerical solution of the pressure for the Barry & Mercer problem (at the final time $T_f = 10^{-4}$ with hydraulic conductivity $K = 10^{-6}$, Poisson ratio $\nu = 0.1$, and mesh spacing $h = 1/64$).

stabilize the arising discrete problem. The main idea is to add the term $L\dfrac{\partial p}{\partial t}$ to both sides in the flow equation (12), and discretizing the two new terms in a different way: we use mass matrix for the discretization of the term in the right hand side and the row-sum lumpled mass matrix on the left hand side term. This leads to the following discrete variational formulation:

$$a(\boldsymbol{u}_h^n, \boldsymbol{v}_h) - \alpha(p_h^n, \operatorname{div} \boldsymbol{v}_h) = (\boldsymbol{f}_h^n, \boldsymbol{v}_h), \quad \forall \boldsymbol{v}_h \in \boldsymbol{V}_h, \tag{25}$$

$$\begin{aligned} &\frac{1}{\beta}(\bar{\partial}_t p_h^n, q_h) + \alpha(\operatorname{div} \bar{\partial}_t \boldsymbol{u}_h^n, q_h) + a_p(p_h^n, q_h) + L(\bar{\partial}_t p_h^n, q_h)_0 - L(\bar{\partial}_t p_h^n, q_h) \\ &\quad = (g_h^n, q_h), \forall q_h \in Q_h, \end{aligned} \tag{26}$$

where $(\cdot,\cdot)_0$ is an approximation of the $L^2(\Omega)$ inner product defined by mass lumping, *i.e.*, for continuous functions $p$ and $q$ defined on $\bar{\Omega}$, we have

$$(p, q)_0 = \sum_{T \in \mathcal{T}_h} \int_T (pq)_I \, d\boldsymbol{x} = \sum_{T \in \mathcal{T}_h} \frac{|T|}{d+1} \sum_{j=1}^{d+1} (pq)(P_{T,j}),$$

where $(pq)_I$ denotes the linear interpolant of the continuous function $(pq)$ and $P_{T,j}$ are the coordinates of the $j$-th vertex of $T \in \mathcal{T}_h$. In (26), $L$ is a parameter appropriately chosen to remove the non-physical oscillations. In particular, for the considered P1-P1 discretization, the parameter

is chosen as

$$L = \frac{1}{\beta} + \frac{3\alpha^2}{2\left(\lambda + \frac{2\mu}{d}\right)}. \tag{27}$$

The choice of this parameter is done in the one-dimensional case in the way that it is the optimal value to provide a monotone scheme that eliminates the oscillations without inducing extra diffusion effects in the numerical solution.

**Remark 3.1.** *The considered stabilized scheme is identical to the one given in [5] for one-dimensional problems. This scheme has been widely cited in the porous media community and was theoretically analyzed in [69], where it was observed numerically that oscillations were eliminated also in problems with two and three spatial dimensions, though supporting theory for such observation is missing. The stabilization considered in this work also leads to a monotone scheme, and it has several advantages with respect to the techniques proposed in [5, 69]. Some of these benefits are the fact that the stabilization parameter L does not depend on the mesh size, and that it has been derived for any value of the storage coefficient. In addition, as it is shown in next sections, the current stabilization scheme provides a way to derive decoupled solvers for Biot's model which are convergent without the need to introduce other stabilization terms (as it is the case for the well-known fixed stress split method).*

Following the notation introduced in (22) and (23), the fully-discrete stabilized scheme (25)-(26) can be written in block form as follows:

$$\mathcal{A}_{stab} \begin{pmatrix} \boldsymbol{u} \\ p \end{pmatrix} = \begin{pmatrix} f \\ g \end{pmatrix}, \quad \text{with} \quad \mathcal{A}_{stab} = \begin{pmatrix} A & G \\ D & \tau A_p + \beta^{-1} M + L(M_l - M) \end{pmatrix}, \tag{28}$$

where $M$ and $M_l$ the mass matrix and the lumped mass matrix, respectively.

Next, we prove the stabilized scheme's stability in order to demonstrate the well-posedness of the discrete problem (25)-(26). With this purpose, we show a relationship between the stabilization technique studied in [69] and the stabilized scheme considered in this work.

**Lemma 3.2.** *The difference between the lumped mass matrix $M_l$ and the mass matrix $M$ on a simplicial grid, that is $M_l - M$, is spectrally equivalent to the scaled stiffness matrix $h^2 L_p$, where $\langle h^2 L_p p, q\rangle := \sum_{T\in\mathcal{T}} h_T^2 \int_T |\nabla p|^2$), that is,*

$$C_1\langle (M_l - M)p, q\rangle \leq \langle h^2 L_p p, q\rangle \leq C_2\langle (M_l - M)p, q\rangle. \tag{29}$$

*Proof.* Let $p$ and $q$ be piecewise linear continuous functions, then we have the following

$$\langle Mp, q\rangle = \sum_{T\in\mathcal{T}_h} \int_T pq \, d\boldsymbol{x},$$
$$\langle M_l p, q\rangle = \sum_{T\in\mathcal{T}_h} \int_T (pq)_I \, d\boldsymbol{x}.$$

Let us define $Z = (M_l - M)$, then we can write,

$$\langle Zp, q\rangle = \sum_{T\in\mathcal{T}_h} \langle Z_T p_T, q_T\rangle,$$

where, for a fixed $T \in \mathcal{T}_h$, $\langle Z_T p_T, q_T\rangle$ is the difference between the integrals in the definitions of $M_l$ and $M$ and $p_T \in \mathbb{R}^{d+1}$ is the vector that represents the degrees of freedom of $p(x)$ with components $\{p_{T,k}\}_{k=1}^{d+1}$ on $T$.
Evaluating the integrals on $T \in \mathcal{T}_h$ and using the Poincaré inequality for convex domains [10, Theorem 3.2], we have that

$$\frac{1}{d+1}\langle Z_T p_T, p_T\rangle = \int_T \left(p - \frac{1}{|T|}\int_T p \, d\boldsymbol{x}\right)^2 d\boldsymbol{x} \le \frac{h_T^2}{\pi^2}\int_T |\nabla p|^2 \, d\boldsymbol{x}.$$

On the other hand, from [81, Equations (2.3)-(2.4)], we obtain the bound

$$h_T^2 \int_T |\nabla p|^2 \, d\boldsymbol{x} \le \frac{c_T|T|}{2}\sum_{j=1}^{d+1}\sum_{k=1}^{d+1}(p_{T,j} - p_{T,k})^2 = c_T(d+1)(d+2)\langle Z_T p_T, p_T\rangle, \tag{30}$$

with $c_T := \max\limits_{\substack{1\le j,k\le(d+1)\\ j\neq k}} \left\{\dfrac{h_T^2}{|h_j||h_k|}\right\}$, where $h_j$ (and similarly $h_k$) is the distance from the vertex $P_{T,j}$ ($P_{T,k}$ for $h_k$) to the face of $T$ opposite to this vertex. Summing over all elements $T \in \mathcal{T}_h$ shows that $Z = (M_l - M)$ is spectrally equivalent to the scaled stiffness matrix corresponding to the Laplace operator $h^2 L_p$, and we obtain the spectral equivalence in (29). □

Consequentially, we can derive an inf-sup condition that guarantees the well-posedness of the stabilized discrete problem.

**Theorem 3.3.** *The following weak inf-sup condition*

$$\sup_{\boldsymbol{w}_h \in \boldsymbol{V}_h} \frac{(q, \operatorname{div} \boldsymbol{w}_h)}{\|\boldsymbol{w}_h\|_A} \geq \eta \frac{1}{\sqrt{\lambda + 2\mu/d}} \|q\| - \epsilon \frac{1}{\sqrt{\lambda + 2\mu/d}} h \|\nabla q\|, \quad \forall\, q \in Q_h, \tag{31}$$

*where* $h = \max_T h_T$ *and* $\eta > 0$ *and* $\epsilon > 0$ *are constants that do not depend on the mesh size or the physical parameters, is fulfilled.*

*Proof.* The proof of the inf-sup condition follows from the application of Lemma 3.2 and the theoretical results derived in [69, 3, 71]. In particular, the inf-sup condition is similar to the one shown in [69, Theorem 1]. □

Summarizing, the stabilization terms and the stabilization parameters are derived in a mathematically consistent manner, and the computationally convenient equal-order interpolation of all the field variables has been shown to be stable.

Finally, we demonstrate that the stabilized scheme (25)-(26) provides numerical solutions that are free of non-physical oscillations. With this purpose, we solve the problems considered in the three examples presented above in Section 3.1 by using the proposed scheme. The numerical solution of the pressure for each of these problems is depicted in Figure 4, and we can observe that the spurious oscillations are completely eliminated for all the cases.

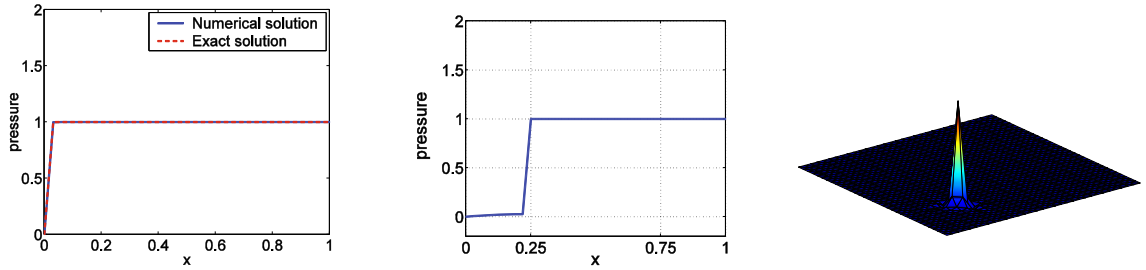


(a) Example 1 (b) Example 2 (c) Example 3

Figure 4: Numerical solution of the pressure field for the examples introduced in Section 3.1: (a) Terzaghi problem, (b) Two-layer problem and (c) Barry & Mercer problem.

## 4 Efficient decoupled solvers

An alternative to the classical monolithic or fully coupled schemes is the use of decoupled solvers, which address the coupled poroelastic problem by splitting it into a sequence of subproblems that

can be solved separately. In such approaches, the flow and mechanics equations are treated independently, with information exchanged between the subproblems through an iterative or staggered procedure. This partitioned strategy can significantly reduce computational costs and facilitate the use of existing solvers optimized for each physical field.

In the next two sections, we present iterative and non-iterative coupling methods for solving Biot's model by using simple piecewise linear finite elements for both displacement and pressure variables. These solution methods are straightforwardly derived from the stabilized scheme introduced in Section 3.2.

### *4.1 Iterative coupling method*

From the considered stabilized discrete scheme (25)-(26), we straightforwardly obtain a sequential-implicit method, which is similar to the fixed-stress splitting method, but with the advantage that no additional stabilization of the iteration is required for convergence. The idea is first to solve the flow problem and then the mechanics, and iterate until a converged solution is obtained. Therefore, at each time level $t_n$, we consider the following iterative method for the solution of (25)-(26):

Given the initial guess for the coupling iteration at time $t_n$, $\boldsymbol{u}_h^{n,0} = \boldsymbol{u}_h^{n-1}$ and $p_h^{n,0} = p_h^{n-1}$, the algorithm provides a sequence of approximations ($\boldsymbol{u}_h^{n,i}$ and $p_h^{n,i}$), $i \geq 1$, as follows:

**Step 1:** Given $(\boldsymbol{u}_h^{n,i-1}, p_h^{n,i-1}) \in \boldsymbol{V}_h \times Q_h$, find $p_h^{n,i} \in Q_h$ such that:

$$\frac{1}{\beta}\left(\frac{p_h^{n,i}-p_h^{n-1}}{\tau}, q_h\right) + L\left(\frac{p_h^{n,i}-p_h^{n-1}}{\tau}, q_h\right)_0 + a_p(p_h^{n,i}, q_h) = -\alpha\left(\operatorname{div}\frac{\boldsymbol{u}_h^{n,i-1}-\boldsymbol{u}_h^{n-1}}{\tau}, q_h\right) + L\left(\frac{p_h^{n,i-1}-p_h^{n-1}}{\tau}, q_h\right) + (g_h^n, q_h), \quad \forall\, q_h \in Q_h, \tag{32}$$

**Step 2:** Given $p_h^{n,i} \in Q_h$, find $\boldsymbol{u}_h^{n,i} \in \boldsymbol{V}_h$ such that

$$a(\boldsymbol{u}_h^{n,i}, \boldsymbol{v}_h) = \alpha(p_h^{n,i}, \operatorname{div}\boldsymbol{v}_h) + (\boldsymbol{f}_h^n, \boldsymbol{v}_h), \quad \forall\, \boldsymbol{v}_h \in \boldsymbol{V}_h. \tag{33}$$

The previous algorithm is based on the following splitting of $\mathcal{A}_{stab}$,

$$\mathcal{A}_{stab} = \begin{pmatrix} A & G \\ D & C \end{pmatrix} = \begin{pmatrix} A & G \\ 0 & \tau A_p + \beta^{-1} M + L M_l \end{pmatrix} - \begin{pmatrix} 0 & 0 \\ -D & LM \end{pmatrix}.$$

Although we can prove the robust convergence of algorithm (32)-(33), we aim to optimize the convergence of the iterative coupling method. With this purpose, we have to distinguish two different cases: the case when $\beta^{-1}$ is very close to zero and a more general fluid regime that implies a bigger value of $\beta^{-1}$. For simplicity in the presentation, we will focus on the first case, that is, the proposed approach is presented in detail for the case in which the storage coefficient $\beta^{-1}$ is close to zero and therefore the appropriate stabilization parameter given in (27) reduces to $L = \dfrac{3\alpha^2}{2\left(\lambda + \frac{2\mu}{d}\right)}$. At the end of the section, its extension to a more general case which includes the regime with larger values of $1/\beta$ is briefly introduced.

In this case, in order to optimize the convergence of the scheme, we introduce a parameter $\gamma$ to split the term corresponding to $M_l$ and have more flexibility when studying the convergence. In this way, the proposed iterative method at each time step $t_n$ is defined as:

Given the initial guess for the coupling iteration at time $t_n$, $\boldsymbol{u}_h^{n,0} = \boldsymbol{u}_h^{n-1}$ and $p_h^{n,0} = p_h^{n-1}$, the algorithm provides a sequence of approximations ($\boldsymbol{u}_h^{n,i}$ and $p_h^{n,i}$), $i \geq 1$, as follows:

**Step 1:** Given $(\boldsymbol{u}_h^{n,i-1}, p_h^{n,i-1}) \in \boldsymbol{V}_h \times Q_h$, find $p_h^{n,i} \in Q_h$ such that:

$$\begin{aligned} &\frac{1}{\beta}\left(\frac{p_h^{n,i} - p_h^{n-1}}{\tau}, q_h\right) + \gamma L \left(\frac{p_h^{n,i} - p_h^{n-1}}{\tau}, q_h\right)_0 + a_p(p_h^{n,i}, q_h) = -\alpha \left(\operatorname{div} \frac{\boldsymbol{u}_h^{n,i-1} - \boldsymbol{u}_h^{n-1}}{\tau}, q_h\right) \\ &+ L\left(\frac{p_h^{n,i-1} - p_h^{n-1}}{\tau}, q_h\right) + (\gamma - 1) L \left(\frac{p_h^{n,i-1} - p_h^{n-1}}{\tau}, q_h\right)_0 + (g_h^n, q_h), \quad \forall\, q_h \in Q_h, \end{aligned} \tag{34}$$

**Step 2:** Given $p_h^{n,i} \in Q_h$, find $\boldsymbol{u}_h^{n,i} \in \boldsymbol{V}_h$ such that

$$a(\boldsymbol{u}_h^{n,i}, \boldsymbol{v}_h) = \alpha(p_h^{n,i}, \operatorname{div} \boldsymbol{v}_h) + (\boldsymbol{f}_h^n, \boldsymbol{v}_h), \quad \forall\, \boldsymbol{v}_h \in \boldsymbol{V}_h. \tag{35}$$

Equivalently, the iterative method can be written by means of the following splitting of $\mathcal{A}_{stab}$,

$$\mathcal{A}_{stab} = \begin{pmatrix} A & G \\ 0 & \tau A_p + \beta^{-1} M + \gamma L M_l \end{pmatrix} - \begin{pmatrix} 0 & 0 \\ -D & LM + (\gamma - 1) L M_l \end{pmatrix}. \tag{36}$$

Then, our aim is to demonstrate the convergence of the iterative method presented in (34)-(35). In addition, it is important to show a robust convergence with respect to the physical and discretization parameters of the model. With this purpose, let us define $e_u^i = \boldsymbol{u}_h^{n,i} - \boldsymbol{u}_h^n$ and $e_p^i = p_h^{n,i} - p_h^n$ as the errors at iteration $i$ for the displacements and for the pressure, respectively, and in the next result we present the corresponding error estimates.

**Theorem 4.1.** *The iterative method given in* (34)-(35) *is convergent for any parameters* $\gamma \in (2/3, 2]$ *such that* $\gamma L = \omega \frac{\alpha^2}{(\lambda + 2\mu/d)} \geq \frac{\alpha^2}{(\lambda + 2\mu/d)}$, *i.e.,* $\omega \geq 1$. *Additionally,*

$$\|e_p^i\|^2 + \frac{|1-\gamma|}{\gamma} \|e_p^i\|_Z^2 \leq \frac{1}{1 + \frac{\eta^2}{\omega(1+2\theta^*)}} \left( \|e_p^i\|^2 + \frac{|1-\gamma|}{\gamma} \|e_p^{i-1}\|_Z^2 \right), \tag{37}$$

*where* $\theta^* \geq \frac{\epsilon^2 C_2 \gamma}{4\omega(\gamma - |1-\gamma|)}$ *is a root of the following quadratic equation*

$$q_2(\theta) := \left[ \frac{2(\gamma - |1-\gamma|)}{\gamma} \right] \theta^2 + \left[ \frac{\gamma - |1-\gamma|}{\gamma} - \frac{\eta^2 |1-\gamma|}{2\omega\gamma} - \frac{\epsilon^2 C_2}{2\omega} \right] \theta - \frac{\epsilon^2 C_2}{4\omega} = 0. \tag{38}$$

*Here,* $\eta > 0$ *is the constant appearing in the weak inf-sup condition* (31)*, and* $C_2$ *is the constant for the upper bound of the spectral equivalence condition* (29)*.*

*Proof.* By subtracting equations (25) and (35) tested with $\boldsymbol{v}_h = e_{\boldsymbol{u}}^{i-1} \in V_h$ and equations (26) and (34) tested with $q_h = e_p^i \in Q_h$, adding all together, and using that $M_l - M = Z$, we obtain the following:

$$a(e_{\boldsymbol{u}}^i, e_{\boldsymbol{u}}^{i-1}) + \frac{1}{\beta} \|e_p^i\|^2 + \tau \|e_p^i\|_{A_p}^2 + \gamma L (e_p^i - e_p^{i-1}, e_p^i) + \gamma L (e_p^i, e_p^i)_Z + (1-\gamma) L (e_p^{i-1}, e_p^i)_Z = 0,$$

which implies the following inequality by using a polarization identity and Young's inequality:

$$\begin{aligned} &\frac{1}{2} \|e_{\boldsymbol{u}}^2\|_A^2 + \frac{1}{2} \|e_{\boldsymbol{u}}^{i-1}\|_A^2 + \frac{1}{\beta} \|e_p^i\|^2 + \tau \|e_p^i\|_{A_p}^2 + \frac{\gamma L}{2} \|e_p^i\|^2 + \frac{\gamma L}{2} \|e_p^i - e_p^{i-1}\|^2 + \\ &+ \left( \gamma - \frac{|1-\gamma|}{2} \right) L \|e_p^i\|_Z^2 \leq \frac{\gamma L}{2} \|e_p^{i-1}\|^2 + \frac{1}{2} \|e_{\boldsymbol{u}}^i - e_{\boldsymbol{u}}^{i-1}\|_A^2 + \frac{|1-\gamma|}{2} L \|e_p^{i-1}\|_Z^2. \end{aligned} \tag{39}$$

As a first step, we take the difference between equations (35) and (25) evaluated at iteration $i$ and $i-1$, tested with $\boldsymbol{v}_h = e^i_{\boldsymbol{u}} - e^{i-1}_{\boldsymbol{u}}$ which yields:

$$\begin{aligned}\|e^i_{\boldsymbol{u}} - e^{i-1}_{\boldsymbol{u}}\|^2_A &= \alpha(e^i_p - e^{i-1}_p, \nabla\cdot(e^i_{\boldsymbol{u}} - e^{i-1}_{\boldsymbol{u}})) \leq \alpha\|e^i_p - e^{i-1}_p\|\|\nabla\cdot(e^i_{\boldsymbol{u}} - e^{i-1}_{\boldsymbol{u}})\| \\ &\leq \frac{\alpha}{\sqrt{\lambda+2\mu/d}}\|e^i_p - e^{i-1}_p\|\|e^i_{\boldsymbol{u}} - e^{i-1}_{\boldsymbol{u}}\|_A,\end{aligned}$$

where we use the Cauchy-Schwarz inequality and the fact that $a(\boldsymbol{u},\boldsymbol{u}) \geq (\lambda + \frac{2\mu}{d})\|\nabla\cdot\boldsymbol{u}\|^2$. Thus,

$$\|e^i_{\boldsymbol{u}} - e^{i-1}_{\boldsymbol{u}}\|_A \leq \frac{\alpha}{\sqrt{\lambda+2\mu/d}}\|e^i_p - e^{i-1}_p\|. \tag{40}$$

From the weak inf-sup condition (31), we know that, for any given $e^i_p$, there exists $\boldsymbol{w}_h \in V_h$, such that

$$(e^i_p, \operatorname{div}\boldsymbol{w}_h) \geq \left(\eta\frac{1}{\sqrt{\lambda+2\mu/d}}\|e^i_p\| - \epsilon\frac{1}{\sqrt{\lambda+2\mu/d}}h\|\nabla e^i_p\|\right)\|\boldsymbol{w}_h\|_A, \quad \|\boldsymbol{w}_h\|_A = \|e^i_p\|.$$

Thus, as a second step, subtracting equations (35) and (25) and testing with $\boldsymbol{v}_h = \boldsymbol{w}_h$ we derive that,

$$\begin{aligned}&\alpha\left(\eta\frac{1}{\sqrt{\lambda+2\mu/d}}\|e^i_p\| - \epsilon\frac{1}{\sqrt{\lambda+2\mu/d}}h\|\nabla e^i_p\|\right)\|\boldsymbol{w}_h\|_A \leq \alpha(e^i_p, \operatorname{div}\boldsymbol{w}_h) \\ &= a(e^i_{\boldsymbol{u}}, \boldsymbol{w}_h) \leq \|e^i_{\boldsymbol{u}}\|_A\|\boldsymbol{w}_h\|_A,\end{aligned}$$

which implies

$$\|e^i_{\boldsymbol{u}}\|_A \geq \eta\frac{\alpha}{\sqrt{\lambda+2\mu/d}}\|e^i_p\| - \epsilon\frac{\alpha}{\sqrt{\lambda+2\mu/d}}h\|\nabla e^i_p\|.$$

Now, by using Young's inequality with constant $\theta > 0$, we obtain

$$\|e^i_{\boldsymbol{u}}\|^2_A \geq \frac{\eta^2}{1+2\theta}\frac{\alpha^2}{\lambda+2\mu/d}\|e^i_p\|^2 - \frac{\epsilon^2}{2\theta}\frac{\alpha^2}{\lambda+2\mu/d}h^2\|\nabla e^i_p\|^2. \tag{41}$$

At the end, substituting the inequalities obtained in (40) and (41) back into (39), dropping the

$\frac{1}{2}\|e_{\boldsymbol{u}}^{i-1}\|_A^2$, $\frac{1}{\beta}\|e_p^i\|^2$, and $\tau\|e_p^i\|_{A_p}^2$ terms, we arrive at

$$\left(\frac{1}{2}\frac{\eta^2}{1+2\theta}\frac{\alpha^2}{\lambda+2\mu/d}+\frac{\gamma L}{2}\right)\|e_p^i\|^2+\frac{\gamma L}{2}\|e_p^i-e_p^{i-1}\|^2+\left(\gamma-\frac{|1-\gamma|}{2}\right)L\|e_p^i\|_Z^2$$
$$\leq\frac{\gamma L}{2}\|e_p^{i-1}\|^2+\frac{1}{2}\frac{\alpha^2}{\lambda+2\mu/d}\|e_p^i-e_p^{i-1}\|^2+\frac{|1-\gamma|}{2}L\|e_p^{i-1}\|_Z^2+\frac{\epsilon^2C_2}{4\theta}\frac{\alpha^2}{\lambda+2\mu/d}\|e_p^i\|_Z^2.$$

By applying the theorem's hypothesis $\gamma L=\omega\frac{\alpha^2}{\lambda+2\mu/d}\geq\frac{\alpha^2}{\lambda+2\mu/d}$, i.e., $\omega\geq 1$, we have

$$\left(\frac{1}{2}\frac{\eta^2}{1+2\theta}\frac{\gamma}{\omega}+\frac{\gamma}{2}\right)\|e_p^i\|^2+\left((1-\frac{\epsilon^2C_2}{4\omega\theta})\gamma-\frac{|1-\gamma|}{2}\right)\|e_p^i\|_Z^2\leq\frac{\gamma}{2}\|e_p^{i-1}\|^2+\frac{|1-\gamma|}{2}\|e_p^{i-1}\|_Z^2.$$

Finally, in order to guarantee the convergence, we require that,

$$(1-\frac{\epsilon^2C_2}{4\omega\theta})\gamma-\frac{|1-\gamma|}{2}\geq\frac{|1-\gamma|}{2}\Longrightarrow\theta\geq\frac{\epsilon^2C_2\gamma}{4\omega(\gamma-|1-\gamma|)}.$$

Next, we try to find $\theta=\theta^*\geq\frac{\epsilon^2C_2\gamma}{4\omega(\gamma-|1-\gamma|)}$ such that

$$\frac{(1-\frac{\epsilon^2C_2}{4\omega\theta})\gamma-\frac{|1-\gamma|}{2}}{\frac{1}{2}\frac{\eta^2}{1+2\theta}\frac{\gamma}{\omega}+\frac{\gamma}{2}}=\frac{|1-\gamma|}{\gamma}.$$

Direct calculations show that $\theta^*\geq\frac{\epsilon^2C_2\gamma}{4\omega(\gamma-|1-\gamma|)}$ should be the positive root of the quadratic equation (38). Since $\frac{2(\gamma-|1-\gamma|)}{\gamma}>0$ for $\gamma\in(\frac{2}{3},2]$, the existence of $\theta^*$ is verified by the positiveness of the discriminant, and the fact that $q_2(\frac{\epsilon^2C_2\gamma}{4\omega(\gamma-|1-\gamma|)})\leq 0$. Therefore, we have

$$\left(\frac{\eta^2\gamma}{2\omega(1+2\theta^*)}+\frac{\gamma}{2}\right)\left(\|e_p^i\|^2+\frac{|1-\gamma|}{\gamma}\|e_p^i\|_Z^2\right)\leq\frac{\gamma}{2}\left(\|e_p^i\|^2+\frac{|1-\gamma|}{\gamma}\|e_p^{i-1}\|_Z^2\right),$$

from where we can derive result (37) in the theorem and then complete the proof. □

Summarizing, we have demonstrated the convergence of the iterative method (34)-(35) for a set of values of parameter $\gamma$, in particular for any parameter $\gamma\in(2/3,2]$ such that $\gamma L$ is big enough. It is important to notice that the constants arising within the error estimates are independent of the physical and discretization parameters, what makes the proposed iterative scheme a parameter-robust solver.

From the values of $\gamma$ satisfying the convergence property in Theorem 4.1, however, we want

to choose one that improves the convergence of the initially derived algorithm (32)-(33). In order to do that, we deeply analyze the application of the iterative algorithm to the one-dimensional Terzaghi problem in (24). With this purpose, we consider the reduction of the norm of the residual below $10^{-8}$ as the stopping criterion and we analyze the number of iterations needed for convergence of the proposed scheme for different values of parameter $\gamma$. For illustrative purposes and without restricting the generality of the analysis, we prescribe the following values for the physical parameters of the problem as follows: the hydraulic conductivity is $K = 10^{-10}$, $\lambda + 2\mu = 1$, $\alpha = 1$, and the mesh size is chosen as $h = 1/32$. Notice that hese values are representative and do not affect the generality of the conclusions. Then, in Figure 5, we display the number of iterations needed for convergence when the proposed iterative coupling scheme is used for solving Terzaghi problem with the stabilized P1-P1 discretization derived in (25)-(26), for different values of parameter $\gamma$. It is observed that only two iterations are needed when $\gamma = 2/3$,

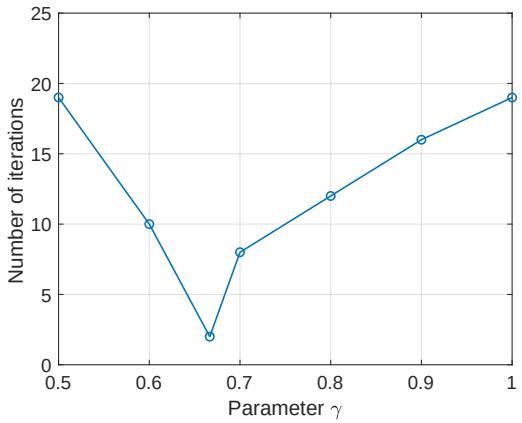


Figure 5: Number of iterations of the iterative coupling method for different values of $\gamma$, when the stabilized P1-P1 discretization of Terzaghi's problem is considered.

which seems to be the optimal value, since other values of $\gamma$ provide a higher number of iterations. Next, based on this numerical insights, we derive and rigorously prove the following result for the one-dimensional case we are dealing with.

**Theorem 4.2.** *Iterative method* (34)-(35) *with parameter* $\gamma = \dfrac{2}{3}$ *converges in two iterations for the stabilized P1-P1 discretization of Terzaghi's problem.*

*Proof.* From the block form of the fully-discrete stabilized scheme given in (28), we can write

the matrix block form including parameter $\gamma$ as follows:

$$\mathcal{A}_{stab} = \begin{pmatrix} A & G \\ D & \tau A_p + \beta^{-1} M + L(M_l - M) \end{pmatrix} = \begin{pmatrix} A & G \\ D & \underbrace{\tau A_p + \beta^{-1} M + \gamma L M_l - LM - (\gamma - 1) L M_l}_{C} \end{pmatrix}$$

Considering the one dimensional Terzaghi problem makes that we can explicitly calculate the Schur complement, $S_p$, for the considered stabilized P1-P1 discretization. In particular, it is easily derived that

$$S_p - C = -DA^{-1}G = \frac{\alpha^2}{\lambda + 2\mu}(\frac{3}{2}M - \frac{1}{2}M_l) = \underbrace{\frac{3\alpha^2}{2(\lambda + 2\mu)}}_{L} M + \underbrace{\left(-\frac{1}{2}\frac{\alpha^2}{\lambda + 2\mu}\right)}_{(\gamma-1)L} M_l = LM + (\gamma - 1) L M_l,$$

where in the last equality we have used that $L = \dfrac{3\alpha^2}{2(\lambda + 2\mu)}$ and $\gamma = \dfrac{2}{3}$. By using the equality that we just obtained, we can write the splitting corresponding to the iterative method (34)-(35) given in (36) in the following way:

$$\begin{aligned} \mathcal{A}_{stab} &= \begin{pmatrix} A & G \\ 0 & \tau A_p + \beta^{-1} M + \gamma L M_l \end{pmatrix} - \begin{pmatrix} 0 & 0 \\ -D & LM + (\gamma - 1) L M_l \end{pmatrix} \\ &= \begin{pmatrix} A & G \\ D & C \end{pmatrix} = \begin{pmatrix} A & G \\ 0 & S_p \end{pmatrix} - \begin{pmatrix} 0 & 0 \\ -D & S_p - C \end{pmatrix}, \end{aligned} \tag{42}$$

If considering the iteration matrix $\mathcal{S}$ corresponding to splitting (42), that is.,

$$\mathcal{S} = \mathcal{I} - \mathcal{B}\mathcal{A}_{stab}, \text{ where } \mathcal{B} = \begin{pmatrix} A & G \\ 0 & S_p \end{pmatrix}^{-1},$$

we can write that

$$\begin{aligned} \mathcal{S}^2 &= (\mathcal{I} - \mathcal{B}\mathcal{A}_{stab})(\mathcal{I} - \mathcal{B}\mathcal{A}_{stab}) = \mathcal{B}(\mathcal{I} - \mathcal{A}_{stab}\mathcal{B})(\mathcal{I} - \mathcal{A}_{stab}\mathcal{B})\mathcal{B}^{-1} \\ &= \mathcal{B}(\mathcal{I} - \mathcal{A}_{stab}\mathcal{B})^2\mathcal{B}^{-1}. \end{aligned} \tag{43}$$

We now consider the block-$\mathcal{LU}$ factorization of $\mathcal{A}_{stab}$, i.e.,

$$\mathcal{A}_{stab} = \begin{pmatrix} A & G \\ D & C \end{pmatrix} = \begin{pmatrix} I & 0 \\ DA^{-1} & I \end{pmatrix} \begin{pmatrix} A & G \\ 0 & S_p \end{pmatrix} =: \mathcal{LU}.$$

Since $\mathcal{B} = \mathcal{U}^{-1}$, then $\mathcal{I} - \mathcal{A}_{stab}\mathcal{B} = \mathcal{I} - \mathcal{LUU}^{-1} = \mathcal{I} - \mathcal{L} = \begin{pmatrix} 0 & 0 \\ -DA^{-1} & 0 \end{pmatrix}$. This implies that $(\mathcal{I} - \mathcal{A}_{stab}\mathcal{B})^2 = 0$ and, consequently, from (43) we obtain that $\mathcal{S}^2 = 0$, what means that the iterative coupling scheme converges in only two iterations. □

Summarizing, we have seen that the proposed iterative coupling method (34)-(35) is optimal in the one-dimensional case when $\gamma = 2/3$ is assumed, since only two iterations are enough for the solution of the complex coupled Biot's problem. The question now is how it behaves for higher dimensional problems. In order to analyze that, we consider here the two-dimensional benchmark problem of Barry & Mercer which has been previously introduced in Example 3.1.3. An example of application for a three-dimensional problem was also studied in [62].

### 4.1.1 Numerical experiment. Barry & Mercer problem

In order to apply the proposed iterative coupling method in higher dimensions, we fix the value of parameter $\gamma$ which was demonstrated to be optimal in the one-dimensional case. Of course, this does not mean that it is optimal for the two-dimensional case, but we will show that this choice provides almost optimal results in all the tests carried out.

In order to numerically illustrate the suitability of the choice of $\gamma$, we consider two different test cases with different values of the Poisson ratio $\nu$ and hydraulic conductivity $K$ and different grid sizes, and we analyze the number of iterations of the proposed scheme for different values of parameter $\gamma$. This can be observed in Figure 6, where we fix $h = 1/32$ and consider two values of hydraulic conductivity: $K = 10^{-10}$ and $K = 10^{-2}$, and two values for the Poisson ratio $\nu = 0.2$ and $\nu = 0.4$. We observe from the figures that the choice of $\gamma$ has little influence when $K$ is large, whereas for small values of $K$ selecting an appropriate value of parameter $\gamma$ becomes crucial. Moreover, unlike in the one-dimensional setting, here the choice of $\gamma = 2/3$ is not optimal for both values of $\nu$: it performs optimally for $\nu = 0.4$ but not for $\nu = 0.2$. Nevertheless, choosing $\gamma = 2/3$ still yields very good, almost optimal, results in both cases, as illustrated in the two pictures.

Next, we analyze the parameter-robustness of the proposed iterative coupling algorithm (34)-(35). With this purpose, in Table 1, we show the number of iterations of the method for

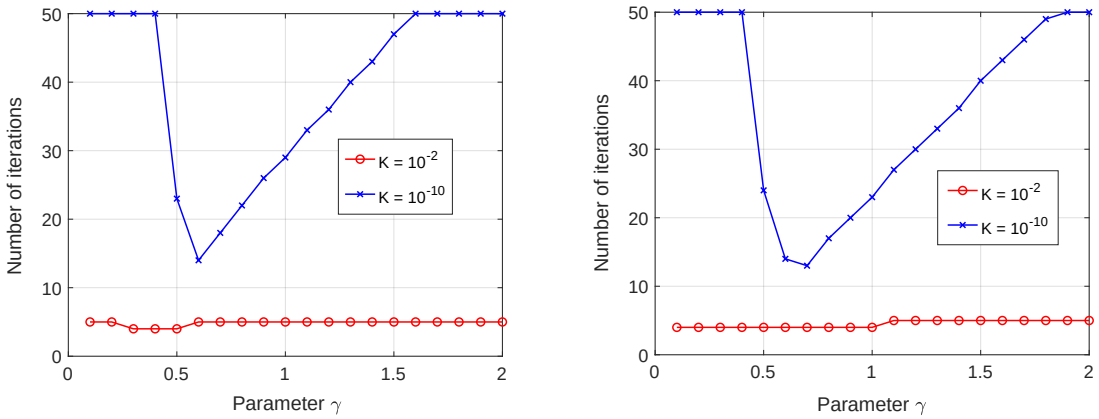


(a) $\nu = 0.2$ (b) $\nu = 0.4$

Figure 6: Number of iterations of the iterative coupling scheme for different values of $\gamma$ for the Barry & Mercer's problem.

several values of the hydraulic conductivity $K$ and the mesh size $h$. The stopping criterion considered to obtain the results is fixed as $\|\delta p^{n,i}\| + \|\delta \mathbf{u}^{n,i}\| \leq 10^{-8}$ where $\delta p_h^{n,i} = p_h^{n,i} - p_h^{n,i-1}$ and $\delta \mathbf{u}_h^{n,i} = \mathbf{u}_h^{n,i} - \mathbf{u}_h^{n,i-1}$ denote the difference between two successive approximations for displacements and for pressure, respectively. From the table, we can observe that the number of iterations stays relatively stable for all the different values of $K$ and $h$.

| $K$ | $h = 1/16$ | $h = 1/32$ | $h = 1/64$ | $h = 1/128$ |
|---|---|---|---|---|
| $10^{-2}$ | 4 | 4 | 4 | 4 |
| $10^{-4}$ | 6 | 6 | 6 | 6 |
| $10^{-6}$ | 11 | 11 | 11 | 11 |
| $10^{-8}$ | 15 | 15 | 15 | 15 |
| $10^{-10}$ | 11 | 11 | 12 | 12 |
| $10^{-12}$ | 6 | 7 | 7 | 8 |

Table 1: Number of iterations of Algorithm (34)-(35) with $\gamma = 2/3$, considering $E = 10^5$, $\nu = 0.4$, different mesh sizes $h$ and different values of the hydraulic conductivity $K$.

We repeat the same numerical test but fixing the value of the hydraulic conductivity to $K = 10^{-10}$ and varying the value of the Poisson ratio in a range from 0.1 to 0.49. Different grid sizes are considered again and the number of iterations of algorithm (34)-(35) is shown in Table 2. Again, the method shows a robust performance with respect to the considered parameters.

| $\nu$ | $h = 1/16$ | $h = 1/32$ | $h = 1/64$ | $h = 1/128$ |
|---|---|---|---|---|
| 0.1 | 18 | 20 | 21 | 22 |
| 0.2 | 16 | 17 | 18 | 19 |
| 0.3 | 13 | 14 | 15 | 16 |
| 0.4 | 11 | 11 | 12 | 12 |
| 0.49 | 12 | 11 | 9 | 8 |

Table 2: Number of iterations of Algorithm (34)-(35) with $\gamma = 2/3$, considering $E = 10^5$, $K = 10^{-10}$, different mesh sizes $h$ and different values of Poisson ratio $\nu$.

**Remark 4.3** (More general fluid regimes)**.** *In a more general case in which the storage coefficient $\beta^{-1}$ is not close to zero, it is not possible to find a parameter $\gamma$ in* (36) *that provides an optimal iterative coupling method that converges in two iterations for the one-dimensional Terzaghi problem. We can include, however, a second parameter into the iterative coupling method in order to obtain similar results to the presented in the previous case. We then consider two parameters $\gamma_1, \gamma_2 > 0$, and if $\boldsymbol{u}_h^{n,0} = \boldsymbol{u}_h^{n-1}$ and $p_h^{n,0} = p_h^{n-1}$ are the initial guesses of the iterative scheme at time $t_n$, the new improved algorithm provides a sequence of approximations $(\boldsymbol{u}_h^{n,i}, p_h^{n,i}), i \geq 1$ as follows:*

**Step 1:** *Given $(\boldsymbol{u}_h^{n,i-1}, p_h^{n,i-1}) \in \boldsymbol{V}_h \times Q_h$, find $p_h^{n,i} \in Q_h$ such that:*

$$\begin{aligned}\frac{1}{\beta}\left(\frac{p_h^{n,i}-p_h^{n-1}}{\tau}, q_h\right) + \gamma_1 L\left(\frac{p_h^{n,i}-p_h^{n-1}}{\tau}, q_h\right)_0 - \gamma_2 L\left(\frac{p_h^{n,i}-p_h^{n-1}}{\tau}, q_h\right) + a_p(p_h^{n,i}, q_h) = \\ +(1-\gamma_2)L\left(\frac{p_h^{n,i-1}-p_h^{n-1}}{\tau}, q_h\right) + (\gamma_1 - 1)L\left(\frac{p_h^{n,i-1}-p_h^{n-1}}{\tau}, q_h\right)_0 \\ -\alpha\left(\operatorname{div}\frac{\boldsymbol{u}_h^{n,i-1}-\boldsymbol{u}_h^{n-1}}{\tau}, q_h\right) + (g_h^n, q_h), \quad \forall\, q_h \in Q_h, \end{aligned} \tag{44}$$

**Step 2:** *Given $p_h^{n,i} \in Q_h$, find $\boldsymbol{u}_h^{n,i} \in \boldsymbol{V}_h$ such that*

$$a(\boldsymbol{u}_h^{n,i}, \boldsymbol{v}_h) = \alpha(p_h^{n,i}, \operatorname{div} \boldsymbol{v}_h) + (\boldsymbol{f}_h^n, \boldsymbol{v}_h), \quad \forall\, \boldsymbol{v}_h \in \boldsymbol{V}_h. \tag{45}$$

*Similarly as previously done in Theorem 4.1, we can prove the convergence of the iterative coupling method* (44) -(45)*, which results to be robust with respect to the physical and discretization parameters of the problem.*

**Theorem 4.4.** *The iterative method given in* (44)-(45) *is convergent for any parameters* $\gamma_1 \in (2/3, 2]$, $\gamma_1 > \gamma_2 \geq 0$, *such that* $(\gamma_1 - \gamma_2)L = \omega \frac{\alpha^2}{(\lambda+2\mu/d)} \geq \frac{\alpha^2}{(\lambda+2\mu/d)}$, *i.e.,* $\omega \geq 1$. *Additionally,*

$$\|e_p^i\|^2 + \frac{|1-\gamma_1|}{\gamma_1-\gamma_2}\|e_p^i\|_Z^2 \leq \frac{1}{1+\frac{\eta^2}{\omega(1+2\theta^*)}}\left(\|e_p^{i-1}\|^2 + \frac{|1-\gamma_1|}{\gamma_1-\gamma_2}\|e_p^{i-1}\|_Z^2\right), \tag{46}$$

*where* $\theta^* \geq \frac{\epsilon^2 C_2 \gamma_1}{4\omega(\gamma_1-|1-\gamma_1|)}$ *is a root of the quadratic equation* (38) *(with* $\gamma$ *replaced by* $\gamma_1$*). Here,* $\eta > 0$ *is the constant appearing in the weak inf-sup condition* (31) *and* $C_2$ *is the constant for the upper bound of the spectral equivalence condition* (29).

*Finally, in order to optimize the convergence of algorithm* (44)-(45)*, we can analyze the one-dimensional problem to obtain the optimal values for* $\gamma_1$ *and* $\gamma_2$.

**Theorem 4.5.** *Iterative method* (44)-(45) *with parameters* $\gamma_1 = 1 - \dfrac{1}{2L(\lambda+2\mu)}$, *and* $\gamma_2 = 1 - \dfrac{3}{2L(\lambda+2\mu)}$, *with* $L$ *as in* (27) *converges in two iterations for the stabilized P1-P1 discretization of Terzaghi's problem.*

*The proofs of Theorems 4.4 and 4.5 can be found in [62], as well as more details for this general case.*

### *4.2 Non-iterative coupling method*

The explicit coupling approach considered here is based on the idea behind the so-called explicit fixed-stress split scheme, which is widely used in practice (see for example [54, 25, 24] and the references therein). In such a decoupled method, the flow problem (12) is solved first with time-lagging the displacement term followed by the mechanic problem (11). As well as in the iterative coupling fixed-stress split method, a stabilization term should be added in the flow equation for convergence reasons. Here, by considering the stabilized scheme in (25)-(26), we can construct a similar decoupled algorithm avoiding the need to add a different parameter to stabilize the solution algorithm. We want to emphasize that the proposed non-iterative coupling method for the stabilized P1-P1 discretization provides one of the simplest numerical scheme for addressing the coupled multiphysics Biot's problem.

In order to define the explicit coupling algorithm, we must slightly change the time-discretization of the stabilized problem. In particular, we now consider the backward Euler method to discretize the terms corresponding to $\dfrac{1}{\beta}(\partial_t p_h, q_h)$ and $L(\partial_t p_h, q_h)_0$ and a forward Euler method for the

terms $L(\partial_t p_h, q_h)$ and $\alpha(\operatorname{div} \partial_t \boldsymbol{u}_h, q_h)$. More concretely, if we again consider a uniform partition of the time interval $(0, T_f]$, $t_n = n\tau$, $n = 0, \ldots, N$, with time-step $\tau = T_f/N$, and let $(\boldsymbol{u}_h^n, p_h^n)$ be the approximation of $(\boldsymbol{u}_h(t), p_h(t))$ at time level $t_n$, we can write the fully discrete stabilized scheme as follows:

$$a(\boldsymbol{u}_h^{n+1}, \boldsymbol{v}_h) - \alpha(p_h^{n+1}, \operatorname{div} \boldsymbol{v}_h) = (\boldsymbol{f}_h^{n+1}, \boldsymbol{v}_h), \quad \forall \boldsymbol{v}_h \in \boldsymbol{V}_h, \tag{47}$$

$$\begin{aligned} &\frac{1}{\beta}(\bar{\partial}_t^f p_h^n, q_h) + \alpha(\operatorname{div} \bar{\partial}_t^b \boldsymbol{u}_h^n, q_h) + a_p(p_h^{n+1}, q_h) + L(\bar{\partial}_t^f p_h^n, q_h)_0 - L(\bar{\partial}_t^b p_h^n, q_h) \\ &\quad = (g_h^{n+1}, q_h), \forall q_h \in Q_h, \end{aligned} \tag{48}$$

where $\bar{\partial}_t^f p_h^n := (p_h^{n+1} - p_h^n)/\tau$, $\bar{\partial}_t^b p_h^n := (p_h^n - p_h^{n-1})/\tau$ and $\bar{\partial}_t^b \boldsymbol{u}_h^n := (\boldsymbol{u}_h^n - \boldsymbol{u}_h^{n-1})/\tau$.

Notice that the resulting fully discrete problem is an explicit coupling approach in which on each time level the flow problem is solved first followed for the mechanic problem, and therefore, there is no coupling between both problems anymore, as shown in the following algorithm:

**For** $n = 1, 2, \ldots, N-1$

**Step 1:** Given $(\boldsymbol{u}_h^n, \boldsymbol{u}_h^{n-1}, p_h^n, p_h^{n-1}) \in \boldsymbol{V}_h \times \boldsymbol{V}_h \times Q_h \times Q_h$, find $p_h^{n+1} \in Q_h$ such that:

$$\begin{aligned} &\frac{1}{\beta}\left(\frac{p_h^{n+1} - p_h^n}{\tau}, q_h\right) + L\left(\frac{p_h^{n+1} - p_h^n}{\tau}, q_h\right)_0 + a_p(p_h^{n+1}, q_h) = -\alpha\left(\operatorname{div} \frac{\boldsymbol{u}_h^n - \boldsymbol{u}_h^{n-1}}{\tau}, q_h\right) + \\ &\qquad + L\left(\frac{p_h^n - p_h^{n-1}}{\tau}, q_h\right) + (g_h^{n+1}, q_h), \quad \forall\, q_h \in Q_h, \end{aligned} \tag{49}$$

**Step 2:** Given $p_h^{n+1} \in Q_h$, find $\boldsymbol{u}_h^{n+1} \in \boldsymbol{V}_h$ such that

$$a(\boldsymbol{u}_h^{n+1}, \boldsymbol{v}_h) = \alpha(p_h^{n+1}, \operatorname{div} \boldsymbol{v}_h) + (\boldsymbol{f}_h^{n+1}, \boldsymbol{v}_h), \quad \forall\, \boldsymbol{v}_h \in \boldsymbol{V}_h. \tag{50}$$

Regarding the initial conditions to apply algorithm (49)-(50), previously we need to obtain $p_h^1$, and therefore a fully implicit scheme is used to obtain the solution at the first time level $(\boldsymbol{u}_h^1, p_h^1)$.

In particular, the following problem is solved:

$$a(\boldsymbol{u}_h^1, \boldsymbol{v}_h) - \alpha(p_h^1, \operatorname{div} \boldsymbol{v}_h) = (\boldsymbol{f}_h^1, \boldsymbol{v}_h), \quad \forall\, \boldsymbol{v}_h \in \boldsymbol{V}_h, \tag{51}$$

$$\frac{1}{\beta}\left(\frac{p_h^1 - p_h^0}{\tau}, q_h\right) + L\left(\frac{p_h^1 - p_h^0}{\tau}, q_h\right)_0 + \alpha\left(\operatorname{div}\frac{\boldsymbol{u}_h^1 - \boldsymbol{u}_h^0}{\tau}, q_h\right) + a_p(p_h^1, q_h)$$

$$-L\left(\frac{p_h^1 - p_h^0}{\tau}, q_h\right) = (g_h^1, q_h), \ \forall\, q_h \in Q_h. \tag{52}$$

Next, we demonstrate that the explicit coupling scheme (49)-(50) is optimally convergent. Let us define the errors at $t = t_n$ as follows $e_{\boldsymbol{u}}^n = \boldsymbol{u}(t_n) - \boldsymbol{u}_h^n$ and $e_p^n = p(t_n) - p_h^n$.

**Theorem 4.6.** *Let $\boldsymbol{u}(t)$ and $p(t)$ be the solutions of* (17) *and* (18)*, and $\boldsymbol{u}_h^n$ and $p_h^n$ be the solutions obtained by Algorithm* (49)-(50)*. If $L = \omega\frac{\alpha^2}{\lambda+2\mu/d}$, $\omega \geq 1$, then the following error estimates hold,*

$$\begin{aligned}
&\|\boldsymbol{u}(t_n) - \boldsymbol{u}_h^n\|_A + \|p(t_n) - p_h^n\| \\
&\leq C\left(\|e_{\boldsymbol{u}}^0\|_A + \|e_p^0\|_{A_p}\right) + Ch\left(|u(t_0)|_2 + |p(t_0)|_1 + |p(t_0)|_2 + |u(t_n)|_2 + |p(t_n)|_1\right) \\
&\quad + C\tau\left[\left(\int_{t_0}^{t_{n+1}} \|\partial_{tt} p(s)\|^2 \,\mathrm{d}s\right)^{\frac{1}{2}} + \left(\int_{t_0}^{t_{n+1}} \|\partial_{tt}\boldsymbol{u}(s)\|_1^2 \,\mathrm{d}s\right)^{\frac{1}{2}}\right] \\
&\quad + Ch\left[\left(\int_{t_0}^{t_{n+1}} h^2|\partial_t p(s)|_2^2 \,\mathrm{d}s\right)^{\frac{1}{2}} + \left(\int_{t_0}^{t_{n+1}} |\partial_t \boldsymbol{u}|_2^2 + |\partial_t p|_1^2 \,\mathrm{d}s\right)^{\frac{1}{2}} + \left(\tau\sum_{j=1}^{n} |\partial_t p(t_{j+1})|_1^2\right)^{\frac{1}{2}}\right] \\
&\quad + Ch\tau\left(\int_{t_0}^{t_{n+1}} |\partial_{tt} p(s)|_1^2 \mathrm{d}s\right)^{\frac{1}{2}}.
\end{aligned} \tag{53}$$

*Proof.* Because of the technical and lengthy nature of the proof, we do not include it here. A detailed proof is provided in [40]. □

### 4.2.1 Numerical experiment. 2D problem with a manufactured solution

Now, we present some numerical results in two-dimensions to validate our theoretical estimates. We consider the unit square as domain, i.e. $\Omega = (0,1) \times (0,1) \subset \mathbb{R}^2$, and we take the source terms, initial and Dirichlet boundary conditions such that the exact solution of problem (11)-(12) is as follows:

$$u(x, y, t) = v(x, y, t) = p(x, y, t) = t^3 \sin(\pi x)\, \sin(\pi y), \tag{54}$$

The following physical parameters are considered: $\lambda = 1, \mu = 2, \alpha = 1, \beta = 100, K = 1$, and a final time of $T_f = 1$ is fixed. Then, we apply the non-iterative coupling algorithm (49)-(50) to solve the stabilized P1-P1 discrete scheme of Biot's model.

We compute the errors between the exact solution and the numerical solution of the pressure obtained by applying algorithm (49)-(50), i.e. $\|u - u_h^{dec}\|_\infty$, and also we compute the corresponding errors when the problem is solved with a fully-implicit method (or an iterative coupling scheme, since the numerical solution is the same) i.e. $\|u - u_h^{fully}\|_\infty$, for comparison. Such errors are calculated in the maximum norm, and are shown in Table 3, where also the convergence rates in the case of the errors for the decoupled scheme are displayed. We observe that by refining the time step $\tau$ and mesh size $h$ appropriately, the errors decrease with a rate of approximately 2, indicating first order of convergence, as expected from the theoretical analysis. Moreover, the obtained errors with the fully-implicit method and the explicit coupling algorithm are both small with similar order of magnitude.

| $h$ | $\tau$ | $\|u - u_h^{fully}\|_\infty$ | $\|u - u_h^{dec}\|_\infty$ | rate |
|---|---|---|---|---|
| $1/100$ | $1/40$ | $2.7646e-03$ | $7.7593e-03$ | |
| $1/200$ | $1/80$ | $1.2669e-03$ | $3.8973e-03$ | 1.99 |
| $1/400$ | $1/160$ | $6.0461e-04$ | $1.9528e-03$ | 1.99 |
| $1/800$ | $1/320$ | $2.9508e-04$ | $9.7740e-04$ | 2.00 |

Table 3: Errors in maximum norm between the exact solution and the numerical solution obtained from the explicit coupling algorithm (49)-(50) $\|u - u_h^{dec}\|_\infty$ and also from the application of a fully-implicit method $\|u - u_h^{fully}\|_\infty$, together with the corresponding convergence rate for the first case, for different values of the time and spatial discretization parameters $\tau$ and $h$, respectively.

## 5 Conclusions

In this work, we have addressed the two central challenges arising in the numerical simulation of Biot's model: the design of a stable discretization strategy capable of producing solutions free from nonphysical oscillations, and the development of an efficient and robust solver for the resulting large linear systems. To this end, we proposed a novel stabilization technique that offers several advantages over existing approaches. First, the method does not depend on the mesh size $h$ or on any other discretization parameters. Second, it is derived for arbitrary values of the storage coefficient, ensuring broad applicability. Third, the particular structure of the stabilization naturally leads to coupling schemes between the fluid and mechanics subproblems (iterative and

non-iterative) that converge without requiring any additional stabilization terms. As a consequence, we obtain parameter-robust decoupled solvers for the fully coupled system. Furthermore, the proposed iterative coupling algorithm can be tuned to achieve optimal convergence behavior in one-dimensional settings and nearly optimal performance in two and three dimensions. The combination of the stabilized finite element scheme, based on simple piecewise linear functions for both displacement and pressure variables, and the resulting decoupled solvers thus provides a simple, efficient, practical and reliable computational framework for the simulation of Biot's model.

## Acknowledgments

I would like to thank all the members of 'Real Academia de Ciencias Exactas, Físicas, Químicas y Naturales de Zaragoza', specially the members of the 'Sección de Exactas' for nominating me for the Academy award. It is a great honor for me to receive such a great distinction. I would also like to thank Prof. Francisco J. Gaspar and Prof. Francisco J. Lisbona for introducing me to the Biot's model and the fascinating world of poromechanics and for their support along my whole research career. Last but not least, I would like to thank my collaborators that contributed to the results presented in this work: Francisco J. Gaspar and Álvaro Pé de la Riva (University of Zaragoza), Xiaozhe Hu and James Adler (Tufts University, USA) and Ludmil Zikatanov (The Pennsylvania State University, USA). This work is partially supported by the Diputación General de Aragón, Spain (Grupo de referencia APEDIF, ref. E24_23R) and by the Spanish Grant PID2022-140108NB-I00 funded by MCIN/AEI/10.13039/501100011033 and by "ERDF A way of making Europe", and by the "European Union NextGenerationEU/PRTR".

## References

[1] Y. Abousleiman, A. H.-D. Cheng, L. Cui, E. Detournay, and J.-C. Roegiers. Mandel's problem revisited. *Géotechnique*, 46(2):187–195, 1996.

[2] J. H. Adler, F. J. Gaspar, X. Hu, P. Ohm, C. Rodrigo, and L. T. Zikatanov. Robust preconditioners for a new stabilized discretization of the poroelastic equations. *SIAM Journal on Scientific Computing*, 42(3):B761–B791, 2020.

[3] James H. Adler, Francisco J. Gaspar, Xiaozhe Hu, Carmen Rodrigo, and Ludmil T. Zikatanov. Robust block preconditioners for Biot's model. In Petter E. Bjørstad, Susanne C. Brenner, Lawrence Halpern, Hyea Hyun Kim, Ralf Kornhuber, Talal Rahman, and Olof B. Widlund, editors, *Domain*

*Decomposition Methods in Science and Engineering XXIV*, pages 3–16, Cham, 2018. Springer International Publishing.

[4] James H. Adler, Yunhui He, Xiaozhe Hu, Scott MacLachlan, and Peter Ohm. Monolithic multigrid for a reduced-quadrature discretization of poroelasticity. *SIAM Journal on Scientific Computing*, 45(3):S54–S81, 2023.

[5] G. Aguilar, F. Gaspar, F. Lisbona, and C. Rodrigo. Numerical stabilization of Biot's consolidation model by a perturbation on the flow equation. *International Journal for Numerical Methods in Engineering*, 75(11):1282–1300, 2008.

[6] T. Almani, K. Kumar, G. Singh, and M.F. Wheeler. Stability of multirate explicit coupling of geomechanics with flow in a poroelastic medium. *Computers & Mathematics with Applications*, 78(8):2682–2699, 2019.

[7] D.N. Arnold, F. Brezzi, and M. Fortin. A stable finite element for the Stokes equations. *Calcolo*, 21(4):337–344, 1985.

[8] Khalid Aziz and Antonín Settari. *Petroleum Reservoir Simulation*. Society of Petroleum Engineers, 1979.

[9] S. I. Barry and G. N. Mercer. Exact solutions for two-dimensional time-dependent flow and deformation within a poroelastic medium. *Journal of Applied Mechanics*, 66(2):536–540, 10 1999.

[10] Mario Bebendorf. A note on the Poincaré inequality for convex domains. *Zeitschrift für Analysis und ihre Anwendungen*, 22(4):751–756, 2003.

[11] F. Ben-Hatira, K. Saidane, and A. Mrabet. A finite element modeling of the human lumbar unit including the spinal cord. *Journal of Biomedical Science and Engineering*, 5:146–152, 2012.

[12] Luca Bergamaschi, Massimiliano Ferronato, and Giuseppe Gambolati. Novel preconditioners for the iterative solution to FE-discretized coupled consolidation equations. *Computer Methods in Applied Mechanics and Engineering*, 196(25):2647–2656, 2007.

[13] Lorenz Berger, Rafel Bordas, David Kay, and Simon Tavener. Stabilized lowest-order finite element approximation for linear three-field poroelasticity. *SIAM Journal on Scientific Computing*, 37(5):A2222–A2245, 2015.

[14] Maurice A. Biot. General theory of three-dimensional consolidation. *Journal of Applied Physics*, 12(2):155–164, 1941.

[15] Maurice A. Biot. Theory of elasticity and consolidation for a porous anisotropic solid. *Journal of Applied Physics*, 26(2):182–185, 1955.

[16] Manuel Borregales, Kundan Kumar, Florin Adrian Radu, Carmen Rodrigo, and Francisco José Gaspar. A partially parallel-in-time fixed-stress splitting method for Biot's consolidation model. *Computers & Mathematics with Applications*, 77(6):1466 – 1478, 2019. 7th International Conference on Advanced Computational Methods in Engineering (ACOMEN 2017).

[17] Jakub Wiktor Both, Manuel Borregales, Jan Martin Nordbotten, Kundan Kumar, and Florin Adrian Radu. Robust fixed stress splitting for Biot's equations in heterogeneous media. *Applied Mathematics Letters*, 68:101 – 108, 2017.

[18] Trygve Bærland, Jeonghun J. Lee, Kent-Andre Mardal, and Ragnar Winther. Weakly imposed symmetry and robust preconditioners for Biot's consolidation model. *Computational Methods in Applied Mathematics*, 17(3):377–396, 2017.

[19] Mingchao Cai, Huipeng Gu, Jingzhi Li, and Mo Mu. Some optimally convergent algorithms for decoupling the computation of Biot's model. *Journal of Scientific Computing*, 97(2):48, 2023.

[20] N. Castelletto, J. A. White, and H. A. Tchelepi. Accuracy and convergence properties of the fixed-stress iterative solution of two-way coupled poromechanics. *International Journal for Numerical and Analytical Methods in Geomechanics*, 39(14):1593–1618, 2015.

[21] Nabil Chaabane and Béatrice Rivière. A splitting-based finite element method for the Biot poroelasticity system. *Computers & Mathematics with Applications*, 75(7):2328–2337, 2018.

[22] Shuangshuang Chen, Qingguo Hong, Jinchao Xu, and Kai Yang. Robust block preconditioners for poroelasticity. *Computer Methods in Applied Mechanics and Engineering*, 369:113229, 2020.

[23] Zhangxin Chen, Guanren Huan, and Yuanle Ma. *Computational Methods for Multiphase Flows in Porous Media*. Society for Industrial and Applied Mathematics, 2006.

[24] R. H. Dean, X. Gai, C. M. Stone, and S. E. Minkoff. A comparison of techniques for coupling porous flow and geomechanics. *SPE Journal*, 11(01):132–140, 03 2006.

[25] Dennis Denney. Coupled reservoir simulation: Management of production- induced stress sensitivity. *Journal of Petroleum Technology*, 53(04):80–81, 04 2001.

[26] M. Favino, A. Grillo, and R. Krause. A stability condition for the numerical simulation of poroelastic systems. In Christian Hellmich, Bernhard Pichler, and Dietmar Adam, editors, *Poromechanics V: Proceedings of the Fifth Biot Conference on Poromechanics*, pages 919–928, 2013.

[27] Massimiliano Ferronato, Luca Bergamaschi, and Giuseppe Gambolati. Performance and robustness of block constraint preconditioners in finite element coupled consolidation problems. *International Journal for Numerical Methods in Engineering*, 81(3):381–402, 2010.

[28] Massimiliano Ferronato, Nicola Castelletto, and Giuseppe Gambolati. A fully coupled 3-d mixed finite element model of Biot consolidation. *Journal of Computational Physics*, 229(12):4813–4830, 2010.

[29] X. Gai. *A coupled geomechanics and reservoir flow model on parallel computers*. PhD thesis, The University of Texas at Austin, Austin, Texas, 2004.

[30] X. Gai, S. Sun, M. F. Wheeler, and H. Klie. A time stepping scheme for coupled reservoir flow and geomechanics on nonmatching grids. volume SPE Annual Technical Conference and Exhibition of *SPE Annual Technical Conference and Exhibition*, pages SPE–97054–MS, October 2005.

[31] F. J. Gaspar, J. L. Gracia, F. J. Lisbona, and C. W. Oosterlee. Distributive smoothers in multigrid for problems with dominating grad-div operators. *Numer. Linear Algebra Appl.*, 15(8):661–683, 2008.

[32] F. J. Gaspar, F. J. Lisbona, C. W. Oosterlee, and R. Wienands. A systematic comparison of coupled and distributive smoothing in multigrid for the poroelasticity system. *Numerical Linear Algebra with Applications*, 11(2-3):93–113, 2004.

[33] F. J. Gaspar, F. J. Lisbona, and P. N. Vabishchevich. A finite difference analysis of Biot's consolidation model. *Appl. Numer. Math.*, 44(4):487–506, 2003.

[34] F. J. Gaspar, F. J. Lisbona, and P. N. Vabishchevich. Staggered grid discretizations for the quasi-static Biot's consolidation problem. *Appl. Numer. Math.*, 56(6):888–898, 2006.

[35] Francisco J. Gaspar and Carmen Rodrigo. On the fixed-stress split scheme as smoother in multigrid methods for coupling flow and geomechanics. *Computer Methods in Applied Mechanics and Engineering*, 326:526 – 540, 2017.

[36] Joachim Berdal Haga, Harald Osnes, and Hans Petter Langtangen. Efficient block preconditioners for the coupled equations of pressure and deformation in highly discontinuous media. *International Journal for Numerical and Analytical Methods in Geomechanics*, 35(13):1466–1482, 2011.

[37] Joachim Berdal Haga, Harald Osnes, and Hans Petter Langtangen. On the causes of pressure oscillations in low-permeable and low-compressible porous media. *International Journal for Numerical and Analytical Methods in Geomechanics*, 36(12):1507–1522, 2012.

[38] Q. Hong and J. Kraus. Parameter-robust stability of classical three-field formulation of Biot's consolidation model. *Elec. Transact. Numer. Anal.*, 48:202–226, 2018.

[39] Qingguo Hong, Johannes Kraus, Maria Lymbery, and Fadi Philo. Conservative discretizations and parameter-robust preconditioners for Biot and multiple-network flux-based poroelasticity models. *Numerical Linear Algebra with Applications*, 26(4):e2242, 2019.

[40] Xiaozhe Hu, Francisco J. Gaspar, and Carmen Rodrigo. Convergence analysis for non-iterative sequential schemes for Biot's model. *Submitted for publication*, 2025.

[41] Xiaozhe Hu, Carmen Rodrigo, Francisco J. Gaspar, and Ludmil T. Zikatanov. A nonconforming finite element method for the Biot's consolidation model in poroelasticity. *Journal of Computational and Applied Mathematics*, 310:143 – 154, 2017.

[42] J. Kim, H.A. Tchelepi, and R. Juanes. Stability and convergence of sequential methods for coupled flow and geomechanics: Drained and undrained splits. *Computer Methods in Applied Mechanics and Engineering*, 200(23):2094–2116, 2011.

[43] J. Kim, H.A. Tchelepi, and R. Juanes. Stability and convergence of sequential methods for coupled flow and geomechanics: Fixed-stress and fixed-strain splits. *Computer Methods in Applied Mechanics and Engineering*, 200(13):1591–1606, 2011.

[44] J.. Kim, H.A.. A. Tchelepi, and R.. Juanes. Stability, Accuracy, and Efficiency of Sequential Methods for Coupled Flow and Geomechanics. *SPE Journal*, 16(02):249–262, 01 2011.

[45] Johannes Korsawe and Gerhard Starke. A least-squares mixed finite element method for Biot's consolidation problem in porous media. *SIAM Journal on Numerical Analysis*, 43(1):318–339, 2005.

[46] Jeonghun J. Lee. Robust three-field finite element methods for Biot's consolidation model in poroelasticity. *BIT Numerical Mathematics*, 58:347–372, 2018.

[47] Jeonghun J. Lee, Kent-Andre Mardal, and Ragnar Winther. Parameter-robust discretization and preconditioning of Biot's consolidation model. *SIAM Journal on Scientific Computing*, 39(1):A1–A24, 2017.

[48] L. J. Lee. Unconditionally stable second order convergent partitioned methods for multiple-network poroelasticity. *arXiv preprint arXiv:1901.06078*, 2019.

[49] Sanghyun Lee and Son-Young Yi. Locking-free and locally-conservative enriched Galerkin method for poroelasticity. *Journal of Scientific Computing*, 94(1), 2023.

[50] R.W. Lewis and B.A. Schrefler. *The Finite Element Method in the Static and Dynamic Deformation and Consolidation of Porous Media*. Wiley: New York, 1998.

[51] P. Luo, C. Rodrigo, F. J. Gaspar, and C. W. Oosterlee. On an Uzawa smoother in multigrid for poroelasticity equations. *Numerical Linear Algebra with Applications*, 24(1):e2074–n/a, 2017. e2074 nla.2074.

[52] J. Mandel. Consolidation des sols (Étude mathématique)*. *Géotechnique*, 3(7):287–299, 09 1953.

[53] Andro Mikelić and Mary F. Wheeler. Convergence of iterative coupling for coupled flow and geomechanics. *Computational Geosciences*, 17(3):455–461, 2013.

[54] Susan E. Minkoff, C.Mike Stone, Steve Bryant, Malgorzata Peszynska, and Mary F. Wheeler. Coupled fluid flow and geomechanical deformation modeling. *Journal of Petroleum Science and Engineering*, 38(1):37–56, 2003.

[55] Márcio A. Murad and Abimael F. D. Loula. Improved accuracy in finite element analysis of Biot's consolidation problem. *Comput. Methods Appl. Mech. Engrg.*, 95(3):359–382, 1992.

[56] Márcio A. Murad and Abimael F. D. Loula. On stability and convergence of finite element approximations of Biot's consolidation problem. *Internat. J. Numer. Methods Engrg.*, 37(4):645–667, 1994.

[57] Márcio A. Murad, Vidar Thomée, and Abimael F. D. Loula. Asymptotic behavior of semidiscrete finite-element approximations of Biot's consolidation problem. *SIAM J. Numer. Anal.*, 33(3):1065–1083, 1996.

[58] Jan Martin Nordbotten. Cell-centered finite volume discretizations for deformable porous media. *International Journal for Numerical Methods in Engineering*, 100(6):399–418, 2014.

[59] Jan Martin Nordbotten. Finite volume hydromechanical simulation in porous media. *Water Resources Research*, 50(5):4379–4394, 2014.

[60] Jan Martin Nordbotten. Stable cell-centered finite volume discretization for Biot equations. *SIAM Journal on Numerical Analysis*, 54(2):942–968, 2016.

[61] Ricardo Oyarzúa and Ricardo Ruiz-Baier. Locking-free finite element methods for poroelasticity. *SIAM Journal on Numerical Analysis*, 54(5):2951–2973, 2016.

[62] Álvaro Pé de la Riva, Francisco J. Gaspar, Xiaozhe Hu, James H. Adler, Carmen Rodrigo, and Ludmil T. Zikatanov. Oscillation-free numerical schemes for biot's model and their iterative coupling solution. *SIAM Journal on Scientific Computing*, 47(3):A1809–A1834, 2025.

[63] Phillip Joseph Phillips and Mary F. Wheeler. A coupling of mixed and continuous Galerkin finite element methods for poroelasticity I: the continuous in time case. *Computational Geosciences*, 11(2):131 – 144, 2007.

[64] Phillip Joseph Phillips and Mary F. Wheeler. A coupling of mixed and continuous Galerkin finite element methods for poroelasticity II: the discrete-in-time case. *Computational Geosciences*, 11(2):145 – 158, 2007.

[65] Phillip Joseph Phillips and Mary F. Wheeler. A coupling of mixed and discontinuous Galerkin finite-element methods for poroelasticity. *Computational Geosciences*, 12(4):417 – 435, 2008.

[66] PhillipJoseph Phillips and MaryF. Wheeler. Overcoming the problem of locking in linear elasticity and poroelasticity: an heuristic approach. *Computational Geosciences*, 13(1):5–12, 2009.

[67] K. K. Phoon, K. C. Toh, S. H. Chan, and F. H. Lee. An efficient diagonal preconditioner for finite element solution of Biot's consolidation equations. *International Journal for Numerical Methods in Engineering*, 55(4):377–400, 2002.

[68] R. Maier R. Altmann and B. Unger. Semi-explicit discretization schemes for weakly coupled elliptic-parabolic problems. *Mathematics of Computation*, 90:1089–1118, 2021.

[69] C Rodrigo, FJ Gaspar, X Hu, and LT Zikatanov. Stability and monotonicity for some discretizations of the Biot's consolidation model. *Computer Methods in Applied Mechanics and Engineering*, 298:183–204, 2016.

[70] C. Rodrigo, X. Hu, P. Ohm, J.H. Adler, F.J. Gaspar, and L.T. Zikatanov. New stabilized discretizations for poroelasticity and the Stokes' equations. *Computer Methods in Applied Mechanics and Engineering*, 341:467–484, 2018.

[71] Carmen Rodrigo, Francisco J. Gaspar, James Adler, Xiaozhe Hu, Peter Ohm, and Ludmil Zikatanov. Parameter-robust preconditioners for Biot's model. *SeMA Journal*, 81:51–80, 2024.

[72] R.E. Showalter. Diffusion in poro-elastic media. *Journal of Mathematical Analysis and Applications*, 251(1):310–340, 2000.

[73] J.H. Smith and J.A. Humphrey. Interstitial transport and transvascular fluid exchange during infusion into brain and tumor tissue. *Microvasc Res*, 73(1):58–73, 2007.

[74] Erlend Storvik, Jakub W. Both, Kundan Kumar, Jan M. Nordbotten, and Florin A. Radu. On the optimization of the fixed-stress splitting for Biot's equations. *International Journal for Numerical Methods in Engineering*, 120(2):179–194, 2019.

[75] K.H. Støverud, M. Alnæs, H.P. Langtangen, V. Haughton, and K.A. Mardal. Poro-elastic modeling of syringomyelia - a systematic study of the effects of pia mater, central canal, median fissure, white and gray matter on pressure wave propagation and fluid movement within the cervical spinal cord. *Comput Methods Biomech Biomed Engin*, 19(6):686–698, 2016.

[76] C. Taylor and P. Hood. A numerical solution of the Navier-Stokes equations using the finite element technique. *Internat. J. Comput. & Fluids*, 1(1):73–100, 1973.

[77] Maria Tchonkova, John Peters, and Stein Sture. A new mixed finite element method for poro-elasticity. *International Journal for Numerical and Analytical Methods in Geomechanics*, 32(6):579–606, 2008.

[78] K. Terzaghi. *Theoretical Soil Mechanics*. Wiley, New York, 1943.

[79] P. A. Vermeer and A. Verruijt. An accuracy condition for consolidation by finite elements. *International Journal for Numerical and Analytical Methods in Geomechanics*, 5(1):1–14, 1981.

[80] H. F. Wang. *Theory of Linear Poroelasticity with Applications to Geomechanics and Hydrogeology*. Princeton University Press, Princeton, 2001.

[81] Jinchao Xu and Ludmil Zikatanov. A monotone finite element scheme for convection-diffusion equations. *Math. Comp.*, 68(228):1429–1446, 1999.

[82] Son-Young Yi. A coupling of nonconforming and mixed finite element methods for Biot's consolidation model. *Numerical Methods for Partial Differential Equations*, 29(5):1749–1777, 2013.

[83] Son-Young Yi. A study of two modes of locking in poroelasticity. *SIAM Journal on Numerical Analysis*, 55(4):1915–1936, 2017.

[84] Alexander Ženíšek. The existence and uniqueness theorem in Biot's consolidation theory. *Aplikace matematiky*, 29(3):194–211, 1984.

[85] Jijing Zhao, Huangxin Chen, Mingchao Cai, and Shuyu Sun. An optimally convergent parallel splitting algorithm for the multiple-network poroelasticity model. *Journal of Computational Physics*, 539:114214, 2025.

*Rev. Real Academia de Ciencias. Zaragoza.* **80:** 47–92, (2025).
ISSN: 0370-3207

# Ab-initio thermal transport calculations in single crystals and beyond: a review

Jesús Carrete

https://scholar.google.com/citations?user=6VfkdRwAAAAJ
Instituto de Nanociencia y Materiales de Aragón (INMA),
CSIC-Universidad de Zaragoza, 50009 Zaragoza,
Spain

*Premio a la Investigación de la Academia 2025. Sección de Físicas*

**Abstract**

First-principles lattice thermal transport calculations based on the Boltzmann transport equation have emerged, in the last two decades, as a powerful family of methods with high predictive power and wide applicability. This review begins with a summary of the basic ingredients of their formulation and then presents a selection of their applications. The starting point is the relatively simple case of a single crystal in the steady state and then, one by one, the complexities necessary to model realistic devices are introduced, including defects, interfaces and time-dependent processes. Among the examples discussed are nanostructures of all dimensionalities, binary superlattices and high-temperature phases. The main computational bottlenecks of these high-cost calculations, and some of the strategies devised to alleviate them, are also emphasized.

*The Boltzmann equation is so exceedingly complex that it seems hopeless to expect to generate a solution from it directly.*
[Zim1960]

## 1 Introduction.

Thermal transport is a fascinating area of study from the point of view of fundamental physics, as well as a critical practical consideration in the design of materials and devices. The concept of heat itself has had a complex historical development and is intricately linked to the second principle of thermodynamics, whose rigorous macroscopic formulation is a recent achievement [LY1999] and whose implications, validity and generalizations in the atomistic world and in connection with quantum information are a matter of intense ongoing research [DS2025]. At the same time, the tendency of areas at different temperatures to achieve balance and the concepts of good and poor thermal conductors are deeply ingrained in our intuition and connected to everyday experience, and have been harnessed by humanity since the very early stages in the development of tool use. Modern technology has only accentuated the importance of understanding and controlling thermal transport. The most paradigmatic domain where this happens is electronics: the notion of thermal throttling — automatic performance reduction to avoid overheating — is well known among consumers of personal computing hardware, thermal management is such a major concern when designing datacenters that the impact of their evaporative cooling systems on local water reserves has become a political question, and simply limiting the temperature swings in power-electronics components of electric vehicles can extend their lifetime [CXH+2023] by more than 60%. While these examples mostly involve the search for improved thermal conductors, tailored thermal insulators are equally necessary, be it to enhance the efficiency of thermoelectric energy recovery [CLM+2014] or as advanced coatings to decrease the working temperature of turbine blades.

The starting point of the modern theoretical study of heat transfer is typically taken as the work of Joseph Fourier [Fou1822], originally published in 1822. In particular, Fourier's law of heat conduction states that the heat current ($I_Q$) along a block of material suspended between a hot and a cold reservoir is proportional to the difference in temperatures ($\Delta T$) between the reservoirs:

$$I_Q = -G\Delta T. \tag{1}$$

Here, $G$ is the thermal conductance, which is both geometry- and composition- (or structure-

) dependent, and the minus sign accounts for the fact that hot and cold reservoirs act as sources and sinks, respectively. Although other mechanisms of heat transfer, like convection and radiation, also exist, this review will focus on conduction due to its singular importance for crystalline solids. A local form of the law is straightforward to formulate, expressing a generalized linear relationship between the temperature gradient ($\nabla T$) and the heat flux ($\boldsymbol{j}_Q$),

$$\boldsymbol{j}_Q = -\boldsymbol{\kappa}\nabla T, \tag{2}$$

where $\boldsymbol{\kappa}$ is the thermal conductivity, which in general is a rank-2 tensor. Fourier's law is analogous to Ohm's law of electric conduction or Fick's law of diffusion in that it expresses a phenomenological linear connection between a thermodynamic force and its corresponding flux. These relations and their connection to entropy production in nonequilibrium thermodynamics were systematically studied by Onsager in the first half of the 20th century [Ons1931]. This more systematic framework also comprises cross phenomena, of which the most important in this context fall under the umbrella of thermoelectricity, i.e., the mutual influences between electric fields ($\boldsymbol{E}$), temperature gradients, heat and electric ($\boldsymbol{j}_e$) currents, expressed by the equations:

$$\begin{aligned}\boldsymbol{j}_e &= \boldsymbol{\sigma}\boldsymbol{E} + \boldsymbol{\sigma}\boldsymbol{S}(-\nabla T)\\ \boldsymbol{j}_Q &= \boldsymbol{\sigma}\boldsymbol{\Pi}\boldsymbol{E} + \left(\boldsymbol{\kappa} + T\boldsymbol{\sigma}\boldsymbol{S}^2\right)(-\nabla T).\end{aligned}$$

The new phenomenological coefficients appearing in these equations are the electric conductivity tensor $\boldsymbol{\sigma}$, the Seebeck coefficient $\boldsymbol{S}$ and the Peltier coefficient $\boldsymbol{\Pi}$, all of them rank-2 tensors. A result of Onsager's theory is that $\boldsymbol{\Pi} = T\boldsymbol{S}$. Although some manifestations of the thermoelectric effects (Seebeck and Peltier) had been known experimentally for more than a century, Onsager's unified treatment opened the door to systematic research into more powerful thermoelectric materials. For example, the maximum performance that can be extracted from a single, homogeneous thermoelectric element operating as an electric generator between a hot and a cold reservoir can be shown to be a monotonically increasing function of its dimensionless thermoelectric figure of merit,

$$ZT = T\frac{\sigma S^2}{\kappa}, \tag{3}$$

where all the coefficients are treated as scalars corresponding to the orientation of the material in the device. This formula motivates the aforementioned search for low-$\kappa$ materials for thermoelectric applications.

Being able to predict the thermal conductivity tensor of a given material is therefore a primary objective of theoretical and computational materials science as applied to thermal transport. The key ingredient is a microscopic expression of the heat flux that can be calculated and compared with Eq. (2). The first step to achieving such an expression is identifying the mechanisms of energy transfer that may be activated by a temperature gradient. In the specific case of crystalline solids, the main contributors are generally electrons and phonons [Zim1960], although other excitations such as magnons can be relevant in certain materials [LGHC2025]. Many of the applications mentioned in this introduction — in particular, electronic devices and thermoelectric systems — are built from semiconductors, where the charge carrier contribution can be neglected up to very high temperatures, leaving phonons as the dominant heat carriers. Thermal transport by lattice vibrations, and the ab-initio characterization thereof, will be the main object of this review.

I will begin by formulating the phonon contribution to the heat current in a semiclassical setting and continue by obtaining the Boltzmann transport equation for phonons that can provide the non-equilibrium phonon populations necessary to calculate that heat current. Next I will explain how that equation can be solved and how each of the required ingredients can be obtained from ab-initio calculations. This initial explanation will focus on the case of a bulk perfect crystal in the steady state. I will then move on to more complex systems containing defects and nanostructural features, as well as to time-dependent problems. The selection of references and examples is biased towards my own contributions to the field.

## 2 Basic formulation for pristine crystalline solids.

### *2.1 The phonon heat current and the linear regime.*

Phonons, the low-energy mechanical excitations of a crystal lattice around equilibrium, are bosons that, in rigor, require a fully quantum treatment [SMM2019a]. However, a semiclas-

sical picture, derived heuristically, provides an excellent compromise to tackle problems at a variety of space and time scales. That will be, therefore, be the approach adopted here.

The starting point is a single crystal with a unit cell characterized (at equilibrium) by three linearly independent lattice vectors $(\boldsymbol{\ell}_1, \boldsymbol{\ell}_2, \boldsymbol{\ell}_3)$ and a motif of $M$ atoms placed at positions $\{\boldsymbol{r}_1 \dots \boldsymbol{r}_M\}$. Therefore, the position of an arbitrary atom of the crystal can be expressed as $\boldsymbol{r}_{\boldsymbol{I},i} = \boldsymbol{R}_{\boldsymbol{I}} + \boldsymbol{r}_i$, i.e., as the sum of a lattice vector $\boldsymbol{R}_{\boldsymbol{I}} = I_1\boldsymbol{\ell}_1 + I_2\boldsymbol{\ell}_2 + I_3\boldsymbol{\ell}_3$ for some triplet of integers $\boldsymbol{I} = (I_1, I_2, I_3) \in \mathbb{Z}^3$, and a vector from the motif. If $\boldsymbol{\mathcal{L}}$ is a matrix with the lattice vectors as columns, the columns of $\boldsymbol{\mathcal{R}} = 2\pi\boldsymbol{\mathcal{L}}^{-t}$ are the basis vectors of the reciprocal lattice, formed by all their integer linear combinations.

Each normal mode of the crystal is identified by a vector $\boldsymbol{q}$ in reciprocal space and a branch index $\boxdot \in \{1 \dots 3M\}$, which I will summarize in a compound index $\lambda \coloneqq (\boldsymbol{q}, \boxdot)$. That mode will have an angular frequency $\omega_\lambda$ and a polarization $\boldsymbol{\psi}_\lambda$ (expressed as a finite vector over a finite subset of the crystal). In the second-quantization picture, each phonon carries an energy $\hbar\omega_\lambda$ and a momentum $\hbar\boldsymbol{q}$. The discrete translation symmetry of the crystal in real space endows the functions defined in reciprocal space with periodicity, so each phonon branch $\omega_\boxdot(\boldsymbol{q})$ is completely specified by its values in the first Brillouin zone (BZ), i.e., the Voronoi polyhedron of any point from the reciprocal lattice. Phonons carry energy at a speed corresponding to their group velocity, $\boldsymbol{v}_\lambda = \frac{\mathrm{d}\omega_\lambda}{\mathrm{d}\boldsymbol{q}}$.

A crucial conceptual assumption for this simplified development is that, at each point in space — interpreted in a convenient mesoscopic sense — and for each phonon mode, a time-dependent phonon population $f_\lambda(\boldsymbol{r}, t)$ can be defined, corresponding to a volumetric phonon density $f_\lambda/V$ for a finite, but large enough, crystal sample of volume $V$. At thermal equilibrium at a temperature $T$, that corresponds to the Bose-Einstein distribution with zero chemical potential, $f_{\mathrm{BE},\lambda} = \left(e^{\frac{\hbar\omega}{k_\mathrm{B}T}} - 1\right)^{-1}$. It is convenient to define $f_{1,\lambda} = f_\lambda - f_{\mathrm{BE},\lambda}$, the nonequilibrium component of the population.

In this picture, the energy density around each $\boldsymbol{r}$ due to phonons of mode $\lambda$ is equal to $\frac{1}{V} f_\lambda \hbar\omega_\lambda$ and the associated heat flux is $\frac{1}{V} f_\lambda \hbar\omega_\lambda \boldsymbol{v}_\lambda$. The total heat flux is obtained by aggregating these contributions:

$$\boldsymbol{j}_Q = \frac{1}{V}\sum_\lambda f_\lambda \hbar\omega_\lambda \boldsymbol{v}_\lambda. \tag{4}$$

Here and in the rest of this review, the notation $\sum_\lambda$ comprises both a literal sum over phonon branches $\boxdot$ and a sum over the $\boldsymbol{q}$ allowed by the boundary conditions of the finite volume, with the latter sum approximated by an integral over the Brillouin zone:

$$\sum_\lambda \coloneqq \frac{V}{(2\pi)^3} \sum_{\boxdot=1}^{3M} \int_{\mathrm{BZ}} \mathrm{d}^3\boldsymbol{q}.$$

The equilibrium component of $f_\lambda$ obviously cannot create any current, so $f_\lambda$ can be replaced by $f_{1,\lambda}$ in Eq. (4). To obtain an expression that can be compared with Fourier's law [Eq. (2)], the next step is to assume that the only force driving phonons out of equilibrium is a thermal gradient, and to introduce a linear dependence on $\nabla T$, under the hypothesis that $f_{1,\lambda}$ is a small enough perturbation:

$$f_{1,\lambda} =: -\boldsymbol{F}_\lambda \cdot \nabla T \frac{\partial f_{\mathrm{BE},\lambda}}{\partial T} = -\boldsymbol{F}_\lambda \cdot \nabla T f_{\mathrm{BE},\lambda}(f_{\mathrm{BE},\lambda}+1)\frac{\hbar\omega_\lambda}{k_\mathrm{B}T^2}. \tag{5}$$

Computing the heat current in this simplified setting amounts to obtaining the set of first-order Taylor coefficients $\boldsymbol{F}_\lambda$ for all phonon modes in the system. In fact, inserting Eq. (5) into Eq. (4) yields an explicit expression for the thermal conductivity:

$$\boldsymbol{\kappa}_\ell = \frac{1}{k_\mathrm{B}T^2V} \sum_\lambda f_{\mathrm{BE},\lambda}(f_{\mathrm{BE},\lambda}+1)(\hbar\omega_\lambda)^2 \boldsymbol{v}_\lambda \otimes \boldsymbol{F}_\lambda. \tag{6}$$

I have explicitly added the subscript $\ell$ to this thermal conductivity to indicate it refers only to the lattice contribution. In metals or in doped semiconductors at high temperature, where the charge carriers also act as significant carriers of heat, the total thermal conductivity can be written as the sum of both contributions: $\boldsymbol{\kappa} = \boldsymbol{\kappa}_\ell + \boldsymbol{\kappa}_\mathrm{ch}$.

### *2.2 The Peierls-Boltzmann transport equation.*

The Boltzmann transport equation (BTE) was formulated by Ludwig Boltzmann [Bol1872] in 1872 to describe the evolution of a distribution of classical pointlike particles over their phase space and over time under the effect of forces, diffusion and binary collisions. The BTE was a landmark in the development of the kinetic theory of gases, and the analysis of

its consequences made an important contribution to the evolution of statistical mechanics, connecting the mechanical/microscopic and thermodynamic/macroscopic worlds. In 1929, Rudolph Peierls adapted the BTE to the study of phonons in solids [Pei1929]. In this section, I will provide a brief derivation of the Peierls-Boltzmann equation, and in the next one I will focus on its specific form used for steady-state calculations in crystalline solids.

The BTE can be considered a specialized form of a master equation for Markovian processes [Rei2016]. The population of state $\lambda$ is decreased by processes $\lambda \to \lambda'$ that scatter phonons to a different state $\lambda'$, and increased by processes $\lambda' \to \lambda$ that scatter phonons into $\lambda$ from a different state. The time evolution of the occupation can thus be expressed, in this abstract formulation, as

$$\frac{\mathrm{d}f_\lambda}{\mathrm{d}t} = \sum_{\lambda' \neq \lambda} w_{\lambda' \to \lambda} f_{\lambda'} - \sum_{\lambda' \neq \lambda} w_{\lambda \to \lambda'} f_\lambda, \tag{7}$$

where $w_{\lambda \to \lambda'}$ is the transition rate from $\lambda$ to $\lambda'$ for each phonon. The left-hand side can be expanded as $\frac{\mathrm{d}f_\lambda}{\mathrm{d}t} = \frac{\partial f_\lambda}{\partial t} + \boldsymbol{v} \cdot \nabla_{\boldsymbol{r}} f_\lambda$; note that a possible third term involving a gradient with respect to the momentum does not appear because of the lack of fields exerting a force on phonons, as opposed to e.g. the case of charged particles. For now, the right-hand side can be summarized as $\left(\frac{\partial f_\lambda}{\partial t}\right)_{\text{scatt}}$. With this, the following form of the Peierls-Boltzmann transport is obtained:

$$\frac{\partial f_\lambda}{\partial t} = -\boldsymbol{v}_\lambda \cdot \nabla_{\boldsymbol{r}} f_\lambda + \left(\frac{\partial f_\lambda}{\partial t}\right)_{\text{scatt}}. \tag{8}$$

In the steady state, the time derivative on the left-hand side is zero. Furthermore, under the hypothesis of a small perturbation with respect to equilibrium (necessary for the linear regime to hold), the dominant contribution to $\nabla_{\boldsymbol{r}} f_\lambda$ is $\nabla_{\boldsymbol{r}} f_{\text{BE},\lambda}$. Since the position dependence of the Bose-Einstein term is mediated by the temperature, the phonon BTE in this regime takes a much simpler form:

$$\left(\frac{\partial f_\lambda}{\partial t}\right)_{\text{scatt}} = \frac{\partial f_{\text{BE},\lambda}}{\partial T} \boldsymbol{v}_\lambda \cdot \nabla T. \tag{9}$$

*2.3 The linearized phonon BTE for single crystals in the steady state.*

Around a potential energy minimum, the potential energy per unit cell of the crystal can be expanded in a Taylor series:

$$E_{\text{pot}} = \frac{1}{2!}\sum_{\substack{\mathbf{0},\boldsymbol{J}\\ i,j\\ \alpha,\beta}} \phi^{(\alpha\beta)}_{\substack{\mathbf{0},\boldsymbol{J}\\ i,j}} u^{(\alpha)}_{\mathbf{0},i} u^{(\beta)}_{\boldsymbol{J},j} + \frac{1}{3!}\sum_{\substack{\mathbf{0},\boldsymbol{J},\boldsymbol{K}\\ i,j,k\\ \alpha,\beta,\gamma}} \phi^{(\alpha\beta)}_{\substack{\mathbf{0},\boldsymbol{J}\\ i,j}} u^{(\alpha)}_{\mathbf{0},i} u^{(\beta)}_{\boldsymbol{J},j} u^{(\gamma)}_{\boldsymbol{K},k} + \dots \tag{10}$$

In this expression, Greek superscripts run over Cartesian axes, and some shorthand notation has been introduced. Specifically, each of the variables denoted as $u^{(\alpha)}_{\boldsymbol{I},i}$ is a component of an atomic position $\boldsymbol{R}_{\boldsymbol{I},i}$, but measured from the equilibrium position $\boldsymbol{R}_{0,\boldsymbol{I},i}$ and scaled by the corresponding atomic mass,

$$u^{(\alpha)}_{\boldsymbol{I},i} \coloneqq \sqrt{m_i}\Big[X^{(\alpha)}_{\boldsymbol{I},i} - X^{(\alpha)}_{0,\boldsymbol{I},i}\Big], \tag{11}$$

and the coefficients of the series are embedded in the so-called order-k interatomic force constants (IFCs),

$$\phi^{(\alpha\beta\dots)}_{\substack{\boldsymbol{I}_1,\boldsymbol{I}_2\dots\boldsymbol{I}_k\\ i_1 i_2\dots i_k\\ \alpha_1,\alpha_2\dots\alpha_k}} \coloneqq \frac{1}{\sqrt{m_{i_1} m_{i_2}\cdots m_{i_k}}}\left(\frac{\partial^k E_{\text{pot}}}{\partial X^{(\alpha_1)}_{\boldsymbol{I}_1,i_1} X^{(\alpha_2)}_{\boldsymbol{I}_2,i_2}\cdots X^{(\alpha_k)}_{\boldsymbol{I}_k,i_k}}\right)_0 = \left(\frac{\partial^k E_{\text{pot}}}{\partial u^{(\alpha_1)}_{\boldsymbol{I}_1,i_1} u^{(\alpha_2)}_{\boldsymbol{I}_2,i_2}\cdots u^{(\alpha_k)}_{\boldsymbol{I}_k,i_k}}\right)_0. \tag{12}$$

The expression in Eq. (10) makes use of the discrete translation symmetry of the lattice to include only IFCs involving unit cell $\mathbf{0}$.

Phonons are the eigenstates of a perfectly harmonic crystal, i.e., one whose Hamiltonian only contains the first term from Eq. (10). Their angular frequencies and polarizations can be obtained from an explicit diagonalization of that Hamiltonian after block-diagonalizing it over a basis adapted to the irreducible representations of the group formed by its translations, leading to the following finite eigenvalue equation at each point in reciprocal space:

$$\boldsymbol{D}(\boldsymbol{q})\boldsymbol{\psi}_\lambda = \omega_\lambda^2 \boldsymbol{\psi}_\lambda, \text{ with } D_{j,k}^{(\alpha\beta)}(\boldsymbol{q}) \coloneqq \sum_{\mathbf{K}} \phi_{\mathbf{0},\boldsymbol{K}\,j,k}^{(\alpha\beta)} e^{-i\boldsymbol{q}\cdot\boldsymbol{R_J}}. \tag{13}$$

$\boldsymbol{D}$, referred to as the dynamical matrix, also contains the group velocity information, as

$$2\omega_\lambda v_\lambda^{(\alpha)} = \boldsymbol{\psi}_\lambda^* \cdot \frac{\partial \boldsymbol{D}(q)}{\partial q^{(\alpha)}} \boldsymbol{\psi}_\lambda. \tag{14}$$

The atomic displacements can also be conveniently reexpressed in terms of creation and annihilation operators of the phonon modes:

$$u_{\boldsymbol{J},j}^{(\alpha)} = \sqrt{\frac{\hbar}{2Mm_j}} \sum_\lambda \left[ \boldsymbol{a}_\lambda e^{-i\omega_\lambda t} + \boldsymbol{a}_\lambda^\dagger e^{i\omega_\lambda t} \right] e^{i\boldsymbol{q}\cdot\boldsymbol{R_J}} \frac{\psi_{\lambda,\boldsymbol{J},j}^{(\alpha)}}{\sqrt{\omega_\lambda}}. \tag{15}$$

Any element that breaks either the periodicity or the harmonicity of the Hamiltonian will lead to eigenstates different from pure phonons. However, as long as those elements can be treated as perturbations, the phonon picture will still provide a useful description, but with finite-lifetime phonons due to scattering.

In a typical weakly anharmonic single crystal, phonon scattering is dominated by the third-order term of the Hamiltonian, explicitly presented in Eq. (10). When each of the atomic displacements is expressed as in Eq. (15), that third-order anharmonicity adopts the form of a combination of products of triplets of phonon creation and annihilation operators. Thus, in the second-quantization picture, this term accounts for scattering due to three-phonon processes. Conservation laws restrict the processes that can contribute to only two kinds:

**Phonon absorption** ($\lambda + \lambda' \to \lambda''$)**:** two phonons are annihilated, one phonon is created.

**Phonon emission** ($\lambda \to \lambda' + \lambda''$)**:** one phonon is annihilated, two phonons are created.

The conservation laws for energy and momentum take the forms

(16a) $$\omega_\lambda \pm \omega_{\lambda'} = \omega_{\lambda''}, \text{ and}$$

(16b) $$\boldsymbol{q}_\lambda \pm \boldsymbol{q}_{\lambda'} = \boldsymbol{q}_{\lambda''} + \boldsymbol{K_I},$$

where the + and − signs refer to absorption and emission processes, respectively. The conservation of momentum holds in a modular sense, as in the equation above $\boldsymbol{K_I}$ can be any arbitrary vector from the reciprocal lattice. It is possible to make a distinction between *Normal* (N) processes, where $\boldsymbol{K_I} = 0$, and *Umklapp* (U) processes; traditional approximations to the lattice thermal conductivity have often emphasized that distinction as fundamental to their role of anharmonic processes in depressing thermal transport, but many of those conclusions rely on the use of drastic, unphysical simplifications like the Debye model and are in fact myths [MW2014]. The frequency and group velocity, which determine each phonon's contributions to the thermal flux, are well defined regardless of the image of the BZ that is considered, and in modern computational approaches the conservation of momentum is enforced via modular arithmetic with no consideration made to whether a process is N or U; in fact, that classification is not unambiguous, but depends on the choice of unit cell. Direct tests have shown that such approximations based on the N/U dichotomy perform quite poorly [ZA2014].

Inserting Eq. (15) into the third-order term in Eq. (10) and using Fermi's golden rule we obtain a form of the scattering term of the phonon BTE including only third-order anharmonicity:

(17)
$$\begin{aligned}\left(\frac{\partial f_\lambda}{\partial t}\right)_{\text{scatt}} =& \frac{2\pi}{\hbar^2} \sum_{\lambda',\lambda''}^{+} \left|V^{+}_{\lambda\lambda'\lambda''}\right|^2 \delta(\omega_\lambda + \omega_{\lambda'} - \omega_{\lambda''})[(f_\lambda + 1)(f_{\lambda'} + 1)f_{\lambda''} - f_\lambda f_{\lambda'}(f_{\lambda''} + 1)] + \\ & \frac{\pi}{\hbar^2} \sum_{\lambda',\lambda''}^{-} \left|V^{-}_{\lambda\lambda'\lambda''}\right|^2 \delta(\omega_\lambda - \omega_{\lambda'} - \omega_{\lambda''})[(f_\lambda + 1)f_{\lambda'}f_{\lambda''} - f_\lambda(f_{\lambda'} + 1)(f_{\lambda''} + 1)],\end{aligned}$$

with the matrix elements

(18)
$$V^{\pm}_{\lambda\lambda'\lambda''} = \sum_{\substack{\boldsymbol{J},\boldsymbol{K}\\ i,j,k\\ \alpha,\beta,\gamma}} \phi^{(\alpha\beta\gamma)}_{\boldsymbol{0},\boldsymbol{J},\boldsymbol{K}\\ i,j,k} \frac{\psi^{(\alpha)}_{\lambda,\boldsymbol{0},i}\psi^{(\beta)}_{\pm\lambda',\boldsymbol{J},j}\psi^{(\gamma)}_{-\lambda'',\boldsymbol{K},k}}{\sqrt{m_i m_j m_k}}.$$

In both of these expressions, the + and − signs again denote absorption and emission processes, respectively, and the shorthand $-\lambda$ stands for $(-\boldsymbol{q}, \boxdot)$ when $\lambda \coloneqq (\boldsymbol{q}, \boxdot)$. In Eq. (17), + and − over the sums indicate that they only run over processes of the corresponding kind allowed by the conservation of momentum.

The fact that each of the distributions only deviates from its equilibrium value by a small perturbation leads to a more useful, linearized version of the scattering term,

(19)
$$\begin{aligned}\left(\frac{\partial f_\lambda}{\partial t}\right)_{\text{scatt}} =& \frac{2\pi}{\hbar^2}\sum_{\lambda',\lambda''}^{+} \left|V^{+}_{\lambda\lambda'\lambda''}\right|^2 \delta(\omega_\lambda + \omega_{\lambda'} - \omega_{\lambda''}) \times \Big[ \\ & (f_{\text{BE},\lambda''} - f_{\text{BE},\lambda}) f_{1,\lambda'} + (f_{\text{BE},\lambda} + f_{\text{BE},\lambda'} + 1) f_{1,\lambda''} + (f_{\text{BE},\lambda''} - f_{\text{BE},\lambda'}) f_{1,\lambda} \Big] + \\ & \frac{\pi}{\hbar^2}\sum_{\lambda',\lambda''}^{-} \left|V^{-}_{\lambda\lambda'\lambda''}\right|^2 \delta(\omega_\lambda - \omega_{\lambda'} - \omega_{\lambda''}) \times \Big[ \\ & (f_{\text{BE},\lambda''} - f_{\text{BE},\lambda}) f_{1,\lambda'} + (f_{\text{BE},\lambda'} - f_{\text{BE},\lambda}) f_{1,\lambda''} - (f_{\text{BE},\lambda''} + f_{\text{BE},\lambda'} + 1) f_{1,\lambda} \Big].\end{aligned}$$

This expression is, however, not complete yet, due to a less obvious but crucial perturbation upon the basic harmonic Hamiltonian, namely isotopic disorder. From a physical standpoint, this is interesting for two reasons: firstly, it provides an easily measurable macroscopic manifestation of a nuclear feature whose effect on electrons is, in contrast, very subtle; secondly, it is a source of scattering originating in a breakdown of translation symmetry that, however, does not break the homogeneity of the crystal.

Consider a chemical element with a given isotopic distribution in a given sample (which can be based on natural isotopic abundances, but also controllably altered during manufacturing) characterized by an average mass $\bar{M}$ and a variance $\sigma_M^2$. A structure where the occupancy of each site is independent from all others and determined only by the global

isotopic distribution can be modelled as a virtual crystal with a reference Hamiltonian where all atoms of that element are assumed to have mass $\bar{M}$ and each individual atom acts as a point-like perturbation [Tam1983]. From the equation of motion of the system it is straightforward to show that the form of that perturbation is $\frac{\Delta M}{M}\omega^2$, affecting the harmonic term of the Hamiltonian and therefore causing two-phonon (elastic) scattering. Applying Fermi's golden rule again and considering all crystallographic sites with their corresponding elements, Tamura showed in 1983 that the elastic scattering rate between modes $\lambda$ and $\lambda'$ due to this mechanism is proportional to $\sum_i \left(\frac{\sigma_{M,i}}{\bar{M}_i}\right)^2 \left|\sum_\alpha \left[\psi^{(\alpha)}_{\lambda,\mathbf{0},i}\right]^* \psi^{(\alpha)}_{\lambda',\mathbf{0},i}\right|^2 \delta(\omega_{\lambda'} - \omega_\lambda)$, and thus essentially determined by the local density of states of the incoming mode at each scattering center [Tam1983]. Adding this contribution to the linearized scattering term of Eq. (19) and using Eq. (5) explicitly delivers the final form of the BTE for a single, weakly anharmonic crystal,

$$\boldsymbol{F}_\lambda = \tau^0_\lambda(\boldsymbol{v}_\lambda + \boldsymbol{\Delta}_\lambda), \tag{20}$$

where the coefficients are defined as

$$\frac{1}{\tau^{(0)}_\lambda} = \sum^{+}_{\lambda'\lambda''} \Gamma^{+}_{\lambda\lambda'\lambda''} + \sum^{-}_{\lambda'\lambda''} \frac{1}{2}\Gamma^{-}_{\lambda\lambda'\lambda''} + \sum_{\lambda'} \Gamma_{\lambda\lambda'} \text{ and} \tag{21a}$$

$$\boldsymbol{\Delta}_\lambda = \sum^{+}_{\lambda'\lambda''} \Gamma^{+}_{\lambda\lambda'\lambda''} \left(\frac{\omega_{\lambda''}}{\omega_\lambda}\boldsymbol{F}_{\lambda''} - \frac{\omega_{\lambda'}}{\omega_\lambda}\boldsymbol{F}_{\lambda'}\right) + \sum^{-}_{\lambda'\lambda''} \frac{1}{2}\Gamma^{-}_{\lambda\lambda'\lambda''} \left(\frac{\omega_{\lambda''}}{\omega_\lambda}\boldsymbol{F}_{\lambda''} + \frac{\omega_{\lambda'}}{\omega_\lambda}\boldsymbol{F}_{\lambda'}\right) + \sum_{\lambda'} \Gamma_{\lambda\lambda'} \frac{\omega_{\lambda'}}{\omega_\lambda}\boldsymbol{F}_{\lambda'}, \tag{21b}$$

and each $\Gamma$ is a transition rate due to a particular kind of process:

$$\Gamma^{+}_{\lambda\lambda'\lambda''} = \frac{\hbar\pi}{4}\frac{f_{\mathrm{BE},\lambda'} - f_{\mathrm{BE},\lambda''}}{\omega_\lambda\omega_{\lambda'}\omega_{\lambda''}}\left|V^{+}_{\lambda\lambda'\lambda''}\right|^2\delta\left(\omega_\lambda + \omega_{\lambda'} - \omega_{\lambda''}\right) \tag{22a}$$

$$\Gamma^{-}_{\lambda\lambda'\lambda''} = \frac{\hbar\pi}{4}\frac{f_{\mathrm{BE},\lambda'} + f_{\mathrm{BE},\lambda''} + 1}{\omega_\lambda\omega_{\lambda'}\omega_{\lambda''}}\left|V^{-}_{\lambda\lambda'\lambda''}\right|^2\delta\left(\omega_\lambda - \omega_{\lambda'} - \omega_{\lambda''}\right) \tag{22b}$$

$$\Gamma_{\lambda\lambda'} = \frac{\pi\omega_\lambda^2}{2}\sum_i\left(\frac{\sigma_{M,i}}{\bar{M}_i}\right)^2\left|\sum_\alpha\left[\psi^{(\alpha)}_{\lambda,\mathbf{0},i}\right]^*\psi^{(\alpha)}_{\lambda',\mathbf{0},i}\right|^2\delta(\omega_{\lambda'} - \omega_\lambda). \tag{22c}$$

This is now a large set of algebraic linear equations for the $\boldsymbol{F}_\lambda$ with completely explicit expressions for all the coefficients, which in principle can be solved. The details of the solution method will be discussed in the next section; however, it is worth mentioning that historically this was still considered a nearly impossible task. Clear evidence of this, in addition to the quote from Ziman that opens this article, is that Callaway [Cal1959] wrote in 1959 that "Although an exact calculation of lattice thermal conductivity is possible in principle, lack of knowledge of crystal vibration spectra and of anharmonic forces in crystals and the difficulty of obtaining exact solutions of the Boltzmann equation are formidable barriers to progress." One of the most usual workarounds was working under the so-called relaxation time approximation (RTA), where each phonon mode $\lambda$ is assumed to relax to thermal equilibrium through a single kind of process, whose characteristic time is therefore equal to that mode's lifetime. The inverse of that lifetime is the total scattering rate of the mode, that is, the sum of the scattering rates of all independent scattering processes, which is precisely what Eq. (21a) expresses. Indeed, the RTA amounts to assuming that $\boldsymbol{\Delta}_\lambda = 0$ in Eq. (20), yielding the explicit solution $\boldsymbol{F}_\lambda = \tau^{(0)}_\lambda \boldsymbol{v}_\lambda$. This can be substituted into Eq. (6) to recover the well know (but merely approximate) expression for the thermal conductivity in the RTA:

$$\boldsymbol{\kappa}_\ell = \frac{1}{k_\mathrm{B}T^2V}\sum_\lambda f_{\mathrm{BE},\lambda}(f_{\mathrm{BE},\lambda}+1)(\hbar\omega_\lambda)^2\boldsymbol{v}_\lambda\otimes\boldsymbol{v}_\lambda\tau^{(0)}_\lambda. \tag{23}$$

For many common semiconductors, the RTA incurs an error in the conductivity of 10% or less [WBSD2009], even if the individual non-equilibrium populations may be quite inaccurate. However, for high-conductivity systems like diamond the results can be much more dramatically wrong [WB2010].

While the RTA eliminates the problem of solving the linearized BTE, it does not alleviate the burden of obtaining all the ingredients needed to compute the coefficients. Thus, the historical trend before first-principles approaches became available was to use parameterized forms of $\tau_\lambda^{(0)}$, often based on analytical assumptions like the Debye model and valid only for small $|\boldsymbol{q}|$. Such methods require fitting their parameters to experimental data and therefore lack predictive power, but even with the best fitting their performance is often poor due to their limited flexibility.

### *2.4 Solving the linearized BTE.*

The first practical method to solve the system of linear equations and obtain the non-equilibrium populations was proposed in 1996 by Omini and Sparavigna [OS1996]. It is a simple iterative strategy that starts from the RTA result $\boldsymbol{F}_\lambda^{(0)} = \tau_\lambda^{(0)} \boldsymbol{v}_\lambda$ and then enters a loop where $\boldsymbol{\Delta}_\lambda$ is evaluated according to Eq. (21b) and then its value is substituted into Eq. (20) to obtain a new estimate of $\boldsymbol{F}_\lambda$ for the next iteration, until convergence is achieved. In the decade that followed, the Omini-Sparavigna method was applied to some systems using mostly application-specific code and interaction models of varying quality (e.g. [BMB+2007; WB2010; WBSD2009]). However, the first public general-purpose software package for this purpose was `ShengBTE` [LCKM2014], released in 2014 and of which I am a coauthor. I will describe the steps of the solution algorithm as implemented in `ShengBTE`:

1. A Γ-centered discrete regular grid of $N_1 \times N_2 \times N_3$ $\boldsymbol{q}$ points is built to sample the Brillouin zone.

2. The space group of the system is detected using the `spglib` library [AT2024] and its elements used to split the $\boldsymbol{q}$ points into equivalence classes.

3. At each point in the grid the angular frequencies, group velocities and polarizations of all phonon branches are obtaining. They are then explicitly symmetrized over equivalence classes.

4. Using Tamura's formula, the contribution to phonon scattering from isotopic disorder is calculated.

5. A search for allowed three-phonon processes is run by iterating over all possible pairs of $\boldsymbol{q}$ and $\boldsymbol{q}'$, using the conservation of momentum to compute the $\boldsymbol{q}''$ that might complete valid absorption or emission processes, and then checking all triplets formed by a phonon mode at each point to see if they can satisfy the conservation of energy. The condition in Eq. (16a) will never be fulfilled exactly by three modes sampled from the grid, and each $\boldsymbol{q}$ point actually stands for the area of the BZ around it, so a tolerance must be applied in this search. `ShengBTE` uses a parameter-free, locally adaptive regularization [LML+2012] of the Dirac $\delta$ in Eqs. (22b) and (22a) to accomplish this without losing predictive power.

6. The scattering amplitude for each of the allowed processes is calculated according to Eqs. (22a) and (22b).

7. The Omini-Sparavigna iterative scheme is set up and run until convergence.

8. The thermal conductivity is computed and symmetrized as a rank-2 tensor.

This outline is somewhat simplified and omits many additional harmonic and anharmonic results calculated during a typical run [LCKM2014].

The publication introducing ShengBTE has been cited almost 3000 times, the program having been used with success for many different kinds of crystals, both experimentally known and hypothetical. A typical example for a relatively simple semiconductor, InAs, is shown in figure 1. Crucial to this success is the thorough and automatic integration of the symmetries in reciprocal space, since small deviations from the perfect symmetry can derail the convergence or yield completely unphysical results.

Most of the computational cost of the algorithm, in terms of both CPU and memory, comes from the detection of allowed processes and the calculation of their amplitudes, since the numbers of absorption and emission processes typically range from $10^7$ to $10^{10}$. Fortunately, it can be parallelized over $\boldsymbol{q}$ and over phonon processes.

More recent phonon BTE solvers, like almaBTE [CVK+2017] have tended to move on from the Omini-Sparavigna iterative algorithm and use either a direct solver of the linear system or a more standard, general-purpose iterative approach. Those procedures generally result in a more stable and accurate solution.

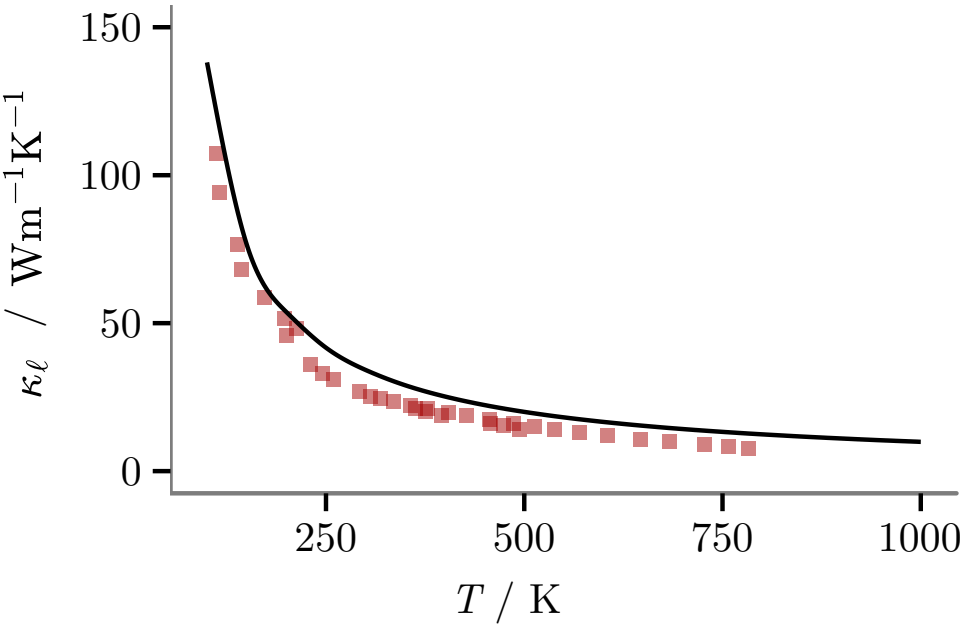


Figure 1: Thermal conductivity of bulk InAs computed using `ShengBTE` (solid line) compared to data from multiple experiments (red squares) [BUBC1959; LA1972; OPG1972; TS1971]. Plot reconstructed with data from [LCKM2014].

### *2.5 Obtaining the IFCs and other ingredients of the BTE.*

Based on the expressions handled in the preceding section, and besides some tabulated quantities like atomic masses and isotopic distributions, the inputs needed to fully formulate the BTE are the equilibrium atomic positions and a set of second- and third-order derivatives of the potential energy at those positions, i.e., the harmonic and anharmonic IFCs. To keep the method parameter free, it is desirable to extract those pieces of information from ab-initio calculations, and due to its favorable tradeoffs between accuracy and scalability, methods based on density functional theory (DFT) have become the standard choice.

DFT [PY1989] is a reformulation of the electronic problem in terms of a single scalar field, the electronic density, which therefore avoids the exponential scaling barrier of wavefunction-based methods [Koh1999]. Although DFT is formally an exact theory for the ground state, in practice the need to use relatively simple approximations to the so-called exchange and correlation terms of the Hamiltonian places some important practical limitations on its precision and accuracy [Fei2010]. Some of those limitations are systematic,

such as a tendency to underestimate electron localization (mispredicting semiconductors as metals) and its neglect of van-der-Waals-like interactions, and there are approximate strategies to correct for those; however, others are system-dependent and sometimes difficult to detect.

The many DFT implementations available differ in what kind of functions they use to represent the solution (the basis), the techniques they offer to abstract away the core electrons (pseudopotentials, plane-augmented waves or PAW…), the platform they are implemented on, the amount of postprocessing they are able to do, whether they are proprietary or open-source, and so on and so forth. Software based on the PAW formalism [Blö1994], using plane waves for its basis, is particularly well suited for the efficient and accurate study of bulk crystals, and is therefore the most popular choice for phonon calculations. The main representatives of this category are `VASP` [KF1996] on the proprietary side, and `Quantum ESPRESSO` [GBB+2009] among open-source packages.

A typical DFT calculation takes atomic positions as input and outputs the total energy and the forces on each atom — the latter being relatively inexpensive to obtain through the Hellmann-Feynman theorem — as well as the stress tensor on the simulation box. That information can be used to run a local, possibly constrained, minimization to reach an equilibrium configuration. From that starting point, in very broad terms there are three families of approaches to obtain the IFCs:

**Density-functional perturbation theory (DFPT):** A perturbation, be it a displacement of a single atoms or a periodic displacement with a periodicity corresponding to $\boldsymbol{q}$, can be applied to the DFT Hamiltonian and the corresponding changes to the energies and wave functions of the eigenstates studied with the methods of perturbation theory [BdGDG2001]. Doing so up to the first order, the Hellmann-Feynman theorem can be recovered, the second order makes possible to extract the dynamical matrix $\boldsymbol{D}(\boldsymbol{q})$, and the third order opens the door to obtaining anharmonic information as well. A crucial result is the $2n + 1$ theorem, which states that the $n$-th derivative of the wave functions is needed to access up to the $(2n + 1)$-th perturbation to the energy, making the calculation of $\boldsymbol{D}(q)$ significantly more costly than that of the forces.

**Finite differences:** A second-order IFC can be approximated by a suitable difference between two forces on atoms in different configurations. For instance, the $xy$ force

constant between two atoms $i$ and $j \neq i$ can be estimated as

$$K_{i,j}^{(xy)} = \frac{1}{\sqrt{m_i m_j}} \frac{\partial^2 E_{\text{pot}}}{\partial x_i \, \partial y_j} \simeq \frac{1}{\sqrt{m_i m_j}} \frac{f_i^{(x)}(y_j = y_{j,0} - h) - f_i^{(x)}(y_j = y_{j,0} + h)}{h},$$

where $h$ is an appropriately small displacement (typically in the order of $10^{-2}$ Å), $f_i^{(x)}$ is the $x$ component of the force on atom $i$, and all coordinates other than $y_j$ are assumed to retain their equilibrium values. Two DFT runs, with atom $j$ in different positions, are needed, although one is enough if a (less accurate) single-sided finite-difference formula is deemed acceptable. Similar expressions can be developed for IFCs of any order, and specifically the third.

**Regression:** The Taylor expansion in Eq. (10), when truncated to any given order, can be regarded as a linear equation with the IFCs as unknowns and products of the $u_{\boldsymbol{J},j}^{(\beta)}$ as coefficients. The same applies to the derivative of that equation with respect to one of the displacements. Therefore, if DFT results are available for the right number of different configurations of atomic displacements, a system of linear equations with forces as its independent term and products of displacements as coefficients can be formulated and solved to obtain the IFCs. That would constitute a small variation on the finite-difference approach described above, but this idea comes onto its own when it is formulated as a fit instead of just a system of equations. By formulating a loss function that quantifies the differences between the DFT forces and those obtained from the finite Taylor expansion and minimizing that loss subject to constraints, the best-fit IFCs can be obtained with a controlled tradeoff between quality and computational effort. In particular, a sparsity constraint can be applied to employ fewer (and possibly far fewer) calculations than would be demanded by the finite-difference formulas, while still recovering satisfactory values of the most important IFCs up to the desired order [ZNXO2014].

DFPT-based methods are theoretically appealing but incur significant implementation costs, specifically due to the need to evaluate derivatives of the different mathematical components of the DFT-based methods being used in each calculation. The magnitude of those costs comes into relief when the large variety of exchange and correlation functionals, kinds of pseudopotentials, types of spin configurations (unpolarized, collinear or non-collinear),

iterative methods and so on that a single DFT package may implement is taken into account. Adding a new feature to the program becomes much more complex if everything must be kept DFPT-compatible. It is thus understandable that full second-order DFPT implementations for phonon calculations are relatively scarce, and third-order implementations are even more exceptional. The best example is `D3Q` [PML2013], part of the `Quantum ESPRESSO` ecosystem. The program imposes strong restrictions on the underlying DFT calculations: no spin polarization, no noncollinear magnetism, no ultrasoft pseudopotentials or PAW are allowed [GAB+2017]. Moreover the performance of the method is not good enough to directly extract $\boldsymbol{D}(\boldsymbol{q})$ at every point of the relatively dense grid employed in the solution of the BTE: a sparser sampling is used instead, which is then transformed back to real space, resulting in a set of second-order IFCs from which $\boldsymbol{D}(\boldsymbol{q})$ can be interpolated at any other $\boldsymbol{q}$ point.

In contrast, the finite-difference and regression-based methods can be implemented on top of any DFT package capable of calculating forces on atoms in arbitrary configurations, and therefore enables access to most of the power of those implementations, including beyond-DFT corrections. Likewise, a package can be designed that is able to interface with several or many DFT backends, and it is easy to extend it to new backends. A very user-friendly and fully featured example of such a package is `Phonopy` [TT2015], widely used in finite-difference calculations of second-order IFCs. For third-order calculations, one of the possibilities is `thirdorder.py` [LCKM2014], designed to be used with `ShengBTE`. Regarding regression methods, `hiPhive` [EFE2019] is an open-source implementation of a wide array of feature selection and compressive-sensing methods enabling access to IFCs of arbitrary order at reasonable cost.

DFT calculations for bulk crystals are performed using a finite simulation box — often either an irreducible or a conventional unit cell — and periodic boundary conditions. Strictly speaking, this is incompatible with representing a configuration where a single atom is displaced with respect to equilibrium (like those entering the finite-difference formulas), since all of the periodic images of that atom will be displaced in the same fashion. To obtain even a reasonable approximation, a supercell containing multiple instances of that unit cell needs to be constructed. The simplest and most usual case involves a diagonal supercell, in which the unit cell is repeated $s_1 \times s_2 \times s_3$ times along the crystallographic axes. The forces computed in such a supercell still contain artifacts of periodicity, but it is

straightforward to show [PLK1997] that the dynamical matrix computed from those cumulant force constants matches the exact one at the $s_1 \times s_2 \times s_3$ $\boldsymbol{q}$ points of the Brillouin zone that are commensurate with the supercell. At any other point, $\boldsymbol{D}(\boldsymbol{q})$ can be considered an interpolation. The quality and the cost of the approximation both increase with supercell size.

A crucial part of the practical deployment of any of these methods is the use of crystal symmetry, both to reduce the number of DFT runs and to ensure the physical correctness of the result. From the point of view of a supercell, any operation from the crystal's space group amounts to the combination of a (possibly improper) rotation and an atomic permutation. The $n$-th order IFCs must transform as a rank-$n$ tensor under the effect of these operations, but the transformed values must be identical to the untransformed ones. Thus, each symmetry operation defines a set of homogeneous linear constraints that the IFCs must fulfill [LCKM2014; PLK1997]. In other words, the IFCs are restricted to belong to the nullspace of the homogeneous system of linear equations induced by the space group. Therefore, to determine the full IFC tensor it is enough to determine a set of coefficients to build the right linear combination of the elements of a basis of that nullspace. This, combined with the fact that each DFT run outputs $3M$ different force components, and the invariance of mixed partial derivatives under an exchange of the order of differentiation, enables drastic reductions in the number of DFT runs required by a calculation: the full phonon spectrum of Si can be extracted from DFT forces for a single configuration, and a sufficient set of third-order IFCs for the 6H phase of SiC (comprising 56754 elements) require just 216 runs.

The continuous symmetries of free space cannot be ignored in IFCs calculations either: rigid rotations and translations of the full crystal cannot change the energy of the system or generate any forces. Inserting the condition of zero forces under translations into Eq. (10) yields an additional set of homogeneous linear equations known as the acoustic sum rules (ASRs). Unfortunately, IFCs obtained from DFT contain artifacts that cause large departures from the ASRs and require corrections. Failure to fix those deviations will cause the phonon spectrum to lack true acoustic branches that have zero angular frequencies at the $\Gamma$ point, a feature so critical from a physical standpoint that phonon spectra containing such artifacts can be considered useless. Similarly, third-order IFCs that violate the ASRs give rise to unphysical anharmonic scattering rates with the wrong behavior in the $\omega \to 0$

limit. Symmetrization of the IFCs to satisfy the ASRs can be performed a posteriori, using a least-squares criterion to keep the changes to a minimum; alternatively, the ASRs can be directly added to the linear system derived from the discrete symmetries.

A more fundamental limitation of the supercell approach is its inability to capture long-range interactions, and specifically electrostatic interactions. The consequences are significant for compounds with polar bonds: figure 2 (left) illustrates this for the example of rocksalt PbS, with a sequence of calculations with supercells of increasing size. I have chosen particularly elongated supercells along a single axis to obtain large numbers of commensurate $\boldsymbol{q}$ points along the corresponding direction in reciprocal space. From this sequence it is obvious that, even with those extreme sizes, the calculation is not well converged with respect to supercell size, and shows no sign of convergence. In particular, the longitudinal and transverse optical branches (LO and TO, depicted in red and brick colors) always have the same frequency at Γ but are no longer degenerate at the first commensurate point away from Γ, no matter how close that point gets. To solve this properly, a nonanalytic correction (NAC) needs to be added to the dynamical matrix to account for those interactions that cannot be captured by any supercell. The result is shown in the right-hand-side panel of figure 2, confirming that the LO/TO split begins at Γ and is much wider than could be expected from the supercell calculations.

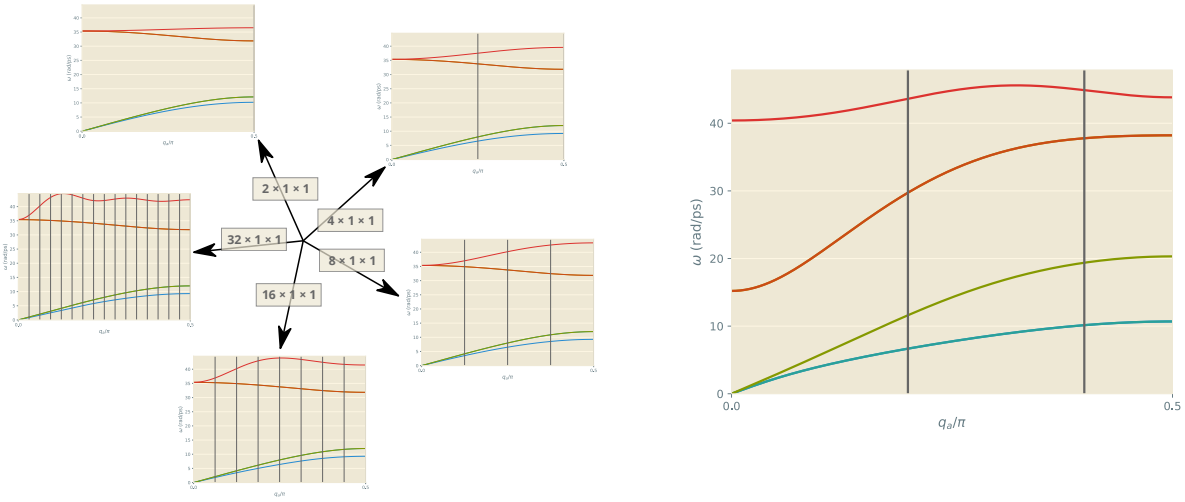


Figure 2: Left: Evolution of the phonon spectrum of rocksalt PbS along the $\Gamma \to X$ direction estimated using supercell-calculated IFCs with different supercell sizes. The vertical bars represent commensurate $\boldsymbol{q}$ points. Right: Same spectrum, computed using a $5 \times 5 \times 5$ supercell and a nonanalytic correction.

There are several different approaches to the NAC [GAT1994; GL1997; WWK+2010], but they generally share a common set of ingredients: the high-frequency dielectric tensor of the crystal ($\boldsymbol{\varepsilon}$) and the Born effective charge tensors [Spa2012] for all atoms, defined as $Z_i^{(\alpha\beta)} = \frac{1}{e}\frac{\partial p^{(\beta)}}{\partial X_i^{\alpha}}$, where $\boldsymbol{p}$ is the electric dipole moment of the solid. Mainstream plane-wave DFT codes can provide access to those quantities through DFPT [GHK+2006]. An important feature of the NAC, which gives it its name, is that the correction depends on matrix elements such as $\boldsymbol{q}\cdot\boldsymbol{\varepsilon}\boldsymbol{q}$ and $(\boldsymbol{Z}_i\boldsymbol{q})\cdot(\boldsymbol{Z}_j\boldsymbol{q})$ that need not have a well defined $\boldsymbol{q}\to\boldsymbol{0}$ limit; thus, the optical frequencies near $\Gamma$ are direction-dependent, and finite jumps can appear in a band diagram along a path that crosses that point.

In summary, the most well-established recipe to obtain all the ingredients of the BTE from ab-initio calculations involves using a plane-wave-based DFT engine to run three series of calculations, not counting the minimization: a short series of runs to compute the second-order IFCs, a perturbative calculation to extract the dielectric parameters, and a much longer series to obtain the third-order IFCs, but regression-based approaches can merge the first and last of these with significantly lower cost.

## 3 Extensions.

### *3.1 Defect-laden crystals.*

Although pristine semiconductor samples — and even isotopically pure ones — are experimentally accessible and serve as a benchmark of ab-initio-based phonon BTE calculations, they are not the most frequently found kind of sample in practical use. As a matter of fact, control of defects is an integral part of semiconductor technology, whether they be an accidental result of the synthesis procedure or introduced on purpose. As an example of the former, part of the contributions leading to Shuji Nakamura's 2014 Nobel Prize for co-inventing the blue LED was related to the reduction of dislocation density [Nak2015]. As for the intentional introduction of defects, it is the mechanism behind doping, key to modulating the electrical and optical properties of semiconductors. In thermoelectricity, an application where the thermal conductivity is a primary design consideration, doping densities are extremely high (often in the order of $10^{21}\,\mathrm{cm}^{-3}$). It is therefore desirable to extend the success of phonon BTE calculations to defect-laden samples while retaining their high predictive power.

Defects come in many shapes and types, which can be classified according to their

dimensionality. 0D defects are confined in a region of a size comparable to a few interatomic distances along all directions, and include vacancies, substitutions, interstitials, antisites, and so on. 1D defects are extended along a particular direction, the best known example being dislocations. Finally, 2D defects, extended along two different directions, comprise boundaries and interfaces.

A common feature of defects is that they break the periodicity of the crystal structure, and therefore they act as a perturbation to the harmonic part of the Hamiltonian, introducing elastic scattering. This was also the case with isotopic disorder (which is, in fact, a particular distribution of defects); however, as opposed to that case and to many instances in the theory of electron scattering, the magnitude of the perturbation is such that Fermi's golden rule is not applicable [KCLM2014], and fully converged perturbation theory must be used. The central object in this treatment is the t matrix,

$$\boldsymbol{t} = \left(\mathbf{1} - \boldsymbol{V}\boldsymbol{g}^{+}\right)^{-1}\boldsymbol{V}, \tag{24}$$

which encodes both the information about the perfect system where the defect is embedded (through its causal Green's function, $\boldsymbol{g}^{+}$) and the perturbation itself (in the perturbation matrix, $\boldsymbol{V}$). The elastic scattering rates, $\Gamma_{\lambda\lambda'}$, can be extracted from $\boldsymbol{\psi}^{*}_{\lambda'} \cdot \boldsymbol{t}\boldsymbol{\psi}_{\lambda}$, instead of from $\boldsymbol{\psi}^{*}_{\lambda'} \cdot \boldsymbol{V}\boldsymbol{\psi}_{\lambda}$ as in Eq. (22c). However, it is more efficient, generally sufficient, and therefore customary to include phonon-defect scattering only at the RTA level and use the optical theorem [Eco2006] to compute their contribution to the scattering rate,

$$\tau^{-1}_{\lambda,\mathrm{def}} = -\frac{n_{\mathrm{def}} V_{\mathrm{uc}}}{\omega_{\lambda}} \operatorname{Im}\{\boldsymbol{\psi}^{*}_{\lambda} \cdot \boldsymbol{t}\boldsymbol{\psi}_{\lambda}\}, \tag{25}$$

where $V_{\mathrm{uc}}$ is the unit cell volume and $n_{\mathrm{def}}$ is the volumetric concentration of defects.

For spatially confined defects, Eq. (25) can be evaluated in real space. The $3 \times 3$ block of the Green's function connecting atoms $(\boldsymbol{I}, i)$ and $(\boldsymbol{J}, j)$ is defined as

$$\boldsymbol{g}^{+}_{\substack{\boldsymbol{I},\boldsymbol{J} \\ i,j}}(\omega) = \lim_{\epsilon \to 0^{+}} \sum_{\lambda} \frac{\boldsymbol{\psi}_{\lambda,\boldsymbol{I},i} \boldsymbol{\psi}^{\dagger}_{\lambda,\boldsymbol{J},j}}{\omega^2 + i\epsilon - \omega^2_{\lambda}}, \tag{26}$$

and the singular form of the denominator demands very specific integration techniques. For bulk crystals, the usual choice is the linear tetrahedron method (introduced in [LV1984], but see [Eye2012] for formulas correcting some typos in the original). It starts by subdividing each minizone defined by a $s_1 \times s_2 \times s_3$ sampling of the BZ into six nonoverlapping tetrahedra. Then, the frequencies of each phonon band are linearly interpolated within each tetrahedron, starting from their values at the four corners and using barycentric coordinates. Those integrals and their $\epsilon \to 0^+$ can be solved analytically, and the total $\boldsymbol{g}^+$ is recovered a sum of the contributions from each tetrahedron. The other ingredient of the calculation is the perturbation matrix, which contains two contributions: the first, $V_{\boldsymbol{M}}$ from the mass difference of the defect with respect to the host system, with the same form as in the case of isotopic disorder, and the second, $V_{\boldsymbol{K}}$, from the difference in second order IFCS:

$$V^{(\alpha\beta)}_{\boldsymbol{K},\substack{\boldsymbol{I},\boldsymbol{J}\\i,j}} \coloneqq K^{(\alpha\beta)}_{0,\substack{\boldsymbol{I},\boldsymbol{J}\\i,j}} - K^{(\alpha\beta)}_{\substack{\boldsymbol{I},\boldsymbol{J}\\i,j}}. \tag{27}$$

The IFCs of the perfect and defect-laden systems must satisfy the ASRs, and the difference must be adjusted so that it is strictly bounded within the area where the Green's function is calculated.

This formalism has been successfully applied to cases such as diamond [KCLM2014], GaN [KCW+2018] and highly doped Si [DCW+2020], always showing excellent predictive ability with no other input parameters than the defect concentration. The level of quantitative agreement is so high that relatively inexpensive thermal conductivity measurements can be used, in conjunction with these calculations, to determine the type and concentration of defects in a sample, as was done in [KCM2016], where it was revealed that Ni/vacancy antisites are the dominant scattering mechanism in thermoelectric ZrNiSn samples, solving a controversy between different experimental measurements. This stands in stark contrast with traditional approximations like the Klemens-Callaway model [AV1962], which rely on fitted parameters and can produce unphysical results. An example of the latter is that, for vacancies, where the magnitude of the mass perturbation $V_{\boldsymbol{M}}$ is completely irrelevant because the atom is disconnected from the lattice in the perturbed configuration, the Klemens-Callaway model still predicts nonzero scattering rates from that mass perturbation; meanwhile, the Green's function method yields the right result without

any adjustment. The availability of quantitative models has also revealed the existence of superscatterers such as B substitutions in SiC [KCD+2017]: those are defects that reduce the thermal conductivity of their host to a much larger degree than most other impurities at similar concentrations, by introducing strong resonances in frequency bands that are especially important for thermal transport.

The same methods can be used to study random alloys, modelled as an effective medium with a random distribution of substitutions that scatter phonons. Employing a single-site-averaged perturbation extracted from DFT calculations on special quasirandom structures representative of the alloy [ZWFB1990], quantitative agreement with experiment is achieved even for InAs/GaAs alloys, where there is significant structural distortion with respect to the parent compounds [ACMM2018].

Extending the method to 1D defects involves treating one of the dimensions in reciprocal space and replacing the tetrahedron method by its 2D equivalent, the linear triangle method [AL1987]. This enabled the treatment of dislocations in GaN [WCMM2019], for which the structural deformation and the corresponding long-range IFC perturbation had to be modelled using a matched combination of an elastic deformation model and actual atomistic calculations.

On the whole, Green's-function-based methods for characterizing the effect of defects on phonon transport have proven themselves as a viable strategy to obtain predictive estimates without experimental input; however, their computational cost is significant, both because of the need to study the complex local relaxations around defects and because of the large number of DFT calculations on low-symmetry configurations that are required to obtain the IFC perturbation. Additionally, defects may exist in different charge states, and in a doped semiconductor mapping a measured charge-carrier density to an actual defect concentration is a decidedly nontrivial problem in computational thermodynamics [BGS+2015].

### *3.2 Interfaces and superlattices.*

The most common kind of 2D defect is the sample boundary, which is present in every measurement. Boundaries are responsible for the characteristic low-temperature behavior of thermal conductivity curves, which go to zero as $T \to 0$: it can be shown that for an infinite sample $\kappa_\ell$ would diverge in that limit [Zim1960]. The same kind of result is obtained from a typical phonon BTE calculation of the kind outlined here, but only as a numerical

artifact due to the discretization of the BZ using a regular grid: proper integration and allowed process detection at lower temperatures would require much denser sampling close to the Γ point. Luckily, relatively simple approximations can account for the presence of a boundary with different geometries, like wires [LML+2012] and films [CVK+2017]. For a generic bulk system where the geometry of the boundary is unknown or not strictly relevant, the usual choice is to include an additional contribution to the scattering rates that reflects a mean free path of the order of the characteristic sample size $L$, with an expression $\tau^{-1}_{\lambda,\text{boundary}} = |\boldsymbol{v}_\lambda|/(FL)$ for a suitable form factor $F$. This can be justified heuristically, as an estimate of the average distance between boundary scattering events. Its main downside is that $F$ often needs to be treated as a fitting parameter, breaking the parameter-free nature of the approach at low temperatures.

Interfaces between media, on the other hand, are some of the more complex defects from the perspective of phonon transport. In the directions parallel to the surface there are often reconstructions that break the periodicity of the bulk, while in the perpendicular direction other phenomena like interdiffusion, polarity and composition gradients create very involved atomistic configurations. Insofar as those configurations can be determined, they can be modelled in detail and their effect on phonons computed employing Green's functions, albeit using quite specific techniques. A good synthesis can be found in [Ong2018]; a crucial part is the realization that a periodicity still exists in the directions parallel to the surface, even if it is different from that of the bulk, so a parallel wave vector $\boldsymbol{q}_\parallel$ can be defined that is conserved in interface scattering processes. Therefore, the problem can solved individually for each $\boldsymbol{q}_\parallel$, and is decoupled into a set of effective 1D phonon transmission calculations with a typical Landauer-Büttiker setup, illustrated in Fig. 3. Reconstruction is assumed to be confined to a finite region around the interface, the scattering region, beyond which the system maintains its bulk structure and is therefore translationally symmetric in the direction perpendicular to the interface. Each of the sides of the interface, acting as a lead, is split into blocks thick enough that interblock IFCs can be neglected beyond the first neighbors, and hence each lead is characterized by a pair of "on-site" and "hopping" IFC blocks, by analogy with a 1D electronic tight-binding problem. Each of the leads is also connected to the scattering region through another IFC block, and that region has its own "on-site" term, but there is no direct connection between the leads (which can be accomplished by taking a large enough scattering region). The Green's functions of the uncoupled leads are

obtained from the corresponding blocks using a real-space technique known as decimation [GTFL1983; ZFM2007], an iterative process that starts by constructing a small version of the lead and doubles the size of that construction in each iteration. From there, two self-energies can be defined and finally the Green's function of the coupled system in the central region is readily recovered. That allows the total phonon transmission at a given frequency to be extracted from the usual Caroli formula; however, it is often more useful to obtain the mode-to-mode transmissions from the left to the right lead across the interface, which are encoded in the so-called Bloch matrices [Ong2018]. Through this formalism, the fine details of phonon transmission across precisely characterized interfaces, such as phase and twin boundaries in group-IV and III-V semiconductors, can be recovered [CLR+2019]. Once more, this contrasts with traditional simplified models, in this case the acoustic-mismatch and diffuse-mismatch models [RCM2005], which rely on very crude hypotheses about how phonons are reemitted and ignore most of the characteristics of those phonons; particularly noteworthy are the effects of polarization, evident in the different behavior of transverse and longitudinal modes at those phase and twin boundaries.

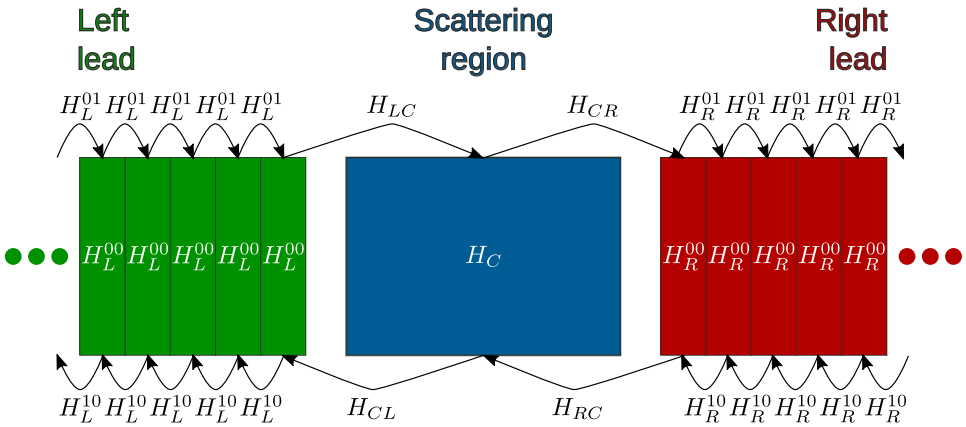


Figure 3: Diagram of the partition of the harmonic IFC matrix in blocks used for calculating the phonon transmission across an interface.

Directly connected to the problem of a single interface is the study of binary superlattices, structures with a periodic composition profile along the growth axis. Superlattices are highly tunable through modifications to that profile, and their physical properties are not determined by their net composition, making them very attractive from a technological standpoint. As an example, Si/Ge superlattices with a reduced Ge concentration can be designed to have a thermal conductivity as low or lower than the random Si/Ge allows used

in thermoelectric products [CKF+2013]; this is very interesting because most of the cost of the alloy is driven by that germanium content. That kind of behavior can be reproduced quantitatively if the superlattice is modelled as an effective medium on top of which two different perturbations are imposed, one due to the composition profile along the growth direction (the barrier component) and the other caused by chemical disorder in the two perpendicular directions (the alloy component). The former, a significant perturbation, must be treated using Green's functions, while the latter can be handled with a slightly adapted version of Tamura's perturbative formula for isotopes. This has been shown to provide excellent agreement with measurements when paired with a thermodynamic model of superlattice growth, for instance in the cases of Ge/Si [TCV+2018] and InAs/GaAs [CVT+2018] superlattices, to the point that a profile can be designed to target a particular thermal conductivity that is later confirmed after its synthesis and measurement. Figure 4 shown some examples for InAs/GaAs superlattices. A special integration method had to be devised to obtain the Green's function for this application, since the linear tetrahedron method exhibits poor behavior when extrapolated to 1D. Using cubic (instead of linear) interpolation for each phonon band within each segment of the 1D BZ fixes the problem without compromising the analytic integration. To determine the coefficients a cubic polynomial, the phonon group velocities must be used in the interpolation, in addition to the angular frequencies; as a beneficial side effect, the approximation is satisfactory over longer segments and therefore sparser grids can be used.

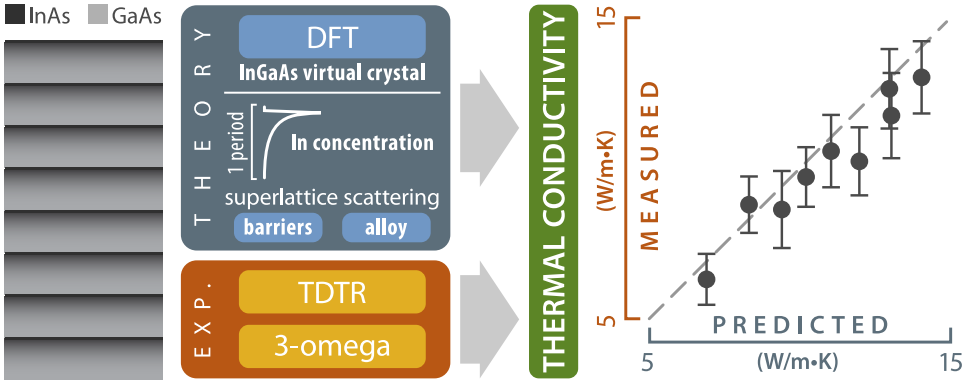


Figure 4: Schematic representation of the calculation and measurement workflow for InAs/GaAs superlattices, and comparison between calculations and experiment. Reproduced with permission from [TCV+2018].

### *3.3 Subperiodic systems.*

In the last decades, nanosystems have risen to prominence because of their seemingly infinite versatility in manifesting new physical phenomena and the tunability of their properties for technological applications. The field of thermal transport is no exception to this trend: silicon nitride nanostructures were used to measure the quantum of thermal conductance [SHWR2000], Si nanowires with rough boundaries have been proposed as candidates for ultralow thermal conductivities [HCD+2008] and graphene may have the highest thermal conductivity of any known material, in competition only with diamond [PVR2012].

Quasi-2D monolayers and multilayers have been tackled very successfully using the BTE formalism outlined, both in pristine form [LLC+2014] and in the presence of defects [MCI+2024]. Nevertheless, special care must be exercised when computing their phonon spectra, since the effect of the symmetries of free space is different in each dimensionality. Specifically, the phonon spectrum any quasi-2D crystalline system — not just monolayers, but any system that is only periodic in two dimensions — must possess a quadratic branch with zero group velocity around the $\Gamma$ point, corresponding to vibrations perpendicular to the plane of periodicity [CLL+2016]. This is a requirement of continuous rotational invariance, resulting in a second set of ASRs that do not have a direct effect on the spectra of 3D systems [GW1966]. Those ASRs need to be enforced on the raw IFCs obtained from DFT, which typically violate them by large margins. It is also necessary for consistency with elasticity theory in the long-wavelength limit, since one of the branches of Lamb waves in vibrating membranes is indeed predicted to have a quadratic dispersion curve [LLKP1986]. Unfortunately, the literature is full of proposed phonon spectra for 2D systems that show the effects of such violations: either nonzero group velocities at $\Gamma$ or a characteristic "pocket" of imaginary frequencies in the branch that should be quadratic, placed between $\Gamma$ and the first commensurate $\boldsymbol{q}$ in a given direction (e.g. [FZKS2015; JM2015; MKS2014; XHB2014], among dozens of other published studies). The effects on the calculated conductivity can be catastrophic, as shown in [CLL+2016] and in figure 5, where the numerical artifacts introduced by the neglect of symmetry cause errors of more than 100% and the reversal of the predicted anisotropy.

The situation with quasi-1D structures, such as nanotubes and nanowires, is more nuanced. On the one hand, large-diameter nanowires can be treated as a bounded sample of a bulk material with a suitable boundary scattering term [LML+2012]. On the other hand,

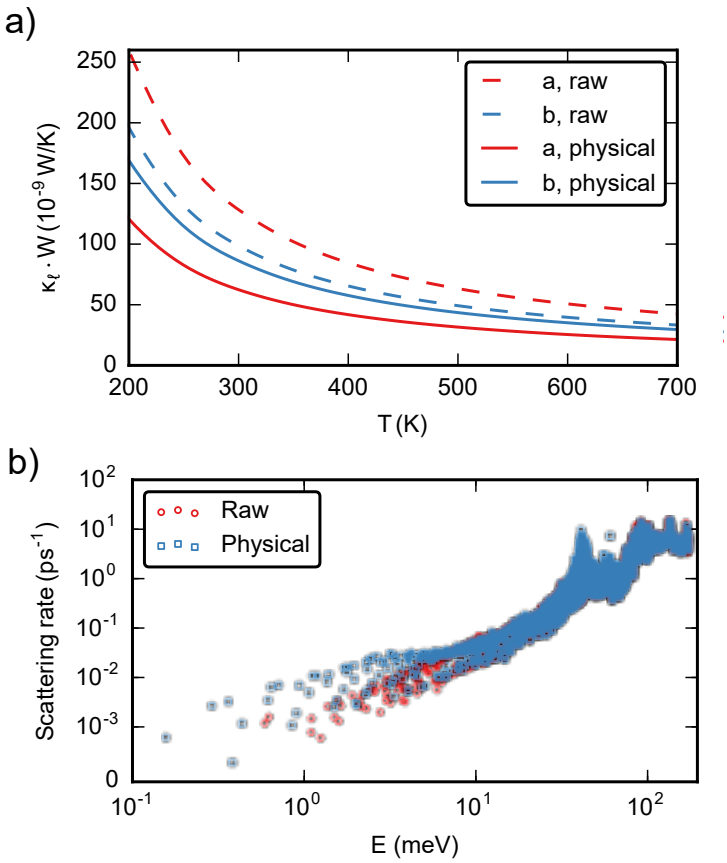


Figure 5: 2D thermal conductivity (a) and three-phonon scattering rates (b) in borophene, with a quasi-2D Pmmn structure, computed using IFCs from DFT fulfilling only the translational ASRs ("raw") or the full set of translational and rotational ASRs ("physical"). Reproduced from [CLL+2016], published under an open access CC-BY-4.0 license.

narrow quasi-1D nanostructures require explicit calculations of their phonon spectra, which is fraught with problems. First, the effect of rotational ASRs is even more marked than in 2D: they must be fulfilled so that the phonon spectrum contains four acoustic branches (instead of three), two of which must be quadratic. Second, the detection and handling of discrete symmetries is also a challenge. When only translations along the periodic axis are taken into account, the unit cell required to generate an infinite nanowire or nanotube contains a very large number of atoms, and accordingly the number of phonon bands is extremely large. As a matter of fact, the right kind of symmetry group to deal with these structures are not space groups but line groups [DM2010], combining generalized translations (including screw operations and glide planes) with axial point groups that are not

subject to the crystallographic restriction theorem and can therefore contain rotations of any order. Studying the vibrational modes of a nanowire or nanotube in terms of the irreducible representations of its line group not only enables the use of a much smaller motif (the so-called symcell), but also yields new quantum numbers to classify the phonon branches according to how they behave under rotations and reflections, analogously to how $\boldsymbol{q}$ characterizes the behavior of a each mode under translation [CNM2019]. The combined effect of neglecting the rotational ASRs and not using the full line group creates a host of numerical artifacts, detailed in figure. 6, that make the phonon spectrum unusable for further calculations. Unfortunately, most of the relevant software packages target 3D crystals and only implement space groups, and awareness about line groups among the community is very limited.

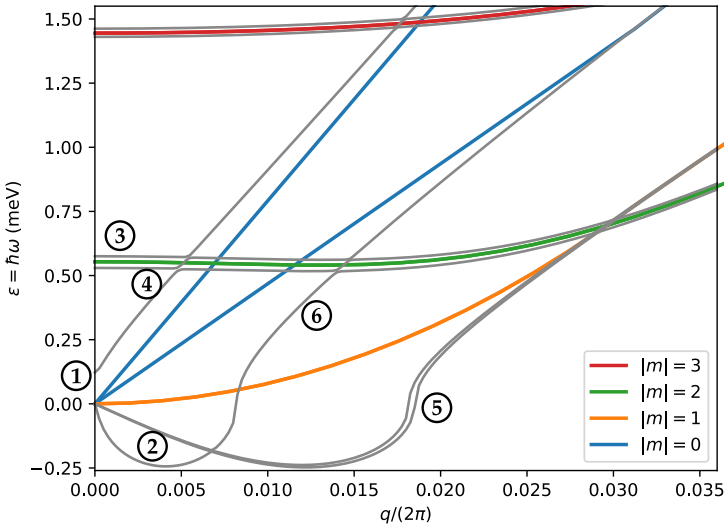


Figure 6: Common artifacts derived from treating phonons in quasi-1D structures using a 3D formalism, in the example of an $MoS_2$ nanotube: (1) wrong number of acoustic branches; (2) imaginary frequencies; (3) spurious breakdown of degeneracies; (4) misprediction of band crossings; (5) finite group velocities in branches that should be quadratic; (6) errors in the speed of sound. Reproduced from [CNM2019], published under an open-access CC-BY-3.0 license.

Regarding phonon scattering and thermal transport, the elastic transmission across several kinds of defects in quasi-1D settings has been studied from first principles [CGVM2011; MSBS2008] using the same Green's function formalism introduced for interfaces in the previous section (with the parallel component of $\boldsymbol{q}$ restricted to zero). However, the BTE formalism in the form explained so far is normally not applicable in this context because

of the high degree of anharmonicity. A rigorous treatment requires the use of anharmonic Green's functions, whose the formalism is known [GZB+2021] but for which no general implementation is in widespread use because of their high cost. Hence, alternative approaches using molecular dynamics [CLR+2019] or Green-Kubo-based methods [ZLL2016] are more often found in the literature when anharmonicity must be explicitly included.

### *3.4 Simulating time-dependent processes in structured systems.*

Motivated by the success of the BTE in treating steady-state lattice thermal transport in pristine and defect-laden crystalline materials, it is natural to wonder whether the formalism can be extended to simulate whole devices, containing regions with different materials and specific geometries. Moreover, for maximum usefulness those simulations should encompass time-dependent processes as well.

In this more general setting, one must go back to the phonon BTE in the form of Eq. (8) and the non-linearized form of the scattering operator in Eq. (17) (plus the relevant contributions from elastic scattering). Unfortunately, this is a large set of partial differential equations formulated over six spatial dimensions (three for $\boldsymbol{r}$ and three for $\boldsymbol{q}$) and over time, and thus runs into the so-called curse of dimensionality, whereby any attempt at a direct solution through the use of basis sets or a discrete grid scales very poorly. Although Monte Carlo (MC) methods are broadly applicable in such situations, MC simulations using phonons as particles have traditionally generated subpar outcomes. The reason is twofold: first, it is very hard to fulfill the conservation of energy in a context where the number of phonons is not conserved; second, the vast majority of the computational effort is wasted on modelling the equilibrium component of the distribution, which does not make any contribution to thermal transport. An alternative approach is energy-based variance-reduced MC (VRMC) [JN2012; PH2011], which deals with the deviation of the local energy distribution with respect to equilibrium at a reference temperature ($T_{\text{ref}}$): $g_\lambda(\boldsymbol{r},t) \coloneqq \hbar\omega_\lambda[f_\lambda(\boldsymbol{r},t) - f_{\text{BE},\lambda}(T_{\text{ref}})]$. That deviational distribution is then split into a fixed number, $N_{\text{part}}$, of samples or "particles":

$$g_\lambda(\boldsymbol{r},t) \simeq E_{\text{eff}} \sum_{p=1}^{N_{\text{part}}} \delta^3[\boldsymbol{r} - \boldsymbol{r}_p(t)]\delta^3[\boldsymbol{q} - \boldsymbol{q}_p]\delta_{\boxdot,\boxdot_p}. \tag{28}$$

Each of these particles has a well defined position and is associated to a phonon branch $\lambda \equiv (\boldsymbol{q}, \boxdot)$, but they represent packets of energy in one mode instead of phonons. By explicitly using $f_{\mathrm{BE},\lambda}(T_{\mathrm{ref}})$ as a reference by using particles whose number is conserved, VRMC avoids both classes of problems from ordinary phonon-based MC.

A particularly efficient implementation of the VRMC can be achieved under the RTA [PLH2014], since a regime can be defined where each deviational particle can be treated independently, and therefore the algorithm can be parallelized. Based on the physics of phonons, deviational particles are emitted and absorbed at isothermal reservoirs and temperature gradients, experience intrinsic scattering in bulk regions (including inelastic scattering with a change of frequency) and are reflected or transmitted at interfaces.

The public, open source version `almaBTE` package, which I coauthored and maintain [CVK+2017], implements this form of VRMC for the efficient and accurate simulation of structured systems. It also implements specific models for treating thin films, superlattices, alloys and transient phenomena in bulk systems, and contains a more advanced version of the capabilities of `ShengBTE`. Additional code implements the Green's functions methods for point defects and interfaces discussed in previous sections.

The computational cost of ab-initio VRMC in a full-BTE setting is much higher, due to the loss of the much simpler RTA form of the scattering operator. The formalism was introduced by Landon and Hadjiconstantinou in [LH2014], but using a low-performance scaling-and-squaring method to compute the large matrix exponential involved in the calculation of the propagator. `BTE-Barna` [RCC2022], an extension of `almaBTE` focusing on 2D materials, improves upon that original implementation by using a Krylov-subspace approach much better suited for the problem, along with an interpolation of the propagator for systems with multiple reference temperatures. The results show clear departures from the RTA in systems such as phosphorene nanoribbons, not only in the details of the phonon populations and the thermal flux, but in the effective thermal conductivity as well. This implementation opens the door to simulating phenomena, like second sound [HDC+2019], which are explicitly beyond the reach of the RTA. Figure 7 shows steady-state results for a three-terminal borophene device computed with `BTE-Barna`.

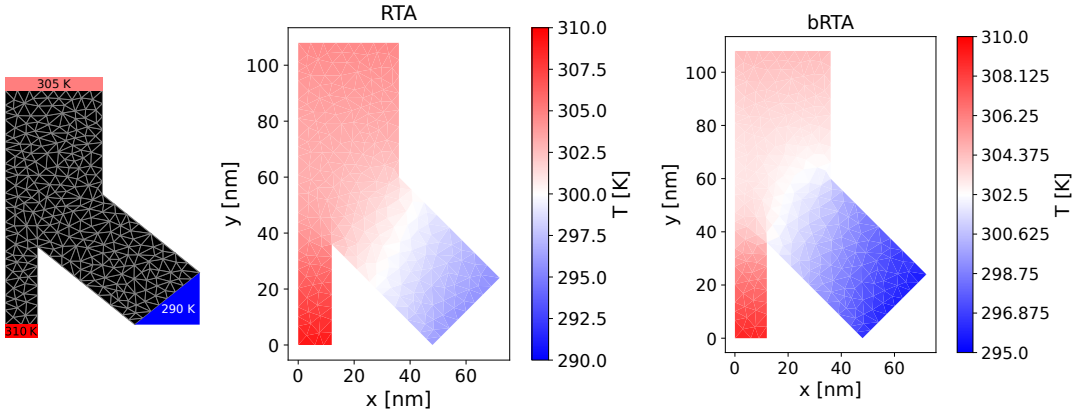


Figure 7: `BTE-Barna` prediction of the steady-state temperature distribution in a three-terminal structure made out of borophene, computed using VRMC. Left: boundary conditions and spatial grid used to gather deviational particle statistics. Center: RTA solution. Right: full-BTE solution. Adapted from [RCC2022], published under an open-access CC-BY-4.0 license.

### *3.5 Beyond three-phonon processes.*

The truncation of Eq. (10) at the third order is physically justifiable, but also born out of necessity, since the treatment of higher-order anharmonicity is computationally very expensive. However, situations exist where four-phonon processes cannot be ignored, either because the temperature is high enough or because three-phonon scattering is relatively weak. While one of the obstacles, namely the calculation of high-order IFCs, has been alleviated by the development of regression-based approaches and user-friendly software like `hiPhive` [EFE2019], the computational complexity of the detection of four-phonon processes and the calculation of their matrix elements remains a challenge, so far palliated mainly by the availability of more powerful computers. Packages like `FourPhonon` [HYL+2022], an extension of `ShengBTE` take care of harnessing the symmetries, running the calculations and solving the BTE, although in practice calculations must normally use a much sparser grid than for the third-order part. As more BTE solutions including higher order anharmonicity become available, the awareness about their importance in materials with extreme thermal behavior grows [LLWX2025]: for example, they are key in describing the ultrahigh thermal conductivity of $\theta$-phase TaN, a semimetal whose thermal transport is dominated by phonons [KYM+2021].

One of the clear signs that the description of thermal transport in a material must

go beyond three-phonon processes comes from the high-temperature behavior of its $\kappa_\ell(T)$ curve, which is characteristically $\propto T^{-1}$ for third-order anharmonicity. While including the four-phonon contribution changes this dependence, in very strongly anharmonic materials $\kappa_\ell(T)$ does not decrease with temperature at all, but instead shows a plateau. This behavior is very characteristic of crystals with very complex unit cells and of amorphous materials, and reproducing it requires going beyond a phonon-based formalism. The first semiquantitative treatment of this was the Allen-Feldman theory [AFFW1999], which classifies normal modes into propagons (extended and propagating), diffusons (extended but nonpropagating) and locons (localized). In a strongly anharmonic system where the scattering rates increase with frequency, the so-called Ioffe-Regel crossover, at which the lifetime of vibrations becomes shorter than half of their oscillation period, marks the threshold between propagons and diffusons. Heat transfer by diffusons depends on their diffusivity and cannot be treated with the BTE in the form seen so far. A modern unified theory was proposed in 2019 by Simoncelli et al. [SMM2019b], with explicit expressions for the diffuson contribution that can be computed ab initio. The diffusivity is related to the off-diagonal elements of the same group velocity operator appearing in Eq. (14).

### *3.6 Temperature-dependent IFCs.*

There are some situations in which the Taylor expansion of the potential energy in Eq. (10), which is intrinsically semilocal, is not a useful description of the energy landscape sampled by the system, but in which most of the associated formalism can still be applied if a different, more suitable effective harmonic approximation to their potential energy can be devised. This is useful, in particular, for two classes of systems: those crystals whose strong anharmonicity lead to temperature-dependent effective phonon bands, and some phases that are mechanically unstable below a certain temperature, and which therefore contain imaginary frequencies in their basic harmonic spectrum.

There are several different strategies to obtain such an effective harmonic potential, such as the temperature-dependent effective potential (TDEP) method [HAS2011], which uses samples from finite-temperature molecular dynamics trajectories, or the stochastic self-consistent harmonic approximation (SSCHA) [ECM2013], based on the minimization of a rigorous upper bound to the free energy of the system. On a practical level, all of them aim to achieve some degree of self-consistency between the configurations visited by

the system at a given temperature according to the effective potential and the energy and forces in those configurations. This is perhaps most explicit in the quantum self-consistent ab-initio lattice dynamics (QSCAILD) method [vCM2021]: starting from a version of the basic harmonic spectrum with the imaginary frequencies removed, it proceeds iteratively by generating a set of samples from the real-space probability density of atomic displacements predicted by quantum statistical mechanics, computing the forces on atoms in each of those configurations with DFT, and fitting a new potential based on those results, until convergence is achieved. QSCAILD has shown its capabilities in scenarios such as a high-throughput exploration of a set of about 400 oxide and fluoride perovskites [vCO+2016], including the detection of those that become cubic at finite temperature and an accurate calculation of their thermal conductivities, or the exploration of the complicated phase diagram of hafnia [BCNM2022]. Figure 8 shows the effective spectrum of cubic hafnia predicted in that reference, and specifically its evolution from unstable to stable at increased temperatures. All of those methods have in common that they require a significantly higher number of DFT calculations; therefore, strategies like importance sampling that enable the reuse of samples are very helpful in those contexts [BCNM2022]. Even beyond these extreme examples, it has been shown that temperature-dependent changes in the phonon spectrum can have a material impact on the predicted thermal conductivity of a variety of systems [LLWX2025].

### *3.7 Accelerated calculation of IFCs.*

A common feature of all the discussed presented in this section is their high computational cost, even compared to the already expensive basic BTE solution for pristine bulk crystals in the steady state presented earlier. Broadly speaking, that cost can be traced to the need to compute more IFCs or higher-order ones, which in turn translates into more or larger DFT calculations. Therefore, techniques that bypass or speed up those calculations can deliver important quantitative advances in terms of the number or complexity of systems that can be treated. This subsection will discuss a sample of such techniques, all emerging from the field of machine learning that is currently having a tremendous impact on materials science, as well as so many other areas of society.

The first example consists in exploiting the regularities among the IFCs of crystals with the same structure but different chemical compositions. While this has been known by

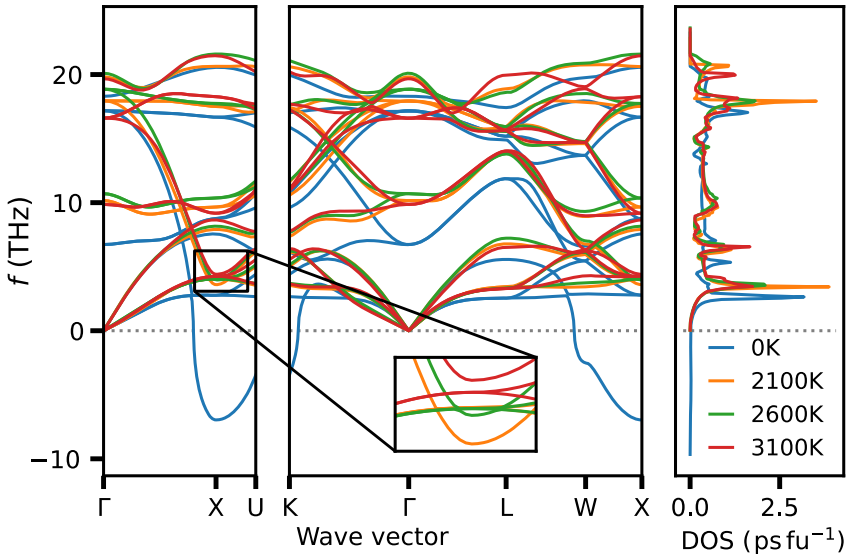


Figure 8: Temperature dependence of the computed effective phonon spectrum of hafnia, showing how that phase reaches mechanical stability. Reproduced from [BCNM2022], published under an open-access CC-BY-NC-4.0 license.

the community for a long time in particularly simple cases (e.g., computing the phonon spectrum of Ge with the harmonic IFCs of Si, and just changing the masses, yields quite a good result [GZB+2021]), modern regression techniques make it exploitable in more general settings. In [CLM+2014], a library formed by the approximately 80000 half Heuslers that could theoretically be built out of the non-radioactive elements of the periodic table is screened in search of promising candidates for thermoelectric applications. After filtering by criteria of mechanical and thermodynamical stability, and keeping only the semiconductors in the set, 75 candidates are left whose thermal conductivity must be obtained. To avoid explicitly calculating all the required anharmonic IFCs, a multiple multivariate linear regression model is built based on a smaller training set. The model exploits approximate linear dependencies between third-order IFCs, and results in a method to reconstruct the full third-order IFC tensor using just four constants as input, while respecting all the symmetries. The result has high predictive power, and was in fact even able to detect an outlier among the "exact" results that was later revealed to contain an error. By using this construction, the number of DFT calculations per compound is reduced from 344 to 16.

At the other end of the spectrum, a regression model can be created to predict the IFCs of compounds with the same chemical composition but different structure, i.e., of

polymorphs. In [LvRC+2018], this idea was applied to 121 non-equivalent mechanically stable minima of $KZnF_3$. Specifically, we used a random-forest regression [Bre2001] with equivariant inputs to predict the harmonic IFC tensors, with very good results for thermodynamic quantities at the quasiharmonic level and even for quantitative features of the IFCs themselves.

By far the most flexible and revolutionary contribution to the field from machine learning, however, is the development of machine-learning interatomic potentials (MLIP), advanced regression models that can model the dynamics of an atomistic system with ab-initio-like quality but at a cost similar to a classical potential. That area of research has exploded in the past decade, and it would be impossible to to present even a small survey of architectures here, so the reader is instead referred to a dedicated review [LZLS2025]. Suffice it to say that at the core of a MLIP is a machine-learning model, most often a kind of neural network, typically implemented on top of a modern framework like `Pytorch` [PGM+2019] or `JAX` [BFH+2018]. A key feature of those frameworks is the fact that they implement high-performance automatic differentiation [BPRS2017], i.e, the propagation of derivatives through a tree of elementary operations using systematic implementations of the chain rule. For instance, JAX implements both of the major modes of automatic differentiation, the forward and reverse modes, whose results are, respectively, a Jacobian-vector-product operator and a vector-Jacobian-product (VJP) operator. A single application of the VJP is enough to extract all the components of the gradient of a scalar-valued multivariate function (such as when extracting the forces on all atoms from the potential energy) at a cost comparable to that of evaluating the function itself, with a high degree of accuracy and almost negligible implementation effort. This marks a huge deviation from the traditional process of potential development when it comes to, e.g., making minimization algorithms or molecular dynamics possible; however, for IFC calculations the implications of automatic differentiation are much more extensive. The whole set of second-order IFCs can be obtained as a Jacobian of a gradient (forward mode composed over reverse mode); alternatively, the dynamical matrix at a $\boldsymbol{q}$ point can be evaluated from a JVP of a JVP and obtained without passing through the IFCs at all, and even the derivative of that dynamical matrix with respect to volume is readily accessible if that kind of anharmonic information is desired. Similarly, a high-order Taylor-series form of the potential energy can be evaluated at a point without computing the IFCs involved — which would be impossible on account

of the geometric growth of their number with the maximum order of the series — through recursive applications of differential operators [BCM2023]. Automatic differentiation blurs the line between classical potentials and ab-initio techniques like DFPT, and is starting to be applied directly in the first-principles world as well to overcome the performance, correctness and cost problems of the direct implementation of derivatives [LSD+2024].

MLIPs are making a fundamental contribution to the study of complex systems for which a direct DFT approach is unfeasible, and their usefulness has been demonstrated, among other cases, for defect-laden quasi-1D [CWMC2025], quasi-2D [PCWM2024] and 3D [DSC+2025] structures. A promising development is the release of so-called "foundation models" [BBC+2023], pretrained over large libraries of materials or molecules, which can be used directly or refined for a particular application, drastically reducing, or even completely eliminating, the effort of generating DFT data to train a model from scratch.

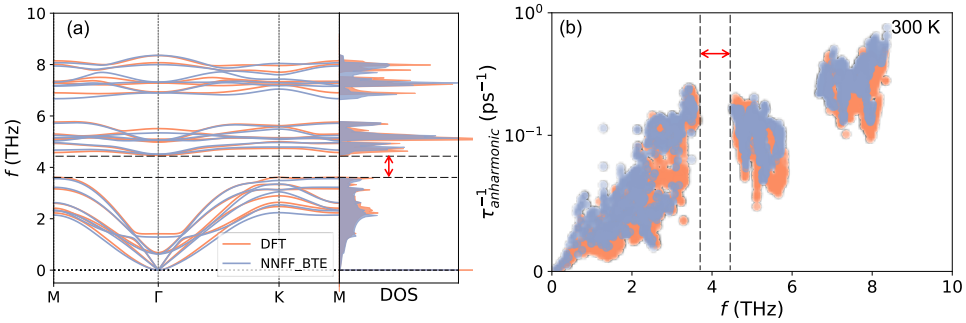


Figure 9: Comparison of the phonon spectrum and anharmonic phonon scattering rates of bilayer PtSTe calculated directly with DFT and through an MLIP based on NeuralIL [CMW+2023]. Reproduced from [PCWM2024], published under an open-access CC-BY-4.0 license.

## 4 Concluding remarks

Thermal transport is such an active field, with so many concurrent developments at different, but partially overlapping, levels of abstraction, that no single review can expect to cover but a small fraction of it. Nevertheless, I hope to have conveyed, at the very least, a message of optimism. After the first breakthroughs in computational solutions to the BTE with ab-initio dispersions, which shattered the traditional perspective that it was an unsolvable problem, progress has been remarkably fast, to the point that simulations of quite realistic models of devices are now possible. Not only have workable approximations

appeared for a large variety of phonon scattering mechanisms and combinations thereof that retain levels of predictive power similar to that of the first solvers for single crystals, but the software ecosystem has matured greatly to allow non-specialists to integrate this kind of research in more classes of studies. Examples of this are the increasing number of high-throughput screenings of thermal conductivities in different settings and the joint treatment of charge carrier and phonon transport from first principles. The next challenge, and one that has proven rather elusive so far despite some notable exceptions, is to make bigger inroads into industry, where a surprising amount of modelling is still done using finite-element solutions to the Fourier equation couple with other macroscopic differential equations.

**Acknowledgments.** I am honored and grateful to receive this prize from the Real Academia de Ciencias de Zaragoza and I extend my sincere thanks to its esteemed members for this recognition.

My work on ab-initio lattice thermal transport would not have been possible without the support of the incredibly talented teams I have been part of. The names of the people to which I owe a big debt of gratitude are too many to cite here, but I would be remiss if I did not mention my PhD advisors, Luis Miguel Varela and Luis Javier Gallego del Hoyo, the ShengBTE and almaBTE teams at CEA Grenoble and elsewhere, and all past and present members of Georg Madsen's group at TU Wien. Working with them has been the privilege and the honor of my lifetime. I am most deeply indebted to Natalio Mingo, a true scientific luminary whose intelligence and tireless creativity are behind many of the innovative techniques discussed in this review. His personality and work have left an indelible mark in me. May he rest in peace.

I cannot neglect to mention my colleagues and friends at INMA, whom I want to thank for creating a welcoming environment and broadening my scientific horizons.

Finally, I must also acknowledge grant PID2023-148359NB-C21 funded by MICIU/AEI /10.13039/501100011033 and the European Union FEDER, as well as all the funding I have received over the years from national and international institutions.

## References

[AV1962] B. K. Agrawal and G. S. Verma, *Phys. Rev.*, vol. 126, pp. 24–29, 1962. DOI: 10.1103/PhysRev.126.24.

[AFFW1999] P. B. Allen, J. L. Feldman, J. Fabian, and F. Wooten, *Philos. Mag. B*, vol. 79, pp. 1715–1731, 1999.

[ACMM2018] M. Arrigoni, J. Carrete, N. Mingo, and G. K. H. Madsen, *Phys. Rev. B*, vol. 98, p. 115 205, 2018. DOI: 10.1103/PhysRevB.98.115205.

[AL1987] J. A. Ashraff and P. D. Loly, *J. Phys. C: Solid State Phys.*, vol. 20, p. 4823, 1987. DOI: 10.1088/0022-3719/20/29/017.

[AT2024] K. S. Atsushi Togo and I. Tanaka, *Sci. Technol. Adv. Mater., Meth.*, vol. 4, pp. 2 384 822–2 384 836, 2024. DOI: 10.1080/27660400.2024.2384822.

[BdGDG2001] S. Baroni, S. de Gironcoli, A. Dal Corso, and P. Giannozzi, *Rev. Mod. Phys.*, vol. 73, pp. 515–562, 2001. DOI: 10.1103/RevModPhys.73.515.

[BBC+2023] I. Batatia *et al.*, 2023. arXiv: 2401.00096 [physics.chem-ph].

[BPRS2017] A. G. Baydin, B. A. Pearlmutter, A. A. Radul, and J. M. Siskind, *J. Mach. Learn. Res.*, vol. 18, pp. 5595–5637, 2017. [Online]. Available: https://dl.acm.org/doi/abs/10.5555/3122009.3242010.

[BGS+2015] S. Bhattacharya, N. S. H. Gunda, R. Stern, S. Jacobs, R. Chmielowski, G. Dennler, and G. K. H. Madsen, *Phys. Chem. Chem. Phys.*, vol. 17, pp. 9161–9166, 2015. DOI: 10.1039/C4CP05991C.

[BCM2023] S. Bichelmaier, J. Carrete, and G. K. H. Madsen, *Int. J. Quantum Chem.*, vol. 123, 2023. DOI: 10.1002/qua.27095.

[BCNM2022] S. Bichelmaier, J. Carrete, M. Nelhiebel, and G. K. H. Madsen, *Phys. Status Solidi RRL*, vol. 16, p. 2 100 642, 2022. DOI: 10.1002/pssr.202100642.

[Blö1994] P. E. Blöchl, *Phys. Rev. B*, vol. 50, p. 17 953, 1994. DOI: 10.1103/PhysRevB.50.17953.

[Bol1872] L. Boltzmann, *Sitzungsber. Kaiserl. Akad. Wiss., Math.-Naturwiss. Cl.*, vol. 66, pp. 275–370, 1872.

[BUBC1959] R. Bowers, R. Ure Jr, J. Bauerle, and A. Cornish, *J. Appl. Phys.*, vol. 30, pp. 930–934, 1959. DOI: 10.1063/1.1735264.

[BFH+2018] J. Bradbury *et al.*, *JAX: Composable transformations of Python+NumPy programs*, version 0.3.13, 2018. [Online]. Available: http://github.com/google/jax.

[Bre2001] L. Breiman, *Mach. Learn.*, vol. 45, pp. 5–32, 2001. DOI: 10.1023/a:1010933404324.

[BMB+2007] D. A. Broido, M. Malorny, G. Birner, N. Mingo, and D. A. Stewart, *Appl. Phys. Lett.*, vol. 91, p. 231 922, 2007. DOI: 10.1063/1.2822891.

[Cal1959] J. Callaway, *Phys. Rev.*, vol. 113, pp. 1046–1051, 1959. DOI: 10.1103/PhysRev.113.1046.

[CGVM2011] J. Carrete, L. J. Gallego, L. M. Varela, and N. Mingo, *Phys. Rev. B*, vol. 84, 2011. DOI: 10.1103/physrevb.84.075403.

[CVT+2018] J. Carrete, B. Vermeersch, L. Thumfart, R. R. Kakodkar, G. Trevisi, P. Frigeri, L. Seravalli, J. P. Feser, A. Rastelli, and N. Mingo, *J. Phys. Chem. C*, vol. 122, pp. 4054–4062, 2018. DOI: 10.1021/acs.jpcc.7b11133.

[CLL+2016] J. Carrete, W. Li, L. Lindsay, D. A. Broido, L. J. Gallego, and N. Mingo, *Mater. Res. Lett.*, vol. 4, pp. 204–211, 2016. DOI: 10.1080/21663831.2016.1174163.

[CLM+2014] J. Carrete, W. Li, N. Mingo, S. Wang, and S. Curtarolo, *Phys. Rev. X*, vol. 4, p. 011 019, 2014. DOI: 10.1103/PhysRevX.4.011019.

[CLR+2019] J. Carrete, M. López-Suárez, M. Raya-Moreno, A. S. Bochkarev, M. Royo, G. K. H. Madsen, X. Cartoixà, N. Mingo, and R. Rurali, *Nanoscale*, vol. 11, pp. 16 007–16 016, 2019. DOI: 10.1039/c9nr05274g.

[CMW+2023] J. Carrete, H. Montes-Campos, R. Wanzenböck, E. Heid, and G. K. H. Madsen, *J. Chem. Phys.*, vol. 158, p. 204 801, 2023. DOI: 10.1063/5.0146905.

[CNM2019] J. Carrete, V. Ngoc Tuoc, and G. K. H. Madsen, *Phys. Chem. Chem. Phys.*, vol. 21, pp. 5215–5223, 2019. DOI: 10.1039/c9cp00052f.

[CVK+2017] J. Carrete, B. Vermeersch, A. Katre, A. van Roekeghem, T. Wang, G. K. Madsen, and N. Mingo, *Comput. Phys. Commun.*, vol. 220, pp. 351–362, 2017. DOI: 10.1016/j.cpc.2017.06.023.

[CWMC2025] Y.-J. Cen, S. Wieser, G. K. H. Madsen, and J. Carrete, *Ab-initio heat transport in defect-laden quasi-1d systems from a symmetry-adapted perspective*, 2025. arXiv: 2508.06882 [cond-mat.mtrl-sci]. [Online]. Available: https://arxiv.org/abs/2508.06882.

[CKF+2013] P. Chen, N. A. Katcho, J. P. Feser, W. Li, M. Glaser, O. G. Schmidt, D. G. Cahill, N. Mingo, and A. Rastelli, *Phys. Rev. Lett.*, vol. 111, p. 115 901, 2013. DOI: 10.1103/PhysRevLett.111.115901.

[CXH+2023] A. Chu, X. Xie, C. M. Hermann, W. Stork, and J. Roth-Stielow, "Towards predictive lifetime-oriented temperature control of power electronics in e-vehicles via reinforcement learning," in *2023 IEEE International Conference on Big Data (BigData)*, 2023, pp. 1667–1676. DOI: 10.1109/BigData59044.2023.10386292.

[DM2010] M. Damnjanovic and I. Milosevic, *Line Groups in Physics: Theory and Applications to Nanotubes and Polymers*. Springer, 2010, ISBN: 9783642111716.

[DS2025] S. Das and U. Sen, *Maximum entropy principle for quantum processes*, 2025. arXiv: 2506.24079 [quant-ph].

[DCW+2020] B. Dongre, J. Carrete, S. Wen, J. Ma, W. Li, N. Mingo, and G. K. H. Madsen, *J. Mater. Chem. A*, vol. 8, pp. 1273–1278, 2020. DOI: 10.1039/c9ta11424f.

[DSC+2025] Y. Dou, K. Shimizu, J. Carrete, H. Fujioka, and S. Watanabe, *Phys. Rev. Mater.*, vol. 9, p. 034 601, 2025. DOI: 10.1103/PhysRevMaterials.9.034601.

[Eco2006] E. N. Economou, *Green's Functions in Quantum Physics*, 3rd ed. Springer, 2006.

[EFE2019] F. Eriksson, E. Fransson, and P. Erhart, *Adv. Theory Simul.*, vol. 2, p. 1 800 184, 2019. DOI: 10.1002/adts.201800184.

[ECM2013] I. Errea, M. Calandra, and F. Mauri, *Phys. Rev. Lett.*, vol. 111, 2013. DOI: 10.1103/physrevlett.111.177002.

[Eye2012] V. Eyert, *The Augmented Spherical Wave Method: A Comprehensive Treatment*. Springer, 2012, ISBN: 978-3-642-25864-0.

[FZKS2015] X. Fan, W. T. Zheng, J.-L. Kuo, and D. J. Singh, *J. Phys.: Cond. Matter*, vol. 27, p. 105 401, 2015. DOI: 10.1088/0953-8984/27/10/105401.

[Fei2010] P. J. Feibelman, *Top. Catal.*, vol. 53, pp. 417–422, 2010. DOI: 10.1007/s11244-010-9451-6.

[Fou1822] J. B. J. Fourier, *Théorie Analytique de la Chaleur*. Didot, 1822, ISBN: 9780486495316.

[GHK+2006] M. Gajdoš, K. Hummer, G. Kresse, J. Furthmüller, and F. Bechstedt, *Phys. Rev. B*, vol. 73, p. 045 112, 2006. DOI: 10.1103/PhysRevB.73.045112.

[GW1966] D. C. Gazis and R. F. Wallis, *Phys. Rev.*, vol. 151, pp. 578–580, 1966. DOI: 10.1103/physrev.151.578.

[GBB+2009] P. Giannozzi *et al.*, *J. Phys. Condens. Matter*, vol. 21, p. 395 502, 2009. DOI: 10.1088/0953-8984/21/39/395502.

[GAB+2017] P. Giannozzi *et al.*, *J. Phys.: Condens. Matter*, vol. 29, p. 465 901, 2017. DOI: 10.1088/1361-648X/aa8f79.

[GAT1994] X. Gonze, D. C. Allan, and M. P. Teter, *Phys. Rev. B*, vol. 50, pp. 13 035–13 038, 1994. DOI: 10.1103/PhysRevB.50.13035.

[GL1997] X. Gonze and C. Lee, *Phys. Rev. B*, vol. 55, pp. 10 355–10 368, 1997. DOI: 10.1103/PhysRevB.55.10355.

[GTFL1983] F. Guinea, C. Tejedor, F. Flores, and E. Louis, *Phys. Rev. B*, vol. 28, pp. 4397–4402, 1983. DOI: 10.1103/PhysRevB.28.4397.

[GZB+2021] Y. Guo, Z. Zhang, M. Bescond, S. Xiong, M. Nomura, and S. Volz, *Phys. Rev. B*, vol. 103, 2021. DOI: 10.1103/physrevb.103.174306.

[HYL+2022] Z. Han, X. Yang, W. Li, T. Feng, and X. Ruan, *Comput. Phys. Commun.*, vol. 270, p. 108 179, 2022. DOI: 10.1016/j.cpc.2021.108179.

[HAS2011] O. Hellman, I. A. Abrikosov, and S. I. Simak, *Phys. Rev. B*, vol. 84, 2011. DOI: 10.1103/physrevb.84.180301.

[HCD+2008] A. I. Hochbaum, R. Chen, R. D. Delgado, W. Liang, E. C. Garnett, M. Najarian, A. Majumdar, and P. Yang, *Nature*, vol. 451, pp. 163–167, 2008. DOI: 10.1038/nature06381.

[HDC+2019] S. Huberman, R. A. Duncan, K. Chen, B. Song, V. Chiloyan, Z. Ding, A. A. Maznev, G. Chen, and K. A. Nelson, *Science*, vol. 364, pp. 375–379, 2019. DOI: 10.1126/science.aav3548.

[JN2012] J.-P. Peraud and N.G. Hadjiconstantinou, *Appl. Phys. Lett.*, vol. 101, p. 153 114, 2012. DOI: 10.1063/1.4942836.

[JM2015] A. Jain and A. J. McGaughey, *Sci. Rep.*, vol. 5, p. 8501, 2015. DOI: 10.1038/srep08501.

[KCLM2014] N. A. Katcho, J. Carrete, W. Li, and N. Mingo, *Phys. Rev. B*, vol. 90, p. 094 117, 2014. DOI: 10.1103/PhysRevB.90.094117.

[KCD+2017] A. Katre, J. Carrete, B. Dongre, G. K. H. Madsen, and N. Mingo, *Phys. Rev. Lett.*, vol. 119, 2017. DOI: 10.1103/PhysRevLett.119.075902.

[KCM2016] A. Katre, J. Carrete, and N. Mingo, *J. Mater. Chem. A*, vol. 4, pp. 15 940–15 944, 2016. DOI: 10.1039/C6TA05868J.

[KCW+2018] A. Katre, J. Carrete, T. Wang, G. K. H. Madsen, and N. Mingo, *Phys. Rev. Materials*, vol. 2, p. 050 602, 2018. DOI: 10.1103/PhysRevMaterials.2.050602.

[Koh1999] W. Kohn, *Rev. Mod. Phys.*, vol. 71, pp. 1253–1266, 1999. DOI: 10.1103/RevModPhys.71.1253.

[KF1996] G. Kresse and J. Furthmüller, *Phys. Rev. B*, vol. 54, pp. 11 169–11 186, 1996. DOI: 10.1103/PhysRevB.54.11169.

[KYM+2021] A. Kundu, X. Yang, J. Ma, T. Feng, J. Carrete, X. Ruan, G. K. H. Madsen, and W. Li, *Phys. Rev. Lett.*, vol. 126, p. 115 901, 2021. DOI: 10.1103/PhysRevLett.126.115901.

[LV1984] P. Lambin and J. P. Vigneron, *Phys. Rev. B*, vol. 29, pp. 3430–3437, 1984. DOI: 10.1103/PhysRevB.29.3430.

[LLKP1986] L. Landau, E. Lifshitz, A. Kosevich, and L. Pitaevskii, *Theory of Elasticity* (Course of Theoretical Physics). Butterworth-Heinemann, 1986, ISBN: 9780750626330.

[LH2014] C. D. Landon and N. G. Hadjiconstantinou, *J. Appl. Phys.*, vol. 116, p. 163 502, 2014. DOI: 10.1063/1.4898090.

[LA1972] G. Le Guillou and H. Albany, *Phys. Rev. B*, vol. 5, p. 2301, 1972. DOI: 10.1103/PhysRevB.5.2301.

[LvRC+2018] F. Legrain, A. van Roekeghem, S. Curtarolo, J. Carrete, G. K. H. Madsen, and N. Mingo, *J. Chem. Inf. Model.*, vol. 58, pp. 2460–2466, 2018. DOI: 10.1021/acs.jcim.8b00279.

[LGHC2025] S. Li, S. Guo, T. Hoke, and X. Chen, *Mater. Today Electron.*, vol. 12, p. 100 156, 2025. DOI: 10.1016/j.mtelec.2025.100156.

[LSD+2024] T. Li, Z. Shi, S. G. Dale, G. Vignale, and M. Lin, "Jrystal: A jax-based differentiable density functional theory framework for materials," in *Machine Learning and the Physical Sciences Workshop at NeurIPS 2024*, 2024.

[LCKM2014] W. Li, J. Carrete, N. A. Katcho, and N. Mingo, *Comput. Phys. Commun.*, vol. 185, pp. 1747–1758, 2014. DOI: 10.1016/j.cpc.2014.02.015.

[LML+2012] W. Li, N. Mingo, L. Lindsay, D. A. Broido, D. A. Stewart, and N. A. Katcho, *Phys. Rev. B*, vol. 85, p. 195 436, 2012. DOI: 10.1103/PhysRevB.85.195436.

[LZLS2025] Y. Li, X. Zhang, M. Liu, and L. Shen, *J. Mater. Inform.*, vol. 5, 2025. DOI: 10.20517/jmi.2025.17.

[LLWX2025] Z. Li, H. Lee, C. Wolverton, and Y. Xia, *High-throughput computational framework for lattice dynamics and thermal transport including high-order anharmonicity: An application to cubic and tetragonal inorganic compounds*, 2025. arXiv: 2507.11750 [cond-mat.mtrl-sci].

[LY1999] E. H. Lieb and J. Yngvason, *Phys. Rep.*, vol. 310, pp. 1–96, 1999. DOI: 10.1017/S0370-1573(98)00082-9.

[LLC+2014] L. Lindsay, W. Li, J. Carrete, N. Mingo, D. A. Broido, and T. L. Reinecke, *Phys. Rev. B*, vol. 89, 2014. DOI: 10.1103/physrevb.89.155426.

[MCI+2024] S. Mahendran, J. Carrete, A. Isacsson, G. K. H. Madsen, and P. Erhart, *J. Phys. Chem. C*, vol. 128, pp. 1709–1716, 2024. DOI: 10.1021/acs.jpcc.3c06820.

[MKS2014] A. Manjanath, V. Kumar, and A. K. Singh, *Phys. Chem. Chem. Phys.*, vol. 16, pp. 1667–1671, 2014. DOI: 10.1039/C3CP54655A.

[MW2014] A. A. Maznev and O. B. Wright, *Am. J. Phys.*, vol. 82, pp. 1062–1066, 2014. DOI: 10.1119/1.4892612.

[MSBS2008] N. Mingo, D. A. Stewart, D. A. Broido, and D. Srivastava, *Phys. Rev. B*, vol. 77, 2008. DOI: 10.1103/physrevb.77.033418.

[Nak2015] S. Nakamura, *Rev. Mod. Phys.*, vol. 87, pp. 1139–1143, 2015. DOI: 10.1103/RevModPhys.87.1139.

[OPG1972] A. Okhotin, A. Pushkarskij, and V. Gorbachev, *Thermophysical Properties of Semiconductors*. Atomizdat, 1972.

[OS1996] M. Omini and A. Sparavigna, *Phys. Rev. B*, vol. 53, pp. 9064–9069, 1996. DOI: 10.1103/PhysRevB.53.9064.

[Ong2018] Z.-Y. Ong, *J. Appl. Phys.*, vol. 124, p. 151 101, 2018. DOI: 10.1063/1.5048234.

[Ons1931] L. Onsager, *Phys. Rev.*, vol. 37, pp. 405–426, 1931. DOI: 10.1103/PhysRev.37.405.

[PCWM2024] L. Pan, J. Carrete, Z. Wang, and G. K. H. Madsen, *J. Phys. Chem. C*, vol. 128, pp. 11 024–11 032, 2024. DOI: 10.1021/acs.jpcc.4c02454.

[PLK1997] K. Parlinski, Z. Q. Li, and Y. Kawazoe, *Phys. Rev. Lett.*, vol. 78, pp. 4063–4066, 1997. DOI: 10.1103/PhysRevLett.78.4063.

[PY1989] R. G. Parr and W. Yang, *Density Functional Theory of Atoms and Molecules*. New York: Oxford University Press, 1989.

[PGM+2019] A. Paszke *et al.*, "PyTorch: An Imperative Style, High-Performance Deep Learning Library," in *Advances in Neural Information Processing Systems 32*, H. Wallach, H. Larochelle, A. Beygelzimer, F. d'Alché-Buc, E. Fox, and R. Garnett, Eds., Curran Associates, Inc., 2019, pp. 8024–8035. [Online]. Available: http://papers.neurips.cc/paper/9015-pytorch-an-imperative-style-high-performance-deep-learning-library.pdf.

[PML2013] L. Paulatto, F. Mauri, and M. Lazzeri, *Phys. Rev. B*, vol. 87, p. 214 303, 2013. DOI: 10.1103/PhysRevB.87.214303.

[Pei1929] R. Peierls, *Ann. Phys.*, vol. 395, pp. 1055–1101, 1929. DOI: 10.1002/andp.19293950803.

[PH2011] J.-P. M. Peraud and N. G. Hadjiconstantinou, *Phys. Rev. B*, vol. 84, p. 205 331, 2011. DOI: 10.1103/PhysRevB.84.205331.

[PLH2014] J.-P. M. Peraud, C. D. Landon, and N. G. Hadjiconstantinou, *Ann. Rev. of Heat Transf.*, vol. 17, pp. 205–265, 2014. DOI: 10.1615/AnnualRevHeatTransfer.2014007381.

[PVR2012] E. Pop, V. Varshney, and A. K. Roy, *MRS Bull.*, vol. 37, pp. 1273–1281, 2012. DOI: 10.1557/mrs.2012.203.

[RCC2022] M. Raya-Moreno, X. Cartoixà, and J. Carrete, *Comput. Phys. Commun.*, vol. 281, p. 108 504, 2022. DOI: 10.1016/j.cpc.2022.108504.

[RCM2005] P. Reddy, K. Castelino, and A. Majumdar, *Appl. Phys. Lett.*, vol. 87, 2005. DOI: 10.1063/1.2133890.

[Rei2016] L. E. Reichl, *A Modern Course in Statistical Physics*, 4th ed. Wiley-VCH, 2016, ISBN: 978-3-527-41349-2.

[SHWR2000] K. Schwab, E. A. Henriksen, J. M. Worlock, and M. L. Roukes, *Nature*, vol. 404, pp. 974–977, 2000. DOI: 10.1038/35010065.

[SMM2019a] M. Simoncelli, N. Marzari, and F. Mauri, *Nat. Phys.*, vol. 15, pp. 809–813, 2019. DOI: 10.1038/s41567-019-0520-x.

[SMM2019b] M. Simoncelli, N. Marzari, and F. Mauri, *Nature Phys.*, vol. 15, pp. 809–813, 2019. DOI: 10.1038/s41567-019-0520-x.

[Spa2012] N. A. Spaldin, *J. Solid State Chem.*, vol. 195, pp. 2–10, 2012. DOI: 10.1016/j.jssc.2012.05.010.

[TS1971] P. Tamarin and S. Shalyt, *Sov. Phys. Semiconductors*, vol. 5, pp. 1097–1098, 1971.

[Tam1983] S. Tamura, *Phys. Rev. B*, vol. 27, pp. 858–866, 1983. DOI: 10.1103/physrevb.27.858.

[TCV+2018] L. Thumfart, J. Carrete, B. Vermeersch, N. Ye, T. Truglas, J. Feser, H. Groiss, N. Mingo, and A. Rastelli, *J. Phys. D: Appl. Phys.*, vol. 51, p. 014 001, 2018. DOI: 10.1088/1361-6463/aa98c5.

[TT2015] A. Togo and I. Tanaka, *Scr. Mater.*, vol. 108, pp. 1–5, 2015. DOI: 10.1016/j.scriptamat.2015.07.021.

[vCM2021] A. van Roekeghem, J. Carrete, and N. Mingo, *Comput. Physics Commun.*, vol. 263, p. 107 945, 2021. DOI: 10.1016/j.cpc.2021.107945.

[vCO+2016] A. van Roekeghem, J. Carrete, C. Oses, S. Curtarolo, and N. Mingo, *Phys. Rev. X*, vol. 6, p. 041 061, 2016. DOI: 10.1103/PhysRevX.6.041061.

[WCMM2019] T. Wang, J. Carrete, N. Mingo, and G. K. H. Madsen, *ACS Appl. Mater. Interfaces.*, vol. 11, pp. 8175–8181, 2019. DOI: 10.1021/acsami.8b17525.

[WWK+2010] Y. Wang, L. L. Wang, S. Kong, M. Lazzeri, and F. Giustino, *J. Phys.: Condens. Matter*, vol. 22, p. 202 201, 2010. DOI: 10.1088/0953-8984/22/20/202201.

[WB2010] A. Ward and D. A. Broido, *Phys. Rev. B*, vol. 81, p. 085 205, 2010. DOI: 10.1103/PhysRevB.81.085205.

[WBSD2009] A. Ward, D. A. Broido, D. A. Stewart, and G. Deinzer, *Phys. Rev. B*, vol. 80, p. 125 203, 2009. DOI: 10.1103/PhysRevB.80.125203.

[XHB2014] H. Xie, M. Hu, and H. Bao, *Appl. Phys. Lett.*, vol. 104, 2014. DOI: 10.1063/1.4870586.

[ZA2014] D.-B. Zhang and P. B. Allen, *Phys. Rev. B*, vol. 90, p. 035 203, 2014. DOI: 10.1103/PhysRevB.90.035203.

[ZFM2007] W. Zhang, T. S. Fisher, and N. Mingo, *Numer. Heat Transf. B: Fundam.*, vol. 51, pp. 333–349, 2007. DOI: 10.1080/10407790601144755.

[ZNXO2014] F. Zhou, W. Nielson, Y. Xia, and V. Ozoliņš, *Phys. Rev. Lett.*, vol. 113, p. 185 501, 2014. DOI: 10.1103/PhysRevLett.113.185501.

[ZLL2016] L. Zhu, B. Li, and W. Li, *Physical Review B*, vol. 94, 2016, ISSN: 2469-9969. DOI: 10.1103/physrevb.94.115420. [Online]. Available: http://dx.doi.org/10.1103/PhysRevB.94.115420.

[Zim1960] J. Ziman, *Electrons and Phonons: The Theory of Transport Phenomena in Solids*. Oxford University Press, 1960, ISBN: 9780198512356.

[ZWFB1990] A. Zunger, S.-H. Wei, L. G. Ferreira, and J. E. Bernard, *Phys. Rev. Lett.*, vol. 65, pp. 353–356, 1990. DOI: 10.1103/PhysRevLett.65.353.

*Rev. Real Academia de Ciencias. Zaragoza.* **80:** 93–96, (2025). ISSN: 0370-3207

# IN MEMORIAM
## Excmo. Sr. D. Luis Boya Balet

Manuel Asorey Carballeira
José Fernando Cariñena Marzo
Académicos numerarios

1936 – 2025

El pasado 1 de octubre falleció en Zaragoza, tras una larga enfermedad, el profesor Luis Joaquín Boya a los 89 años de edad. Boya dedicó toda su vida a la docencia, investigación y divulgación de la Física Teórica y Matemática. Era un experto de primer nivel en esos campos, poseedor de una enorme cultura científica y humanística, todo ello auspiciado por una curiosidad inagotable.

Luis Joaquín Boya nació en Zaragoza en 1936 y cursó sus estudios de Licenciado en Física en la Universidad de Zaragoza, título que obtuvo en 1958 siendo galardonado con el Premio Nacional de Fin de Carrera en 1960. Durante los años 1958-1960 fue profesor

encargado de cátedra de la Universidad de Zaragoza. Para completar su tesis doctoral se desplazó a la Universidad de Birmigham para trabajar en el grupo del profesor Rudolf Peierls durante los años 1960-1962 con ayuda de una Beca de la Fundación Juan March. Retornó a Barcelona donde defendió su tesis doctoral en 1964 bajo la dirección del profesor aragonés Luis Maria Garrido y del propio Rudolf Peierls. El título de la tesis fue *Teoría del Momento de Inercia Nuclear*. Posteriormente fue nombrado profesor adjunto interino en la Universidad de Barcelona (1963-1968) hasta que ganó una plaza de profesor agregado por oposición en la Universidad de Valladolid (1968-1973). Posteriomente obtuvo por traslado una plaza de profesor agregado en la Universidad de Zaragoza (1973-1976). Consiguió una plaza de catedrático de Física Matemática en la Universidad de Salamanca (1976-1981) y finalmente, por traslado, regresó a la Universidad de Zaragoza como catedrático de Mecánica Cuántica donde ejerció como tal hasta su jubilación en 2006, año en el que fue nombrado profesor emérito de su querida *alma mater*.

Su vinculación a Zaragoza no fue óbice para que realizase largas estancias como profesor visitante en las universidades de Californa (dos años), Montreal (dos años) y sobre todo en Austin (1986-2014, 28 años seguidos). En esta última, colaboró con figuras como Arno Bohm, Steven Weinberg y sobre todo George Sudarshan con quien publicó siete artículos científicos.

Una de las peculiares características de Boya es que trataba de evitar la burocracia y gestión en todo lo posible, reservando su tiempo para la docencia e investigación. A pesar de ello, no eludió sus responsabilidades y fue secretario de las facultades de ciencias de Valladolid (1969-1971) y Zaragoza (1974-1976), Decano electo por votación de la Facultad de Ciencias de Salamanca, cargo al que renunció sin llegar a tomar posesión, director del Departamento de Física Teórica de la Universidad de Zaragoza (1985-1987) y decano interino de la Facultad de Ciencias de Zaragoza (1987).

Otro capítulo aparte es su relación con la Real Academia de Ciencias Exactas, Físicas, Químicas y Naturales de Zaragoza en la que Luis Joaquín Boya ingresó el 26 de noviembre de 1996, puesto para el que había sido elegido más de 15 años antes, coincidiendo con una década en la que la Academia desarrolló muy poca actividad. Cuando Boya se incorporó a la Academia ésta se encontraba en una etapa de reactivación bajo la presidencia de Horacio Marco Moll, quien precisamente fue quien dio contestación a su discurso de ingreso titulado *Origen de la vida y evolución de las primeras formas vivientes*. Recibió la medalla número

18, en la que le habían precedido Pedro Ramón y Cajal, y Francisco Grande Covián. Desde entonces tuvo una participación muy activa en la vida de la Academia llegando a ocupar el cargo de vicepresidente de la Academia en 2001, presidente de la sección de Físicas (2004–06), y presidente de la Academia en 2008 hasta las vísperas del centenario. Finalmente, el 16 de mayo de 2019 pasa a Académico honorario. Un año mas tarde de su incorporación como académico, Luis Joaquín Boya también fue galardonado con la medalla de la Real Sociedad Española de Física en 1997. Posteriormente fue elegido presidente del Grupo Especializado de Comunicación y Divulgación de la Física de la RSEF (2014).

En todos los años de su prolongada carrera científica dedicó gran parte de su inagotable energía a estudiar el papel de las simetrías en Física Fundamental, así como los efectos geométricos y topológicos de la física cuántica y la teoría de campos gauge no abelianos.

Destacó por sus sólidos y pioneros conocimientos de geometría diferencial moderna, interesándose por problemas como el confinamiento de los quarks, las aplicaciones de los espacios fibrados a las teorías gauge no abelianas, solitones, teoría de Morse, etc.

Motivado por sus estancias en la Universidad de Texas en Austin, realizó contribuciones a la conexión espín-estadística, a la teoría de cuerdas, a la fase de Berry, a ciertos aspectos de la geometría y la topología de los grupos de Lie, etc. En sus últimos años se apasionó por la teoría de grupos finitos esporádicos y en especial por el 'monstruo'.

En total escribió mas de 120 artículos científicos, además de 40 artículos de divulgación conteniendo algunos de ellos ensayos sobre temas profundos de física y filosofía y numerosas notas de prensa sobre temas de actualidad.

Dirigió una decena de tesis doctorales y codirigió dos más. Sus discípulos han ocupado cátedras en las Universidades de Salamanca, Valencia. Zaragoza y Centros de Investigación del CSIC. También organizó varias conferencias internacionales destacando por relevancia la de Salamanca en 1992 e impartido numerosas conferencias invitadas, destacando también la pronunciada en la *S.N. Bose Conference* de la *Calcutta Mathematical Society.*

Hay una característica de Luis Joaquín que vale la pena destacar, precisamente por lo que escasea: su vasta formación y curiosidad. Quizás no todos conozcan su sólida formación en química, bioquímica, evolución, en cuestiones epistemológicas y en filosofía de la ciencia, ni sus incursiones en temas tan dispares como la fusión fría o el papel de los virus en el origen de la vida organizada, sobre lo que escribió un artículo con su hija Patricia,

bióloga, en 1992. Otra área que fascinaba a Luis Joaquín era la historia de la Ciencia, donde dejó magníficos artículos sobre la *Física teórica en Estados Unidos 1900-2000: de Gibbs a Witten*, *La escuela de Gotinga versus la interpretación de Copenhague*, *El nacimiento de la Mecánica Cuántica, Heisenberg y el proyecto atómico alemán*. Luis Joaquín era un apasionado defensor de Werner Heisenberg y crítico de Niels Bohr, lo que reflejó en estas dos obras suyas: *Mi clásico favorito: Werner Heisenberg y Rejection of the light quantum: the dark side of Niels Bohr* –que le valieron algunas controversias– y en el libro que dejó inconcluso sobre Bohr.

Algunos de sus artículos tuvieron un impacto inesperado: Luis Joaquín publicó en la revista *LLUL* una detallada monografía sobre la cosmología moderna en la que reprochaba a Ralph A. Alpher y a Robert C. Herman, discípulos de George Gamow, su desinterés en una búsqueda sistemática de la radiación de fondo de microondas que habían predicho. Dicha reflexión mereció una respuesta airada de los propios Alpher y Herman afirmando que intentaron convencer repetidamente a sus colegas experimentales para que iniciasen dicha búsqueda, pero que fracasaron en el empeño (Arno A. Penzias y Robert W. Wilson la encontraron por azar y recibieron el Nobel de 1978).

Otra característica de su concepción de la ciencia moderna era su peculiar visión de la filosofía y de la interacción de la ciencia con la religión como se puede entrever en sus obras *Albert Einstein y la religión* y *Dos problemas filosóficos de la mecánica cuántica y relevancia de la ciencia moderna en la enseñanza de la religión*. Además, realizó una amplia labor divulgadora con múltiples conferencias en una gran variedad de centros, tanto nacionales como extranjeros, numerosos artículos en el *Heraldo de Aragón*, la *Revista de Física de la RSEF*, la revista zaragozana *ConCiencia*, *Arbor*, etc.

Creemos que no procede detallar aquí otros aspectos de la vida profesional de Luis Joaquín que le permitieron interaccionar con científicos de numerosos países, su empatía y fluidez en varios idiomas, etc. Uno de los logros más importantes de un profesor e investigador es haber dejado una escuela a través de la cual se perciba su estilo y su influencia. El éxito de Luis Joaquín en este punto ha sido especialmente notorio; estamos seguros de que se sentiría legítimamente orgulloso de la extensa escuela que llegó a crear.

*Rev. Real Academia de Ciencias. Zaragoza.* **80:** 97–101, (2025). ISSN: 0370-3207

# IN MEMORIAM
## Ilmo. Sr. D. Rafael Núñez-Lagos Roglá

Pablo J. Alonso Gascón Presidente de la Sección de Físicas
María Luisa Sarsa Sarsa Académica numeraria

Madrid, 12-02-1936 – 17-11-2025

El 17 de noviembre de 2025 falleció Don Rafael Núñez-Lagos Roglá, gran profesor, respetado y valorado por muchas promociones de licenciados en Física por la Universidad de Zaragoza y querido compañero en la Real Academia de Ciencias Exactas, Físicas, Químicas y Naturales de Zaragoza. En la Academia ostentó la medalla número 7 desde 1997 hasta 2019, cuando pasó a ser académico honorario. Su discurso de ingreso *Cien Años de Radiactividad* lo dedicó a conmemorar el centenario del descubrimiento de la radiactividad, uno

de los temas a los que dedicó una buena parte de su trayectoria investigadora. Fue Presidente de la Sección de Físicas de la Real Academia de Ciencias Exactas, Físicas, Químicas y Naturales de Zaragoza desde 2005 hasta 2015.

En conjunto, y vista con la perspectiva que da el paso del tiempo, su larga trayectoria en el ámbito académico e investigador refleja un notable equilibrio entre excelencia académica y compromiso con la enseñanza universitaria, excelencia investigadora al más alto nivel, y vocación por la transferencia. Todo ello ha contribuido a que Don Rafael se constituyera en una figura destacada y respetada dentro de la comunidad científica española.

Rafael Núñez-Lagos Roglá nació un 12 de febrero de 1936 en Madrid, donde cursó los estudios de Bachiller en el Instituto Nacional Ramiro de Maeztu, titulándose en junio de 1953. Allí también desarrolló sus estudios universitarios, obteniendo el título de Licenciado en Ciencias Físicas por la Universidad Complutense de Madrid en junio de 1958 y el título de Doctor en Ciencias Físicas también por dicha Universidad en octubre de 1961.

Su tesis doctoral, desarrollada en la Junta de Energía Nuclear, se tituló *Campos libres del Neutrino y del Fotón* y fue dirigida por Alberto Galindo, insigne físico teórico de origen aragonés, que hacía poco que se había trasladado de Zaragoza a Madrid. Los años transcurridos en la JEN marcarían su futuro profesional. Allí empezó a trabajar con Ángel Morales Villasevil, también doctorando de Alberto Galindo. En esos años, junto con otros notables físicos de la época, crearon e impulsaron el GIFT (Grupo Interuniversitario de Física Teórica).

Muy pronto se implicó con entusiasmo en las tareas docentes, siendo Profesor Ayudante de Clases Prácticas en la Facultad de Ciencias de la Universidad Complutense de Madrid desde 1958 y Profesor Adjunto Interino desde 1961, siendo becario primero e investigador después en la Junta de Energía Nuclear, donde desarrollaba en paralelo sus tareas investigadoras.

Realizó una estancia postdoctoral de un año en el California Institute of Technology (CalTech), en Estados Unidos, entre 1961 y 1962, así como varias estancias en el *European Centre for Nuclear Research*, CERN, Ginebra, Suiza (1964, 1967, 1974) y en el *International Centre for Theoretical Physics* ICTP, Trieste, Italia (1965, 1970).

En 1967 accedió al cuerpo de catedráticos de Universidad, con solo 31 años. Fue Catedrático en la Universidad de Granada entre el 13-4-1967 y el 31-8-1968, Catedrático en la Universidad de Sevilla entre el 1-9-1968 y el 28-3-1970, y finalmente Catedrático en la Universidad de Zaragoza entre el 29-3-1970 y el 3-9-2006, cuando pasó a ser Profesor Emérito de dicha Universidad. Entre 2007 y 2019 fue Colaborador extraordinario en el Área de Física Atómica, Molecular y Nuclear del Departamento de Física Teórica de la Universidad de Zaragoza.

A lo largo de su amplia labor docente transmitió sus profundos conocimientos y su pasión por la Ciencia con rigor y entusiasmo, siendo recordado por la mayoría de los que fuimos sus alumnos como un excelente docente, en particular en sus clases de Física Cuántica, en tercer curso de la licenciatura en Física, que impartió prácticamente hasta la extinción de dicha titulación e implantación de los estudios de grado.

Ocupó numerosos cargos académicos a lo largo de su carrera. Así, por ejemplo, fue Secretario de la Facultad de Ciencias de la Universidad de Granada durante su breve paso por dicha Universidad, colaborando en la creación de la entonces nueva Facultad de Ciencias. También en la Universidad de Sevilla, poco después, fue Secretario de la recién creada Facultad de Ciencias, siendo además el primer director del Departamento de Física Atómica y Nuclear de dicha Universidad entre 1968 y 1970. Ya en la Universidad de Zaragoza, fue Vicedecano de la Facultad de Ciencias de 1974 a 1981, y decano en funciones en 1980.

En relación a sus actividades investigadoras, pasó de un perfil teórico en sus inicios a un perfil cada vez más experimental, disfrutando del trabajo de laboratorio y colaborando en la puesta a punto de los detectores y blindajes de los experimentos en los que se empezó a involucrar el grupo de investigación que se creó en torno a las figuras de Ángel Morales y Rafael Núñez-Lagos en el área de Física Atómica, Molecular y Nuclear de la Universidad de Zaragoza. En los años 80 empezaron a trabajar en medidas de la desintegración doble beta del Ge-76 en el túnel de Fréjus, en Francia, para a continuación, plantear y proponer un experimento en España, para el que buscaron un emplazamiento adecuado. Rafael Núñez-Lagos fue cofundador y promotor del Laboratorio Subterráneo de Canfranc (LSC), contribuyendo al mantenimento y mejora de sus instalaciones como laboratorio de

la Universidad de Zaragoza. En dichas instalaciones se desarrollaron experimentos tanto de desintegración doble beta como de búsqueda de la materia oscura del Universo, en el marco de importantes colaboraciones internacionales desde 1985.

Entrada del túnel de Somport, 1985

A partir de los años 90, se involucró en distintos proyectos relacionados con la medida de la radiactividad medioambiental y caracterización de materiales, colaborando con el Consejo de Seguridad Nuclear. Fue fundador y director del Laboratorio de Bajas Actividades de Aragón creado y financiado por la Diputación General de Aragón desde 1990 hasta su desaparición en 1996. Continúo la tarea iniciada a partir de 1997, pero desde la Universidad de Zaragoza, siendo fundador y director (hasta 2010) del Laboratorio de Bajas Actividades de la Universidad de Zaragoza, LABAC, perteneciente a la Red Densa REVIRA de Vigilancia Radiactiva Ambiental del Consejo de Seguridad Nuclear. Siguió colaborando en el LABAC después de su jubilación. El LABAC sigue siendo un centro de referencia para medidas de radiactividad, con acreditación ENAC, que gestiona proyectos con empresas y ofrece una cartera de servicios especializada. En esta faceta de transferencia de conocimiento, también fue promotor del Laboratorio del Amplificador de Energía y presidente (de 1997 a 1998) de LAESA, una sociedad anónima creada para su promoción y gestión. Fue este un proyecto controvertido, con alta repercusión mediática, que finalmente no fructificó.

Dirigió 7 tesis doctorales. Sus doctorandos fueron Julio Morales Villasevil, Amalio Fernández-Pacheco Pérez, José V. García Esteve, Pedro Andreo, Nuria Catalán Lasheras, Daniel López Bruna y Carmen Pérez Marín.

Entre los reconocimientos a su trayectoria destaca la Medalla de la Real Sociedad Española de Física en 2005. También fue nombrado Miembro Honorario del Colegio Oficial de Físicos de España en 1996.

Fue un miembro comprometido de la Real Sociedad Española de Física, siendo Vicepresidente de la misma entre noviembre de 1995 y octubre de 1999. Participó activamente en la organización de sus reuniones bienales, destacando la desarrollada en Jaca en 1993, en la que presidió el comité organizador. Consiguió elaborar un programa que contaba con la presencia de varios premios Nobel. Fue también miembro de la *European Physical Society*, la Sociedad Nuclear Española y la Sociedad Española de Protección Radiológica. A nivel internacional, fue el presidente del Comité Español de la Unión Internacional de Física Pura y Aplicada entre 1996 y 2005 y representante de España en la Asamblea General del *International Council of Scientific Unions* (ICSU) en varias ocasiones, siendo Vicepresidente de la Comisión Española en dicho consejo entre 2005 y 2009.

Su gran capacidad de trabajo, su carácter afable, su generosidad y su fineza intelectual se dejó sentir durante los veintidós años que permaneció en la Academia, en particular durante la década que ocupó la presidencia de la sección de Físicas. Durante la misma cuatro nuevos académicos de la sección leyeron su discurso y dos más fueron propuestos al término de su presidencia, completándose el número de académicos de la sección. La modificación del reglamento de premios de investigación cristalizó con el comienzo de su presidencia y los últimos años de su presidencia coincidieron con la organización de los actos del centenario de la Academia que se celebraría en 2016. En particular es de destacar su notable labor en la coordinación de la contribución de la sección al libro conmemorativo *Academia de Ciencias de Zaragoza, un siglo de Servicio a la Sociedad.*

Descanse en paz.

*Rev. Real Academia de Ciencias. Zaragoza.* **80:** 103–105, (2025). ISSN: 0370-3207

# NOTA NECROLÓGICA
## Ilmo. Sr. D. Prof. Francisco García Novo

Juan Pablo Martínez Rica

Académico de Honor

El pasado 15 de Julio falleció, en la ciudad de Sevilla, el Profesor Francisco García Novo, Académico Correspondiente de nuestra Academia.

Francisco García Novo ("Fuco" para los amigos, ante los cuales nunca usaba otro nombre, a pesar de que estaba orgulloso de su nombre de pila, que correspondía, según él, al santo más ecológico) nació en Madrid en 1943. Perteneció al selecto grupo de los "ecólogos de la segunda generación", formados por los "padres fundadores de la ecología española", Ramón Margalef, Fernando González Bernáldez, José Antonio Valverde, Pedro Montserrat, etc. Todos ellos, y también Francisco García Novo, tenían el rasgo común de haber comenzado su formación científica en el CSIC, pasando después, en algunos casos, a la universidad.

García Novo comenzó su preparación científica por la puerta grande: Se licenció en Ciencias Biológicas en la Universidad Complutense (1966), obteniendo el Premio Extraordinario de Licenciatura y el Premio Nacional de Fin de Carrera. Elaboró su tesis doctoral sobre el déficit hídrico en las plantas, bajo la dirección de Fernando González Bernáldez, y la defendió en 1968, obteniendo también el Premio Extraordinario de Doctorado. Su director se había familiarizado con las técnicas estadísticas del análisis multifactorial, y la tesis de García Novo fue la primera tesis ecológica que las empleó en España. También fue García Novo uno de los primeros biólogos que empleó en España aquellos grandes ordenadores de los años 60 que devoraban paquetes de tarjetas perforadas y vomitaban los resultados en largas tiras de grandes hojas martilleadas por impresoras ruidosas.

Continuó su formación científica entre 1966 y 1968 trabajando en el Instituto de Edafología del CSIC (hoy Centro de Ciencias Medioambientales), donde colaboró con González Bernáldez y con Pedro Montserrat. Luego llevó a cabo una corta estancia postdoctoral en Portugal (1968), se casó con Marisa Bouzas en 1968 y para toda la vida, y ambos partieron para una estancia más larga (1968-1975) en la Universidad de St. Andrews, en Escocia, cerca de Edimburgo. Allí, siempre ayudado por su esposa, llevó a cabo estudios sobre los ecosistemas costeros, que ya había iniciado en Doñana, y, bajo la dirección del Profesor Robert Crawford, elaboró una segunda tesis doctoral sobre fisiología vegetal, alcanzando así un doctorado por aquella universidad.

En 1977 obtuvo la cátedra de Ecología de la Universidad de Sevilla, y se trasladó de forma definitiva a esa ciudad, donde su trabajo y su familia podían gozar de claras ventajas. Los frutos de estas oportunidades no tardaron en manifestarse: las publicaciones científicas firmadas por García Novo, y a menudo también por discípulos suyos, superan las 300, el número de tesis doctorales dirigidas se acerca a las 40 y el número de citas de sus trabajos, recibidas por parte de otros autores supera las 3700. De entre este inmenso repertorio de publicaciones cuesta mucho seleccionar las relevantes, pues la mayoría lo son, y sus alumnos y colegas discrepan sobre la selección más acertada. Para nuestra Academia, quizás tienen mayor interés los discursos de ingreso en las distintas Academias científicas a las que perteneció, especialmente en la Real Academia Nacional de Ciencias Exactas, Físicas y Naturales de España.

Ingresó García Novo en esa Academia el día 28 de marzo de 2007, con un discurso de ingreso titulado *"La diversidad biológica"*, un tema que constituye el fundamento de la ecología evolutiva y que permanece actual desde el trabajo seminal de Margalef sobre la teoría de la información en biología (1953). El discurso es un modelo de lectura obligada para los estudiantes que busquen una primera aproximación al contenido de la ecología teórica y de la ecología aplicada, En la Real Academia de Ciencias de España, García Novo ha contribuido además con diversas tareas de importancia, siendo Secretario de la Sección de Ciencias Naturales de esa Real Academia y Presidente de su Comisión de Relaciones Internacionales. Y en su calidad de Presidente de dicha Comisión, ha ayudado a otras academias, y entre ellas a la de Zaragoza, a vincularse con la central, a integrarse en las redes académicas europeas, y a participar de sus proyectos y labores.

No es posible detenerse en las restantes instituciones académicas de las que García Novo formó parte. Fue también Académico Correspondiente de nuestra Casa, y contribuyó a las actividades de la misma con diversas conferencias y publicaciones. Entre éstas últimas destaca el volumen 44 de nuestra serie de Monografías, dedicado a exponer la historia de las Academias de Ciencias en Europa.

García Novo fue director de numerosos cursos de Medio Ambiente, Impactos ambientales, Gestión de Espacios, Ecología de la Conservación, Ecología Humana y Recursos Naturales en universidades e instituciones de España, Portugal, Italia y Argentina.

Fue distinguido con el Premio Rey Jaime I de Medio Ambiente (1995), la Cruz de Alfonso X el Sabio (1967) y la Medalla de Plata de la Universidad de Bari, amén de otras muchas distinciones.

*Rev. Real Academia de Ciencias. Zaragoza.* **80:** 107–110, (2025). ISSN: 0370-3207

# NOTA NECROLÓGICA
## Ilmo. Sr. D. Prof. Charles A. Micchelli

Mariano Gasca González

Académico numerario, sección de Exactas

El profesor Charles A, Micchelli, Académico Correspondiente de la Real Academia de Ciencias de Zaragoza en su Sección de Exactas falleció en su domicilio de Mohegan Lake, N.Y, U.S.A. el 13 de marzo de 2025.

Nacido el 22 de diciembre de 1942 en el seno de una familia italo-americana en Newark, N.J., U.S.A., se graduó en su ciudad natal en la *East Side High School*, en la que conoció a la que sería su esposa, Patricia. Tras graduarse en Matemáticas en *Rutgers University* en 1964, se casó con Pat en 1965 y se graduó como doctor en la *Stanford University* en 1969 bajo la dirección del Profesor Samuel Karlin.

Tras una estancia de investigación de un año en el Depto. de Ciencias Computacionales de la Universidad de Uppsala, Suecia, fue reclutado por el matemático Theodore J. Rivlin de IBM como investigador en el departamento de Ciencias Matemáticas del *IBM Thomas J. Watson Research Center* en Yorktown Heights, Nueva York, donde permaneció durante 30 años. En 2000 pasó a investigador emérito de IBM para ser contratado como profesor por la *State University* de Nueva York en Albany, donde se retiró en 2016.

Fue autor o coautor de más de 275 publicaciones de investigación, con más de 22000 citaciones y con un índice H de 72 según Google Académico. Obviamente figuraba en el ranking del ISI *Highly Cited Researchers*. Tenía contribuciones en muchos campos de la Teoría de Aproximación, como positividad total, splines multivariados, interpolación polinómica en varias variables, subdivisión, modelado geométrico, wavelets, funciones radiales,... Y también en los últimos años en redes neuronales y machine learning. Editor jefe y fundador de la revista *Advances in Computational Mathematics* durante bastantes años, fue editor de más de una decena de revistas de primera fila de Matemática Aplicada. Fue conferenciante plenario invitado en el *International Congress of Mathematicians* en Varsovia en 1983 pero participó también como conferenciante invitado y coorganizó en decenas y decenas de congresos internacionales especializados en todo el mundo. Pocos matemáticos habrán realizado estancias de investigación en más universidades y en más países distintos que el profesor Micchelli. A ello contribuyó la libertad de trabajo que disfrutó en IBM, ya que la importancia y volumen de su investigación hacían que fuera considerado como un embajador científico de la empresa. Suecia, Israel, Italia, India, Indonesia, Alemania, España, Gran Bretaña, Bélgica, Chile, Canadá, Australia, Singapur, China, entre otros muchos son una muestra de países en cuyas universidades investigó, además de lógicamente muchísimas de Estados Unidos.

Nos centraremos ahora en su íntima y fuerte conexión con la Universidad de Zaragoza. En 1982 yo conocía sus trabajos de investigación y me gustaban, cuando coincidimos en el *Mathematisches Forschunginstitute* de Oberwolfach en un meeting semanal titulado *Multivariate Approximation Theory*. Fue mi primera estancia en aquel Instituto y me impresionó. La experiencia de vivir una semana aislados en un paisaje idílico de la Selva Negra una treintena de matemáticos especialistas en el tema y seleccionados por invitación dando charlas en un ambiente distendido fue inolvidable. No existía entonces en el mundo nada comparable en Matemáticas. Una de las maravillas del sitio era su biblioteca, con todas

las revistas y novedades bibliográficas que uno podía soñar. Una noche tras la temprana cena fui a pasar un rato a la biblioteca y me encontré a Charles Micchelli (Charlie, como quería ser llamado) hojeando una revista. Me invitó a sentarme y charlar de Interpolación en varias variables y allí empezó una amistad que duraría más de 40 años.

Tres años más tarde supe que venía a un Congreso Internacional de Polinomios Ortogonales a Segovia como conferenciante invitado y le escribí para invitarle a venir después a Zaragoza para dar un seminario de una semana. Aceptó, y además durante esa semana se encontró tan a gusto en nuestra Universidad que planeamos que viniera un curso sabático, el curso 1988-89. Uno de los frutos de ese curso fue que solicitamos y obtuvimos de la OTAN la organización de un Instituto de Estudios Avanzados con el título de *Computation of Curves and Surfaces* que se celebró en Tenerife en junio de 1989, pasando a ser uno de los congresos que más positivamente se han recordado en la especialidad en los últimos 30 años.

Desde entonces Charlie Miccheli fue asiduo visitante a nuestro Departamento de Matemática Aplicada. Además, en 1994 coorganicé con él un nuevo congreso internacional, esta vez con el título *Total Positivity and its Applications*, en la Residencia de la Universidad de Zaragoza en Jaca. La positividad total de funciones reales de dos variables y en particular la de matrices tiene muchísimas aplicaciones en campos muy diversos, entre ellos splines y modelización geométrica, combinatoria, procesos de difusión estocásticos, matrices, estadística, ecuaciones integrales, etc. Por primera vez se seleccionó a especialistas de todos estos temas para elaborar un volumen como resultado del congreso que llamara la atención sobre esas aplicaciones. Con ello queríamos paliar el vacío que había en bibliografía desde el libro *Total Positivity*, volumen I, de S. Karlin en los años 70, anunciando un volumen II que nunca se escribió. El volumen *Total Positivity and its Applications* consecuencia del congreso tuvo gran éxito entre los especialistas.

Aún colaboró Charlie Micchelli con nosotros en la organización de otro congreso, uno de la serie trienal *Multivariate Approximation and Interpolation with Applications* celebrado en Almuñécar (Granada) en 2001. Siendo él editor jefe de la entonces nueva revista *Advances in Compùtational Mathematics* nos encargó la edición de varios números especiales.

Cuando pasó a excedencia especial en IBM para pasar a ser profesor de la SUNY de Albany siguió atendiendo las invitaciones que le cursamos desde nuestro Departamento para cortas estancias en Zaragoza, hasta su última visita en 2017, poco antes de que se

le diagnosticara la enfermedad que ha causado su fallecimiento. En vista de sus enormes méritos y su dedicación a nuestra Universidad, ésta lo nombró Doctor *Honoris Causa* en 1994, a cuya ceremonia corresponde la foto de arriba, y unos años más tarde la Real Academia de Ciencias de Zaragoza lo nombró Académico Correspondiente de su sección de Exactas.

Le sobreviven su esposa Patricia tras 60 años de matrimonio, los últimos de los cuales con absoluta dedicación a cuidarlo en su enfermedad y sus hijos Craig, nacido en 1970 y profesor de Biología en la *Washington University School of Medicine* en St. Louis y Lisa, nacida en 1972. Descanse en paz tan eminente matemático como buen amigo.

Zaragoza, mayo de 2025

# Actividades de la Real Academia de Ciencias Exactas, Físicas, Químicas y Naturales de Zaragoza durante el año 2025

## Sesiones y actividades corporativas

La Real Academia de Ciencias Exactas, Físicas, Químicas y Naturales de Zaragoza (en adelante Academia) ha celebrado durante el año 2025, nueve sesiones plenarias, cinco de ellas ordinarias y cuatro extraordinarias.

Las sesiones ordinarias tuvieron lugar los días que se indican a continuación, con una breve exposición de los puntos más relevantes tratados:

- 5 de febrero, en la que se dio recepción al discurso de ingreso de José Luis Peña Monné, designando al académico José Luis Simón Gómez para dar el discurso de contestación.
- 25 de abril, en la que se dio recepción al discurso de ingreso de Conrado Rillo Millán, designando al académico Juan Bartolomé Sanjoaquín para dar el discurso de contestación.
- 17 de septiembre, en la que se aprobó la propuesta de nuevo académico de honor a la Fundación Ibercaja.
- 12 de noviembre, en la que se dio recepción al discurso de ingreso de José Nicolau Ibarra, designando al académico Ignacio Pérez-Soba Diez del Corral para dar el discurso de contestación; así como los trabajos correspondientes a los Premios de Investigación 2025 relativos a la Seccion de Matemáticas (Carmen Rodrigo Cardiel) y la Sección de Físicas (Jesús Carrete Montaña).
- 10 de diciembre, en la que se aprobó la propuesta de la Sección de Químicas para el Premio de Investigación 2026: Alberto Concellón Allueva.

Las sesiones extraordinarias tuvieron lugar en las fechas siguientes:

- 26 de febrero, en la Sala de Grados de la Facultad de Ciencias: Ingreso del nuevo académico José Manuel Peña Monné.
- 25 de abril, en el Aula Magna de la Facultad de Ciencias: Ingreso del nuevo académico Conrado Rillo Millán.

- 11 de junio, en la Sala de Grados de la Facultad de Ciencias y organizada conjuntamente con el Colegio Oficial de Ingenieros de Montes de Aragón: Recepción del nuevo académico correspondiente Gregorio Montero González.
- 25 de noviembre, en la Sala Ebro de la sede del Grupo San Valero (plaza Santa Cruz): Entrega de los Premios de Investigación 2025 a los investigadores Carmen Rodrigo Cardiel (Sección de Exactas) y Jesús Carrete Montaña (Sección de Físicas).

Por otra parte, el 29 de octubre, en la Sala Paraninfo de la Universidad de Zaragoza, la Academia organizó el Acto de Apertura de Curso de las Academias de Aragón, en el que el académico José Luis Simón impartió la lección titulada *¿Para qué investigar? ¿Para qué transferir? ¿Para qué divulgar?*.
El 20 de mayo, por iniciativa del Instituto de Estudios Altoaragoneses, tuvo lugar en Huesca un acto en honor a Lucas Mallada, ingeniero de minas oscense, considerado "padre de la Paleontología española", recordando así el homenaje promovido hace 100 años por la Academia de Ciencias. Contó con palabras institucionales del Presidente de la Real Academia y la conferencia *La consideración que se le da a la obra de Lucas Mallada,* impartida por el académico Andrés Pocoví Mieras.

### Altas y bajas de académicos numerarios, de honor y correspondientes

*Bajas, por fallecimiento, de académicos de honor:*

Luis Joaquín Boya Balet, fallecido el 1 de octubre, quien fue académico numerario de la Sección de Físicas desde el 26 de noviembre de 1996 hasta el 16 de mayo de 2019, cuando pasó a ser académico de honor. Luis Boya fue presidente de la Academia desde 2008 hasta 2015.
Rafael Núñez-Lagos Roglá, fallecido el 18 de noviembre, quien fue académico numerario de la Sección de Físicas desde el 22 de enero de 1997 hasta el 9 de octubre de 2019, cuando pasó a ser académico de honor.

*Bajas, por fallecimiento, de académicos de correspondientes:*

Charles Anthony Micchelli, fallecido el 13 de marzo, quien fue académico correspondiente de la Sección de Exactas desde el 9 de mayo de 2002.
Francisco García Novo, fallecido el 15 de julio, quien fue académico correspondiente de la Sección de Naturales desde el 15 de octubre de 2015.
Así mismo, la Academia tuvo noticia del fallecimiento el 3 de abril de 2020, de Albert Figueras Dagá, quien fue académico correspondiente de la Sección de Físicas desde el 25 de septiembre de 2008.

*Ingreso de académicos numerarios:*

El 26 de febrero, el académico electo José Luis Peña Monne presentó su discurso de ingreso *Laderas, paleoambientes y geoarqueología del Holoceno en Aragón*, recibiendo la medalla número 36. Su discurso fue contestado por el académico José Luis Simón Gómez.
El 7 de mayo, el académico electo Conrado Rillo Millán presentó su discurso de ingreso *Un viaje apasionante por la innovación: helio líquido "hecho en Zaragoza"*, recibiendo la medalla número 23. Su discurso fue contestado por el académico Juan Bartolomé Sanjoaquín.

*Nombramiento de académicos de honor:*

En la sesión ordinaria del 17 de septiembre se aprobó la propuesta de nuevo académico de honor: la Fundación Ibercaja.

## Publicaciones de la Academia

Se ha publicado el volumen 79 de la Revista de la Academia de Ciencias de Zaragoza, correspondiente a 2024.
Así mismo, se han publicado los discursos de ingreso de los académicos José Luis Peña Monné y Conrado Rillo Millán, junto a los correspondientes discursos de contestación por los académicos José Luis Simón Gómez y Juan Bartolomé Sanjoaquín, respectivamente, y el discurso del académico José Luis Simón Gómez en el Acto de Apertura de Curso de las Academias de Aragón.
La Academia, como es costumbre, en la solemne apertura del curso 2025-2026 de las Academias de Aragón, celebrado el 29 de octubre, editó y distribuyó entre los asistentes una publicación con el discurso *¿Para qué investigar? ¿Para qué transferir? ¿Para qué divulgar?*, del académico José Luis Simón Gómez, la intervención del Presidente de nuestra Academia, Antonio Elipe Sánchez, y el elenco de los académicos de las cinco academias participantes.
Las publicaciones de la Academia se han beneficiado de una "ayuda para la edición de revistas científicas" del Vicerrectorado de Política Científica de la Universidad de Zaragoza.

## Organización de conferencias y eventos

La Academia durante 2025 ha organizado dos ciclos de divulgación científica de tres conferencias cada uno, que se desarrollaron en primavera y otoño, en las instalaciones de la Fundación Ibercaja en el Patio de la Infanta, c/ San Ignacio de Loyola 16, a las 19 horas y que contaron con una excelente acogida de público.

*Ciclo de conferencias: "Aragoneses en la Agencia Espacial Europea"*

Organizado por la Sección de Exactas, el ciclo de primavera se desarrolló con los títulos de conferencias y protagonistas, todos ellos de la Agencia Espacial Europea, siguientes:

**12 de marzo:** *LSTM: Cómo diseñar una misión espacial*, impartida por Itziar Barat Sanjuán.

**19 de marzo:** *La Innovación Digital en el Sector Espacio*, impartida por Vicente Navarro.

**26 de marzo:** *La Agencia Espacial Europea y su papel en el programa Copérnico*, impartida por Ana Bolea Alamañac.

*Ciclo de conferencias: "Química: una ciencia central"*

Organizado por la Sección de Químicas, el ciclo de otoño se desarrolló con los títulos de conferencias y protagonistas siguientes:

**4 de noviembre:** *Química y desarrollo sostenible*, impartida por el académico Luis A. Oro Giral.

**11 de noviembre:** *El poder de las enzimas en la transición hacia una química más sostenible*, impartida por Francisco J. Plou Gasca, profesor de investigación del Instituto de Catálisis y Petroleoquímica (CSIC).

**18 de noviembre:** *Biomateriales: hacia dónde vamos*, impartida por María Vallet Regí, académica de número de las reales academias nacionales de Farmacia y de Ingeniería.

**Otras actividades**

El 23 de enero tuvo lugar, en el Aula Magna de la Facultad de Ciencias, la conferencia *CERTEST-Biotec. Un caso de éxito. De las aulas a crear una empresa referencia mundial en Biotecnología*, impartida por Carlos Genzor, académico correspondiente por la Sección de Químicas. Al término de la misma, se le hizo entrega del diploma que lo acredita como académico correspondiente.

Con motivo del "Año Internacional de la Ciencia y la Tecnología Cuánticas", se han celebrado una serie de actividades, que comenzaron el 10 de septiembre con una charla del académico Luis Martín Moreno titulada *¿Por qué la naturaleza es tan rara?*, en el Centro

de Historias de Zaragoza. La Academia ha participado también, a través de los académicos Fernando Luis Vitalla y Luis Martín Moreno, con la organización de dos conferencias en el Aula Magna del Paraninfo el día 11 de noviembre, a cargo de José Manuel Sánchez Ron y Rosario González Pérez, además de con una exposición sobre Miguel Catalán en el Paraninfo desde el 6 de noviembre.

El 13 de noviembre Ernesto Estrada impartió una conferencia titulada *¿Qué dicen las matemáticas sobre la difusión de innovaciones?*, en el Salón de Actos del Edificio de Matemáticas de la Universidad de Zaragoza. Tras la conferencia, Ernesto Estrada recibió de manos del Presidente, Antonio Elipe, el diploma acreditativo de académico correspondiente.

### Premios de investigación de la Academia

Al igual que en los años previos, los premios de investigación de la Academia han contado con el apoyo económico de la Fundación San Valero, fruto del convenio existente entre ambas instituciones.

Cumplidos los trámites exigidos de entrega de un artículo de su ámbito y especialidad para su publicación en la Revista de la Academia, en la sesión extraordinaria de 25 de noviembre, celebrada en la Sala Ebro de la sede del Grupo San Valero (plaza Santa Cruz) se procedió a la exposición de los trabajos y a la entrega de los Premios de investigación de la Real Academia de 2025:

Por la Sección de Exactas: Carmen Rodrigo Cardiel, Profesora Titular del Departamento de Matemática Aplicada de la Universidad de Zaragoza, que presentó su trabajo *Efficient numerical solution of Biot's model.*

Por la Sección de Físicas: Jesús Carrete Montaña, Investigador Científico del Instituto de Nanociencia y Materiales de Aragón, CSIC–Universidad de Zaragoza., que presentó su trabajo *Ab-initio thermal transport calculation in single crystals and beyond: a review.*

### Honores, distinciones y nombramientos a académicos

La académica Blanca Bauluz fue elegida decana de la Facultad de Ciencias de la Universidad de Zaragoza el 8 de mayo.

El académico Manuel Doblaré ha sido nombrado miembro del Consejo Científico Técnico de la Agencia Estatal de Investigación por el Consejo Rector de la misma.

El académico Alberto Elduque fue nombrado en mayo miembro del Consejo Científico Asesor de la Fundación Gadea por la Ciencia.

El académico Fernando Luis ha renovado como miembro del comité C5 ("Low Temperature Physics") de la "International Union for Pure and Applied Physics (IUPAP)".

El académico Luis Oro recibió en mayo la "Medalla Echegaray", galardón científico más antiguo que existe en España, creado por Santiago Ramón y Cajal en 1905, por su eminente trayectoria científica.

El académico Ignacio Pérez-Soba Diez del Corral recibió su nombramiento definitivo como Director del Servicio Provincial de Medio Ambiente y Turismo de Zaragoza del Gobierno de Aragón por Decreto 88/2025, de 23 de julio (Boletín Oficial de Aragón nº 145, del 30), del Gobierno de Aragón. Desempeñaba ese puesto en comisión de servicio desde agosto de 2024. Fue también nombrado vocal titular de la Comisión Provincial del Patrimonio Cultural de Zaragoza, por Orden ECD/146/2025, de 21 de enero (Boletín Oficial de Aragón nº 30, de 13 de febrero), del Departamento de Educación, Cultura y Deporte del Gobierno de Aragón.

El académico Conrado Rillo recibió el

- Premio 'Aragón Investiga' en la categoría "Ramón y Cajal", el 19 de noviembre, a proyectos de investigación distinguidos en transferencia de conocimiento.
- Premio Nacional a la Transferencia de Conocimiento IPfest, en la categoría de patente con mayor repercusión, el 20 de noviembre.

La académica María Luisa Sarsa fue elegida como una de las 30 mujeres influyentes de Aragón en 2024 por El Periódico de Aragón.

El académico José Luis Simón recibió el "Premio Medioambiente Jaulín 2025", en Jaulín (Zaragoza), el 25 de enero.

### Participación en la organización de conferencias y congresos

El presidente, Antonio Elipe Sánchez ha sido "co-chair" del Comité Científico del "International Workshop on Celestial Mechanics", celebrado en Vilanova de Cerveira (Portugal), del 26 al 28 de junio.

El académico Alberto Elduque ha formado parte del comité organizador de la "Escuela sobre álgebras de Lie y de Jordan", celebrada en la Universidad de Córdoba,, del 27 al 30 de enero; y en el comité científico de las "VI Jornadas de Educación Matemática de Aragón", celebradas en la Universidad de Zaragoza el 28 de febrero y 1 de marzo.

El académico Fernando Luis ha sido

- Co-organizador (co-chair) de la "30 th International Conference of Low Temperature Physics (LT30)", celebrada en Bilbao del 7 al 13 de agosto.

– Organizador de la sesión divulgativa “Física cuántica, una revolución científica y tecnológica”, que incluyó conferencias impartidas por el académico de la RAE e historiador de la ciencia José Manuel Sánchez Ron y por la catedrática de la Universidad de Granada y presidenta del área de física de la Agencia Estatal de Investigación Rosario González Férez. Aula Magna del Edificio Paraninfo, Universidad de Zaragoza, 11 de noviembre.
– Miembro del “International Scientific Committee” de la “Quantum Matter International Conference & Expo”, Grenoble, 20-23 de mayo.
– Miembro del “International Scientific Advisory Board” de la “4th European Conference on Molecular Spintronics (ESMOLNA)”, Dublín, 2-4 de junio.
– Miembro del “International Advisory Board” de la “19th International Conference on Molecular Magnetism (ICMM)”, Burdeos, 27-31 de octubre.

El académico Luis Martín Moreno ha sido uno de los organizadores de los siguientes congresos:

– “Quantum Nanophotonics”, celebrado en Benasque, del 23 al 29 de marzo.
– “Nanophotonics of 2D Materials”, celebrado en Toruń (Polonia), del 6 al 9 de octubre.

El académico Ignacio Pérez-Soba Diez del Corral ha sido miembro del comité científico del IX Congreso Forestal Español, organizado por la Sociedad Española de Ciencias Forestales y realizado del 16 al 20 de junio en Gijón (Asturias). También ha sido miembro del comité organizador de las Jornadas “Prevención de inundaciones en cuencas mediterráneas: lecciones aprendidas de la DANA de Valencia”, organizadas por el Ayuntamiento de Daroca, la Comarca del Campo de Daroca, el Gobierno de Aragón y el Colegio Oficial de Ingenieros de Montes en Aragón, y celebradas en Daroca del 5 al 6 de junio.
Igualmente, fue coordinador y presentador de estas Jornadas:

– Jornada “Reforestación en la Comunidad Autónoma de Aragón”, organizada por el Departamento de Medio Ambiente y Turismo del Gobierno de Aragón, el Centro Público Integrado de Formación Profesional “San Blas” y el Colegio Oficial de Ingenieros de Montes en Aragón. Barrio de San Blas, Teruel, 23 de enero.
– “Jornada sobre planificación y ejecución de aprovechamientos de madera. Bases para una Gestión Forestal Activa y Sostenible”, organizada por el Ayuntamiento de Jaca, el Departamento de Medio Ambiente y Turismo del Gobierno de Aragón, PEFC-España y el Colegio Oficial de Ingenieros de Montes en Aragón, celebrada en Jaca (Huesca), el 1 de octubre.

Fue también organizador y guía de los siguientes viajes científicos:

– Viaje de campo del Curso de Geología por Navarra y por el Alto Aragón, organizado por la Sociedad internacional de geología y minería para el desarrollo y gestión del territorio (SIGMADOT). Canfranc-Estación (Huesca), mañana del 22 de septiem-

bre.

– Dos viajes de campo en la visita de estudio a España del Proyecto "TERRA-Turkiye ecosystem-based disaster risk reduction approach", desarrollado por la Autoridad de Gestión de Desastres y Emergencias de Turquía (AFAD), con financiación del Instrumento de Ayuda Preadhesión (IPA- II) de la UE. Canfranc-Estación (Huesca), tarde del 22 de septiembre, y Cetina (Zaragoza), el 23 de septiembre.

Además, ha sido (por cuarto año consecutivo) miembro del Jurado de los Premios del Concurso nacional "R7 por el planeta", concedidos por la Fundación Ibercaja para premiar iniciativas de centros educativos para el desarrollo sostenible de la sociedad y de su entorno, y para reconocer actitudes y valores en el ámbito de la protección del medio ambiente.

El académico Conrado Rillo ha sido miembro de los comités científicos de los siguientes congresos:

– "30th International conference on LOW TEMPERATURE PHYSICS -LT30-", celebrado en Bilbao, del 7 al 13 de agosto.
– "Advanced Materials in Spain -AMatS2025-", celebrado en Barcelona, del 24 al 26 de noviembre.

La académica María Luisa Sarsa ha sido:

– Miembro del comité organizador local de la reunión internacional "APPEC Town Meeting 2025", celebrada en Paraninfo de la Universidad de Zaragoza los días 23 y 24 de septiembre.
– Miembro del comité organizador de la reunión nacional "RENATA 2025", celebrada en la Facultad de Ciencias de la Universidad de Zaragoza el 22 de septiembre.

El académico José Luis Simón ha participado, como organizador y moderador, en la mesa redonda *De la DANA a la nada": ¿Tomaremos por fin medidas para prevenir las catástrofes en los ríos mediterráneos?*, organizada por el Geoforo por una Nueva Cultura de la Tierra y celebrada en la Biblioteca de Humanidades María Moliner, Universidad de Zaragoza, el 27 de febrero.

### Conferencias y cursos impartidos por nuestros académicos

El Presidente, Antonio Elipe Sánchez, ha impartido la conferencia invitada titulada *Wrong hypotheses in the Generalizad Restricted Three Body Problem*, en la reunión ADeLA 2025, celebrada en Caldera, región de Atacama (Chile), del 7 al 11 de abril.

El académico Enrique Artal ha impartido los siguientes cursos y conferencias:

- *Curso de orbifolds online organizado por la Red Española de Topología*, entre febrero y abril.
- *Complex Orbifolds. Quotient singularities and weighted projective spaces. Symmetric curves and line arrangements.* Curso impartido en el congreso "Algebraic Geometry, Topology, Combinatorics and Related Topics 2025", celebrado en marzo en Tokushima (Japón).
- *Travelling around singular conjectures with Alejandro*. Conferencia plenaria en la "Jornada Singular en homenaje a Alejandro Melle", celebrado mayo en Madrid.
- *Topology of line arrangements, braids and symmetries*. Conferencia en el congreso "Artin groups, braids and mapping class groups: Celebrating the work of Luis París", celebrado en junio en Cáceres.
- *A suspension formula for Denef-Loeser zeta functions*. Conferencia en el congreso "Moduli, Hilbert Schemes and Singularities", celebrado en septiembre en Cluj-Napoca (Rumanía).
- *Denef-Loeser zeta functions of Lê-Yomdin and suspension singularities II*. Conferencia en el congreso "Iberoamerican Congress on Singularities", celebrado en diciembre en Valparaíso (Chile).
- *Is it possible to use machine learning to simplify braids?*. Conferencia en el "Workshop on Groups and Plane Curves", celebrado en diciembre en Pau (Francia).

El académico Manuel Asorey ha impartido las siguientes conferencias:

- *Vacuum Boundary Effects in Gauge Theories*, en el "Workshop on Standard Model and Beyond", celebrado en Corfu (Grecia).
- *Vacuum Boundary Effects in Gauge Theories*, en el congreso "Cosmology and the Quantum Vacuum", celebrado en Benasque.
- *Vacuum Effects in Gauge Theories*, en el "X International Workshop on Information Geometry, Quantum Mechanics and Applications", celebrado en Policeta, San Rufo (Italia), del 30 de junio al 4 de julio.

El académico Juan Bartolomé ha impartido la conferencia (online) *X-ray Magnetic Circular Dichroism and some contributions to Magnetism*, en el "Kharkiv Quantum Seminar", el 25 de febrero.

La académica Blanca Bauluz ha impartido la conferencia invitada *Arcillas: desde la macro a la nanoescala*, en la Reunión de la Sociedad España de Mineralogía, en la Universidad de Salamanca. el 10 de noviembre.

El académico Manuel Doblaré ha impartido dos conferencias en la Universidad de Nanjing:

- *An overview on the application of some mathematical models in Biomedicine*, en el "1st Sino-Spanish Workshop on Biomaterials, Biomedicine and AI",

– *Some AI Applications in Health Problems at TME Lab group, University of Zaragoza (Spain)*, en el Jiangsu Province Hospital en Nanjing.

El académico Alberto Elduque ha impartido las siguientes conferencias:

– *Giros y cuaterniones*, en los "Miércoles Matemáticos" de la UNED de Calatayud, el 15 de enero.
– *From algebras to superalgebras via tensor categories*, en el "XVII Non-associative day in Madrid", en la Universidad Rey Juan Carlos, el 6 de junio; en el congreso "Hopf Algebras and Related Topics", celebrado del 11 al 15 de agosto en la "Bonne Bay Research Station" de la "Memorial University of Newfoundland", en Canadá, y en el el "mini-workshop Nonassociative algebras and hom-algebra structures", en la Mälardalen University de Suecia, el 23 de octubre.
– *From the Albert algebra to Kac's ten-dimensional Jordan superalgebra*, en el congreso "Algebras and Forms in Geometry and Beyond", celebrado del 11 al 12 de septiembre en la "Université de Haute Alsace", en Mulhouse, Francia.

El académico José Esteban Galé ha impartido la conferencia invitada *Logarithmic decay of means for Cesàro bounded operators*, en el "XVII Congress GAFEVOL, Evolution equations and Functional Analysis", celebrado en Zaragoza, del 10 al 14 de noviembre.

El académico Fernando Luis ha impartido las siguientes conferencias invitadas:

– *De la ciencia a las aplicaciones (y viceversa): un siglo de revoluciones cuánticas*, conferencia inaugural de la Semana de la Ciencia y la Tecnología en el CSIC en Aragón, Delegación del CSIC en Aragón, 4 de noviembre.
– *Wiring up molecular spins with superconducting quantum circuits*, "3rd International Conference on Emerging Quantum Technology" (ICEQT2025), Hefei (China), 17-22 de septiembre.
– *Circuit QED with molecular spin qudits*, "3rd International Workshop on Microwave Research and Applications", Coma–ruga (España), 3 de julio.
– *Circuit QED with molecular spin qudits*, "12th Rochester Conference on Coherence and Quantum Science" (CQS-12)', Rochester (USA), 23-27 de junio.
– *Wiring up molecular spins with superconducting circuits*, "International Conference on Molecular Spin Qubits (ICMSQ)", Sendai (Japón), 7-10 de junio.
– *Quantum circuits with molecular spins: opportunities and challenges*, conferencia tutorial en la "European Conference on Molecular Spintronics" (ECMolS), Dublín (Irlanda), 2-4 de junio.
– *Wiring up molecular spin qubits*, conferencia plenaria en la "European School on MOLecular Nanoscience" (ESMOLNA), Santa Pola (España), 18–23 de mayo.

El académico Luis Martín Moreno ha impartido las conferencias:

- *Overview of the use of AI for Material Science at INMA*, en el congreso "AI4AM Artificial Intelligence for Advanced Materials"en San Sebastián, 8–10 de abril.
- *Ultra-confined Light and Ultra-Strong Coupling Regime with phonon polaritons*, en el "European Optical Society Annual Meeting (EOSAM) 2025", en Delft, 24–28 de agosto.
- *Inteligencia Artificial:qué es y cómo funciona*, Seminario en el Club 33, Zaragoza, el 11 de noviembre.
- *La Física Cuántica: ¿por qué la naturaleza es tan rara?*, Seminario en Cantalojas (Guadalajara), el 20 de agosto, en el Centro de Historias, Zaragoza, el 10 de septiembre, en Huesca el 3 de octubre y en Teruel el 30 de octubre.
- *Inteligencia Artificial en el INMA*, Seminario en el Instituto de Nanociencia y Materiales de Aragón, el 17 de junio.

El académico Luis Oro ha impartido las conferencias:

- *Ciencia, tecnología y desglobalización*, en el ciclo "Los Martes del Paraninfo", el 18 de febrero en Zaragoza.
- *Química Medioambiente y Desarrollo Sostenible*, en el "XXXII Encuentro de la Asociación Alexander Von Humboldt de España", el 5 de septiembre en Castellón.
- *Química y Neutralidad Climática*, en la Universidad de la Experiencia, en Huesca, el 2 de octubre.
- *Química y Desarrollo Sostenible* en la Fundación Ibercaja, en Zaragoza, el 4 de noviembre.
- *El reto de la descarbonización*, en el ciclo "Los Martes del Paraninfo: Cita con los Profesores Eméritos", en Zaragoza, el 11 de noviembre.
- *Tiempos de Cambio: La Química Española a lo largo del Siglo XX*, en el Senatus Científico de Zaragoza, el 20 de noviembre.
- *La controvertida neutralidad climática*, en la Real Academia de Medicina de Zaragoza, el 11 de diciembre.

El académico José Luis Peña Monné ha impartido las siguientes conferencias:

- *Geología y evolución geomorfológica del tossal de Moradilla*, en las II Jornades Tecniques del Tossal de Moradilla, CECS Lleida, el 18 de enero.
- *La evolución de laderas durante el Holoceno superior desde una perspectiva geoarqueológica*, en el ciclo de Charlas Geoarqueológicas de la Sociedad Geológica de España, el 4 de abril.
- *Geología y evolución geomorfológica del tossal de Gardeny*, en la Jornada Tècnica de Gardeny. Gardeny, testimoni actiu de la historia de Lleida. Castell de Gardeny, el 30 de octubre.

– *Centro de interpretación multiespacial a cielo abierto: una alternativa para la gestión patrimonial en los Valles Calchaquíes* y *Espacios persistentes y morfogénesis acelerada en el NOA*, en las "II Jornadas de Arqueología del Noroeste Argentino", organizado por la Universidad Nacional de Tucumán, en octubre.
– *Cluster analysis using portable X ray fluorescence (pXRF) data: a fast and powerful method for regional correlation of ash fall deposits*, en el congreso "Understanding volcanoes and society: the key for risk mitigation", en Puerto Varas (Chile), en noviembre.

El académico Ignacio Pérez-Soba Diez del Corral ha impartido las siguientes conferencias y cursos:

– 8 horas de docencia en el XIX Diploma de Especialización en Derecho Local de Aragón, organizado por la Universidad de Zaragoza y el Departamento de Fomento, Vivienda, Logística y Cohesión Territorial del Gobierno de Aragón, y convocado por la Orden FOM/1233/2024, de 9 de octubre (BOA nº 203, del 17). Fueron dos sesiones de 4 horas cada una, una en Zaragoza (29 de octubre) y una en Huesca (15 de octubre), que se dedicaron a la protección legal de los montes municipales aragoneses, con especial referencia a los declarados de utilidad pública.
– Impartió las siguientes ponencias para la Red Estatal de Montes Públicos (REMP), coordinada por la Fundación Centro de Servicios y Promoción Forestal y de su Industria de Castilla y León (CESEFOR), ambas impartidas por videoconferencia: *Regulación del uso del suelo y de los fondos de mejora en los montes de utilidad pública* (15 de abril; 3 horas) e *Introducción jurídica a los montes públicos y su régimen de propiedad*, esta última en la Acción Formativa "Gestión integral de los montes públicos propiedad de Entidades Locales: aspectos técnicos, legales y económicos" (25 de noviembre; 2,5 horas).
– *Perspectiva histórica de la repoblación forestal en Aragón*, en la Jornada "Reforestación en la Comunidad Autónoma de Aragón", organizada por el Departamento de Medio Ambiente y Turismo del Gobierno de Aragón, el Centro Público Integrado de Formación Profesional "San Blas"; y el Colegio Oficial de Ingenieros de Montes en Aragón. Barrio de San Blas, Teruel, 23 de enero.
– *El agua no sale de los ríos: hagamos restauración hidrológico-forestal de cuencas*, en la Jornada Técnica "El papel de la gestión forestal en la regulación hidrológica de las cuencas", organizada por la Consejería de Medio Ambiente, Infraestructuras y Territorio de la Generalidad Valenciana. Valencia, 19 de febrero.
– *El agua no sale de los ríos: hagamos restauración hidrológico-forestal de cuencas*, que constituyó la Sesión Académica "Memorial José Ángel Carrera Morales 2025" de la Academia Malagueña de Ciencias. Málaga, 20 de febrero.

– *La historia de la Restauración Hidrológico-Forestal en Daroca y su comarca*, en la primera reunión del Grupo de Trabajo sobre el Plan Nacional de Actuaciones Prioritarias de Restauración Hidrológico-Forestal (PNAP), convocada por el Ministerio para la Transición Ecológica y el Reto Demográfico (MITECO). Daroca (Zaragoza), 8 de abril.
– *Obras de corrección torrencial y de restauración hidrológico-forestal para la prevención de inundaciones*, en la mesa redonda nº 2 ("Ingeniería y adaptación al riesgo de riadas e inundaciones"), de la Jornada "Ingeniería y prevención del riesgo de inundaciones y sus efectos", organizada por el Instituto de la Ingeniería de España. Madrid, 10 de abril.
– *Oportunidad, competencia y teleología del Reglamento Europeo de Deforestación*, en la Jornada "Análisis del Reglamento Europeo de Deforestación 1115/2023: problemas para su entrada en vigor", organizada por la Universidad de Valladolid y la Georg-August-Universität de Göttingen (Alemania). Impartida por videoconferencia el 12 de mayo.
– *Actuaciones forestales para la prevención de inundaciones: la restauración hidrológico–forestal*, en las Jornadas "Prevención de inundaciones en cuencas mediterráneas: lecciones aprendidas de la DANA de Valencia", organizadas por el Ayuntamiento de Daroca, la Comarca del Campo de Daroca, el Gobierno de Aragón y el Colegio Oficial de Ingenieros de Montes en Aragón. Daroca (Zaragoza), 5 de junio.
– *El pensamiento económico de G.K. Chesterton, y su actualidad en el medio rural español*, en la Jornada "Por un capitalismo con rostro humano en el medio rural español: el distributismo de G.K. Chesterton", organizada por la Fundación Cultural Ángel Herrera Oria. Universidad San Pablo-CEU (Madrid), 12 de junio.
– *La restauración hidrológico-forestal: cómo minimizar las inundaciones donde se generan*, en las Jornadas Participativas Paiporta 2025, "Disminución de riesgos de inundaciones con intervenciones naturales en el Barranco del Poyo", organizadas por el Ayuntamiento de Paiporta, el Colegio Oficial de Ingenieros de Montes y la Cranfield University, celebradas en Paiporta (Valencia), 19 de junio.
– *El agua no sale de los ríos: hagamos restauración hidrológico-forestal de cuencas*, en el VI Congreso Internacional de Geología y Minería Ambiental para el Desarrollo y el Ordenamiento Territorial, organizado por la Sociedad internacional de geología y minería para el desarrollo y gestión del territorio (SIGMADOT), la Sociedad Española para la Defensa del Patrimonio Geológico y Minero (SEDPGYM), Minería para el Desarrollo (MpD) y el Ayuntamiento de Suria. Suria (Barcelona), 21 de junio.
– *Necesidad, legalidad y eficacia del Reglamento EUDR*, en el "Congreso Internacional EUDR: un análisis para su aplicación práctica en las industrias de la madera", organizado por la Universidad de Valladolid, la Junta de Castilla y León y el Colegio

de Registradores de la Propiedad y Mercantiles de España. Valladolid, 27 de octubre.

- *Los incendios forestales en España: mitos y realidades*, en el X Simposium del Observatorio de Catástrofes de la Asociación Clúster Catástrofes. Instituto de la Ingeniería de España (Madrid), 26 de noviembre.
- *Los incendios forestales y los hongos*, conferencia de apertura de las XI Jornadas Micológicas de Monegros, organizadas por la Asociación Micológica de los Monegros. San Juan del Flumen (Huesca), 28 de noviembre.
- *Régimen jurídico de los aprovechamientos forestales en Montes de Utilidad Pública*, en la Jornada "Gestión municipal y aprovechamientos sostenibles en montes de utilidad pública", organizada por la Fundación ECODES y PEFC España, dentro del proyecto BioPirineo. Palacio de Congresos de Huesca, 4 de diciembre.
- *Aragón y la repoblación forestal: desde el siglo XIX hasta el Plan de Reforestación de Aragón (PREA) 2024-2027.* Ponencia impartida en cada una de las Jornadas de presentación del Plan de Reforestación de Aragón (PREA) organizadas por el Gobierno de Aragón en diciembre de 2025 y celebradas en Ateca (3 de diciembre), Ariza (11 de diciembre) y San Martín de la Virgen de Moncayo (17 de diciembre).

Igualmente, fue miembro de la mesa redonda *Salidas profesionales y oportunidades laborables en el sector primario*, en el VIII Monográfico "Lo que pasa en el campo", organizado por la Corporación Aragonesa de Radio y Televisión con el patrocinio de Ibercaja, en el Espacio Ibercaja Xplora, en Zaragoza, el 26 de junio; y fue el moderador de la mesa redonda *Realidades en España de una economía rural productiva y cercana al ser humano*, en la Jornada "Por un capitalismo con rostro humano en el medio rural español: el distributismo de G.K. Chesterton", organizada por la Fundación Cultural Ángel Herrera Oria en la Universidad San Pablo-CEU (Madrid) el 12 de junio.

El académico Miguel Pocoví Mieras ha impartido la conferencia *Avances en el diagnóstico de la hipercolesterolemia familiar*, en la sesión científica de la Real Academia de Medicina de Zaragoza de 6 de febrero.

El académico Conrado Rillo ha impartido la conferencia *Sustainable helium*, en la SNSSN (SustainableNano – Spanish Network on Safe and Sustainable Nanotechnologies), el 5 de febrero.

El académico Javier San Román ha impartido, con motivo del Año Internacional de los Glaciares, la conferencia titulada *Glaciares, memoria y presente. Un recorrido por los glaciares de los Pirineos*, en Huesca, el 21 de marzo, en Aínsa, el 30 de mayo, y en Jaca, el 14 de noviembre.

También ha impartido, el 9 de noviembre en Jasa, una charla sobre David Attenborough y su libro "Una vida en nuestro planeta", y el 12 de diciembre en Zaragoza una conferencia

sobre el río Huerva, dentro de un ciclo organizado por el Ayuntamiento de Zaragoza.

La académica María Luisa Sarsa ha impartido las siguientes conferencias invitadas:

- *Towards a robust model-independent test of DAMA/LIBRA: ANAIS-112 six-year exposure results and prospects*, impartida en el congreso internacional UCLA-DM2025, celebrado en UCLA Campus, Los Angeles, US entre el 24 y el 27.
- *ANAIS-112 Experiment: searching for the WIMP wind under the Pyrenees to solve the DAMA/LIBRA puzzle*, impartida en el congreso internacional "20th PATRAS Workshop on axions, WIMPS and WISPS", celebrado en La Laguna, Tenerife, entre el 22 y el 26 septiembre.
- *Dark Matter Experiment*, impartida en el "LII International Meeting on Fundamental Physics", celebrado en Santiago de Compostela entre el 7 y el 10 octubre.
- *El hombre y el genio: Einstein y su legado*, impartida el 8 de mayo en el Ámbito Cultural de El Corte Inglés de Zaragoza, dentro del ciclo "Encuentros con la Ciencia".

También ha actuado, como integrante del grupo RISArchers, con el monólogo *Los límites del genio*, el 9 de septiembre en el X Aniversario de Risarchers, en el Pub Rock & Blues de Zaragoza; y ha participado en el debate/coloquio organizado por el grupo STEAM_Unizar2050: "Mujeres creando Futuro: Arte, Ciencia y Rebeldía", celebrado el 10 de marzo en el Centro Joaquín Roncal de Zaragoza.

El académico José Luis Simón ha impartido la conferencia *Cómo nació el Geolodía*, junto al Dr. Luis Alcalá, organizada por la Sociedad Geológica de España, en Aliaga (Teruel), el 25 de abril.

También ha participado en las siguientes actividades de divulgación:

- Acto de celebración del 20 aniversario de Geolodía en Aliaga (Teruel), organizado por la Sociedad Geológica de España (25 abril). En dicho acto fue nombrado socio honorario de la SGE.
- "I Jornadas Geológicas Val d'Echo", organizadas por la Asociación Turística del Valle de Hecho y coordinadas por José Luis Simón, habiendo impartido en ellas la charla divulgativa sobre *Pensamiento mágico y pensamiento racional frente a las catástrofes naturales* y organizado dos salidas de campo. Las jornadas se celebraron en el Valle de Hecho (Huesca), el 31 de mayo y el 1 de junio
- "Jornada geológica en La Hoz de la Vieja", con una visita geológica guiada y una charla divulgativa sobre el proyecto geológico-artístico "Tierra. Poemas y Música de las Esferas". La jornada se celebró en La Hoz de la Vieja (Teruel), el 12 de julio.
- Coordinación de un dossier sobre "Espacios naturales protegidos de la provincia de Teruel", en la revista cultural Turolenses', del Instituto de Estudios Turolenses (nº 25, enero de 2025, pp. 29-43). En el mismo número aparece un artículo de José Luis Simón sobre "Espacios de interés geológico" (p. 40).

El académico José S. Urieta Navarro impartió el seminario *Escalado del proceso de electrosíntesis. Del laboratorio a la producción industrial*, los días 12, 13 y 17 de marzo, dentro de las actividades complementarias del Máster de Química Industrial de la Universidad de Zaragoza.

**Otras contribuciones relevantes de nuestros académicos**

El académico Alberto Elduque organiza la XXI temporada del *Taller de Talento Matemático*, actividad dirigida a estudiantes de secundaria, desde 3º de ESO hasta 2º de Bachillerato, así como la *Fase Aragonesa de la Olimpiada Matemática Española*.

El académico José Esteban Galé ha realizado una visita de investigación al "Institute of Mathematics Simion Stoilow", de la Academia Rumana, en Bucarest, trabajando con Dr. Daniel Beltita sobre "Operator algebras on reproducing kernel Hilbert spaces", del 18 al 25 de noviembre.

El académico Luis Martín Moreno ha realizado una estancia de investigación en el "Donostia International Physics Centre (DIPC)", de San Sebastian, durante el mes de julio, colaborando con el Profesor Javier Aizpurúa.

El académico Ignacio Pérez-Soba Diez del Corral ha sido Decano del Colegio Oficial de Ingenieros de Montes en Aragón, Presidente de la Comisión Deontológica Nacional del Colegio Oficial de Ingenieros de Montes, y Patrono de la Fundación "Capital Natural".

La académica María Luisa Sarsa ha realizado las siguientes contribuciones:

- Participación en la campaña gráfica del Ayuntamiento de Zaragoza: "¿Buscas referentes? Son tus vecinas". Segunda edición de la actividad, con motivo de la celebración del 8 de marzo.
- Miembro del XLZD Pre-Construction oversight committee, dependiente de UKRI - Science & Technology Facilities Council, UK, to provide independent scrutiny and advice on issues of cost, schedule and scope over the lifetime of the project. Starting in 2025.
- Editor invitado de la revista European Physical Journal Plus (EPJ+) para la edición de un volumen especial "Focus Point on Best doctoral theses from the Spanish Royal Physics Society (RSEF) in 2023-24".
- Miembro del comité editorial de la revista conCiencias.digital, revista de la Facultad de Ciencias de la Universidad de Zaragoza.
- Miembro del comité organizador de la XXXVI edición de la Olimpiada Aragonesa de Física, celebrada en la Facultad de Ciencias de la Universidad de Zaragoza el 12 de febrero.

– Miembro del comité organizador de las actividades divulgativas que el Instituto Universitario CAPA desarrolla en torno a la celebración del día internacional de la materia oscura, 31 de octubre.
– Miembro del jurado evaluador del Physicathon Universitario "Physics Around the Clock", 6ª edición, 15-16 febrero.
– Embajadora del Grupo Especializado de Mujeres en Física (GEMF) de la Real Sociedad Española de Física en la Universidad de Zaragoza desde 2023.

El académico José Luis Simón ha participado en las siguientes acciones de transferencia a las administraciones públicas:

– Grupo de trabajo para la elaboración del Plan Nacional de Vigilancia Sísmica, Vulcanológica y de otros Fenómenos Geofísicos, creado por el Ministerio de Transportes, Movilidad y Agenda Urbana.
– 'Workshop' del proyecto INNTEGRA-Innovación de las Políticas de Previsión del Peligro Sísmico en España mediante la Integración de Datos Geológicos Sistematizados. En dicho proyecto se están consensuando y armonizando los criterios para crear, desde la base de datos de fallas activas QAFI, un mapa oficial de fallas activas en España que sirva para la nueva Norma de Construcción Sismorresistente y para la adaptación del Eurocódigo 8 europeo.
– Ponencia *Interacción entre el riesgo de movimientos del terreno y las fallas activas en Aragón. Escenarios de riesgo múltiple combinado*, dentro del curso "Planificación de Protección Civil y gestión de la emergencia ante el riesgo de movimientos del terreno", organizado por la Dirección General de Protección Civil y Emergencias del Ministerio del Interior en la Subdelegación del Gobierno en Zaragoza el 7 de mayo.

# Composición de la Academia a 31 de diciembre de 2024

## Junta de Gobierno

| | |
|---|---|
| *Presidente*: | D. Antonio Elipe Sánchez |
| *Vicepresidente*: | D. Fernando José Lahoz Díaz |
| *Académico Editor*: | D. Enrique Artal Bartolo |
| *Académico Bibliotecario*: | D. Andrés Pocoví Juan |
| *Académico Web*: | D. Pablo Alonso Gascón |
| *Académico Tesorero*: | D. Miguel Ángel Rebolledo Sanz |
| *Académico Secretario*: | D. Alberto Elduque Palomo |

## Académicos Numerarios y de Honor

*A fecha 31 de diciembre de 2025 hay 37 académicos de número, 2 académicos de honor y dos académicos nombrados que no han leído todavía su discurso. Se listan a continuación, por secciones, citando número de medalla y fecha de ingreso o de nombramiento.*

### Sección de Exactas

| | | | |
|---|---|---|---|
| *Presidente*: | Dña. María Teresa Lozano Imízcoz | (medalla 22) | *22 enero 1998* |
| *Académicos*: | D. Mariano Gasca González | (medalla 1) | *1 diciembre 1988* |
| | D. Manuel Calvo Pinilla | (medalla 25) | *10 marzo 1998* |
| | D. Eladio Domínguez Murillo | (medalla 27) | *25 marzo 1999* |
| | D. Antonio Elipe Sánchez | (medalla 16) | *30 marzo 2000* |
| | D. Jesús Bastero Eleizalde | (medalla 17) | *9 noviembre 2000* |
| | D. Manuel Doblaré Castellano | (medalla 19) | *3 noviembre 2005* |
| | D. Alberto Elduque Palomo | (medalla 29) | *23 febrero 2006* |
| | D. Enrique Artal Bartolo | (medalla 4) | *24 noviembre 2009* |
| | D. José Esteban Galé Gimeno | (medalla 10) | *31 enero 2018* |

### Sección de Físicas

| | | | |
|---|---|---|---|
| *Presidente*: | D. Pablo Javier Alonso Gascón | (medalla 35) | *16 mayo 2002* |
| *Académicos*: | D. Miguel Ángel Rebolledo Sanz | (medalla 14) | *11 mayo 2000* |
| | D. José Fernando Cariñena Marzo | (medalla 33) | *6 noviembre 2001* |
| | D. Juan Bartolomé Sanjoaquín | (medalla 3) | *27 octubre 2016* |
| | D. Ricardo Ibarra García | (medalla 20) | *19 diciembre 2016* |
| | D. Manuel Asorey Carballeira | (medalla 18) | *27 mayo 2021* |
| | D. Luis Martín Moreno | (medalla 7) | *25 mayo 2022* |
| | D. Fernando María Luis Vitalla | (medalla 39) | *25 enero 2023* |
| | Dña. María Luisa Sarsa Sarsa | (medalla 40) | *18 septiembre 2024* |
| | D. Conrado Rillo Millán | (medalla 23) | *25 abril de 2025* |

### Sección de Químicas

| | | | |
|---|---|---|---|
| *Presidente*: | D. Luis Antonio Oro Giral | (medalla 11) | *4 junio 1981* |
| *Académicos*: | D. José Santiago Urieta Navarro | (medalla 5) | *2 diciembre 1997* |
| | D. Carlos Gómez-Moreno Calera | (medalla 6) | *21 octubre 1999* |
| | D. Juan Forniés Gracia | (medalla 24) | *26 junio 2000* |
| | D. Ángel García de Jalón Comet | (medalla 30) | *29 noviembre 2001* |
| | D. Juan Francisco Cacho Palomar | (medalla 13) | *2 diciembre 2003* |
| | D. Miguel Pocoví Mieras | (medalla 32) | *20 mayo 2004* |
| | D. José Luis Marqués Insa | (medalla 37) | *24 noviembre 2005* |
| | D. José Luis Serrano Ostáriz | (medalla 26) | *12 diciembre 2006* |
| | D. Fernando Lahoz Díaz | (medalla 2) | *3 mayo 2017* |

### Sección de Naturales*

| | | | |
|---|---|---|---|
| *Presidenta*: | Dña. María Caridad Sánchez Acedo | (medalla 9) | *12 diciembre 2000* |
| *Académicos*: | D. Andrés Pocoví Juan | (medalla 28) | *4 abril 2019* |
| | D. José Luis Simón Gómez | (medalla 12) | *13 julio 2020* |
| | D. Ignacio Pérez-Soba Diez del Corral | (medalla 31) | *28 marzo 2023* |
| | Dña. Blanca Bauluz Lázaro | (medalla 38) | *28 junio 2023* |
| | D. Javier San Román Saldaña | (medalla 8) | *20 septiembre 2023* |
| | D. José Luis Peña Monné | (medalla 36) | *26 febrero 2025* |
| | Dña. Berta Sáez Gutiérrez | *Electa el 17 de abril de 2024* | |
| | D. José Manuel Nicolau Ibarra | *Electo el 17 de abril de 2024* | |

*En esta sección hay una vacante.

## Académicos de Honor

| | |
|---|---|
| D. Juan Pablo Martínez Rica | *14 diciembre 2022* |
| Fundación Ibercaja | *17 septiembre 2025* |

# Académicos Correspondientes

*A fecha de 31 de diciembre hay 46 académicos correspondientes que se han distribuido por secciones y ordenados por fechas de nombramiento.*

**Sección de Exactas**

| | |
|---|---|
| D. José M. Montesinos Amilibia | (7 abril 1992) |
| D. Claude Brezinski | (9 mayo 2002) |
| D. José Luis Fernández Pérez | (24 septiembre 2002) |
| D. Gilles Pisier | (24 septiembre 2002) |
| D. José Ángel Docobo Durántez | (21 abril 2005) |
| D. Sylvio Ferraz Mello | (21 abril 2005) |
| D. Francisco Marcellán Español | (4 noviembre 2004) |
| D. Santos González Jiménez | (27 abril 2006) |
| D. Efim Zelmanov | (5 octubre 2011) |
| D. Jesús Carlos Fernández Asensio | (7 junio 2013) |
| D. José Garay Pablo | (3 junio 2015) |
| D. Juan Luis Vázquez Suárez | (3 junio 2015) |
| D. Jesús Sanz Serna | (24 octubre 2018) |
| D. Ernesto Estrada | (17 diciembre 2024) |

**Sección de Físicas**

| | |
|---|---|
| D. Alberto Galindo Tisaire | (1 octubre 1967) |
| D. Eusebio Bernabeu Martínez | (1982) |
| D. Giuseppe Marmo | (9 mayo 2002) |
| Dña. María Josefa Yzuel Giménez | (9 mayo 2002) |
| D. José Adolfo de Azcárraga | (25 septiembre 2008) |
| D. Fernando María Legarda Ibáñez | (25 septiembre 2008) |
| D. Javier Llorca Martínez | (25 septiembre 2008) |
| D. Miguel V. Andrés Bou | (23 marzo 2009) |
| D. Javier Sesma Bienzobas | (7 mayo 2014) |
| D. Juan Ignacio Cirac Sasturaín | (3 junio 2015)) |
| D. Antonio Hernando Grandes | (16 Febrero 2017)) |
| D. Francisco Javier Solís Céspedes | (4 Octubre 2017) |

**Sección de Químicas**

| | |
|---|---|
| D. Ekkehardt Hahn | (13 junio 2002) |
| D. Pierre Braunstein | (13 junio 2002) |
| D. José María Ordovás Muñoz | (13 febrero 2008) |
| Dña. Mª Carmen Orosia Claver Cabrero | (13 febrero 2008) |
| D. Avelino Corma Canós | (15 octubre 2015) |
| D. Fernando Cossío Mora | (15 octubre 2015) |
| D. Carlos Genzor | (17 de abril de 2024) |

**Sección de Naturales**

| | |
|---|---|
| D. Leandro Sequeiros Sanromán | (9 mayo 2002) |
| D. Luis Villar Pérez | (9 mayo 2002) |
| D. Adrian Michael Harvey | (13 junio 2002) |
| D. Mario Panizza | (13 junio 2002) |
| D. Carlos López Otín | (19 diciembre 2006) |
| D. Miguel Delibes de Castro | (23 febrero 2011) |
| D. Eladio Liñán Guijarro | (3 junio 2015) |
| Dña. Gloria Cuenca Bescós | (4 julio 2022) |
| D. Juan Marín Velázquez | (24 noviembre 2022) |
| Dña. María Luisa Peleato Sánchez | (13 diciembre 2022) |
| D. Eduardo Martínez de Pisón Stampa | (3 julio 2024) |
| D. Gregorio Montero González | (3 julio 2024) |
| Dña. María Patrocinio Morrondo Pelayo | (3 julio 2024) |

Zaragoza, diciembre de 2025

../

# INSTRUCCIONES PARA LOS AUTORES

**Abstract**

The *Revista de la Real Academia de Ciencias* publishes original research contributions in the fields of Mathematics, Physics, Chemistry and Natural Sciences. All the manuscripts are peer reviewed in order to assess the quality of the work. On the basis of the referee's report, the Editors will take the decision either to publish the work (directly or with modifications), or to reject the manuscript.

## 1 Normas generales de publicación

### *1.1 Envío de los manuscritos.*

Para su publicación en esta Revista, los trabajos deberán remitirse a

Académico Editor
Revista de la Academia de Ciencias
Universidad de Zaragoza
50009 Zaragoza

o bien electrónicamente a la cuenta `artal@unizar.es`.

La Revista utiliza el sistema de *offset* de edición, empleando el texto electrónico facilitado por los autores, que deberán cuidar al máximo su confección, siguiendo las normas que aquí aparecen.

Los autores emplearán un procesador de texto. Se recomienda el uso de LaTeX, para el que se han diseñado los estilos `academia.sty` y `academia.cls` que pueden obtenerse directamente por internet en `http://www.raczar.es` o por petición a la cuenta de correo electrónico: `artal@unizar.es`.

### *1.2 Dimensiones*

Se recomienda que el texto de los trabajos, redactados en español, inglés o francés, no exceda de 25 páginas, siendo preferible una extensión de 6 a 20 páginas como promedio. El texto de cada página ocupará una caja de $16 \times 25$ cm, con espacio y medio entre líneas.

## 2 Presentación del trabajo.

Los trabajos se presentarán con arreglo al siguiente orden: En la primera página se incluirán los siguientes datos:

a) *Título del trabajo:* Conciso, pero ilustrativo, con mayúsculas.
b) *Autor:* Nombre y apellidos del autor o autores, con minúscula.
c) *Centro:* Centro donde se ha realizado, con su dirección postal.
d) *Abstract:* En inglés y con una extensión máxima de 200 palabras.
e) *Texto*

A) Los encabezamientos de cada sección, numerados correlativamente, serán escritos con letras **minúsculas** en negrita. Los encabezamientos de subsecciones, numerados en la forma 1.1, 1.2, ..., 2.1, 2.2, ..., se escribirán en *cursiva*.

B) Las fórmulas estarán centradas y numeradas correlativamente.

C) Las referencias bibliogáficas intercaladas en el texto, deben ser fácilmente identificables en la lista de referencias que aparecerá al final del artículo, bien mediante un número, bien mediante el nombre del autor y año de publicación.

D) Las figuras y tablas, numeradas correlativamente, se intercalarán en el texto. Las figuras se enviarán en formatos `EPS, PDF, PNG, JPG`. Los apéndices, si los hay, se incluirán al final del texto, después de la bibliografía.

E) Para las referencias bibliográficas se recomienda el uso de BibTeXcon los estilos `amsplain` o `amsalpha`.

## 3 Notas finales

La Revista permite la inclusión de fotografías o figuras en color, con un coste adicional que correrá a cargo de los autores.

**Enrique Artal**
Académico Editor

## Intercambio de Publicaciones

### Relación de revistas nacionales que recibe en intercambio la Biblioteca de la Academia de Ciencias

1. *A Ciencia Cierta* – Academia Malagueña de Ciencias.
2. *Acta Botanica Barcinonensia* – Dep Biología Vegetal. Univ. Barcelona.
3. *Anales del Jardín Botánico de Madrid*
4. *Anales UNED Calatayud*
5. *Animal Biodiversity and Conservation* – Museu de Zoologia
6. *Anuari de la Reial Acadèmia de Ciencies i Arts de Barcelona*
7. *Boletín de la Academia Malagueña de Ciencias*
8. *Boletín Geológico y Minero* – Instituto Geológico y Minero de España
9. *Collectanea Botanica* – Institut Botànic (Barcelona)
10. *Collectanea Mathematica* – Universitat de Barcelona
11. *Extracta Mathematicæ* - Universidad de Extremadura
12. *Gaceta de la Real Sociedad Matemática Española*
13. *Lucas Mallada: Revista de Ciencias* – Inst. Est. Altoaragoneses.
14. *Manuals del Museu* – Museu de Ciències Naturals de Barcelona
15. *Memòries de la Reial Acadèmia de Ciencies i Arts De Barcelona*
16. *Naturaleza Aragonesa* – Sociedad de Amigos del Museo Paleontológico de la Universidad de Zaragoza.
17. *Trabajos de Geología* – Universidad de Oviedo
18. *Zoologia Bætica*. UNIVERSIDAD DE GRANADA.

**Relación de revistas internacionales que recibe en intercambio la Biblioteca de la Academia de Ciencias**

1. *Abhandlungen der Senckenberg für Naturforschung* – Senckenberg Research Institute
2. *Acta Entomologica Musei Nationalis Pragœ*
3. *Acta Geologica Polonica* - Warszawa
4. *Acta Mathematica Hungarica*
5. *Acta Matematica Sinica* - New Series China
6. *Anales de la Academia Nacional de Ciencias Exactas, Físicas y Naturales de Buenos Aires*
7. *Annalen des Naturhistorischen Museums in Wien. Serie A*
8. *Annalen des Naturhistorischen Museums in Wien. Serie B*
9. *Annales Fennici Mathematici*
10. *Annales Academiæ Scientiarum Fennicæ. Mathematica Dissertationes* – Helsinki, Suomalainen Tiedeakatemia
11. *Annali del Museo Civico di Storia Naturale "Giacomo Doria"*
12. *Arkiv För Matematik*
13. *Atti della Accademia Ligure di Scienze e Lettere. Serie VII*
14. *Boletín de la Sociedad Matemática Mexicana. Tercera Serie.*
15. *Brenesia: Revista de Biodiversidad y Conservación* – Museo Nacional de Costa Rica
16. *Bulletin de la Classe de Sciences* – Academie Royale de Belgique – Bruxelles
17. *Bulletin of the American Mathematical Society. New Series*
18. *Bulletin of the London Mathematical Society*
19. *Bulletin of the Polish Academy of Sciences*
20. *California Agriculture* – University of California
21. *Commentationes Mathematicæ : Annals of the Polish Mathematical Society, Series I*
22. *Dædalus - Journal of the American Academy of Arts and Sciences*
23. *Doriana - Supplementa agli Annali del Museo Civico di Storia Naturale "G. Doria"*
24. *Facta Universitatis - Series: Mathematics And Informatic* – University of Nis, Serbia
25. *Filomat* – University of Nis, Serbia
26. *Folia Zoologica* – Czechoslovak Academy of Sciences
27. *Functiones et Approximatio Commentarii Mathematici* - Poznań
28. *Glasnik Matematički Serija III* - Zagreb

29. *Hiroshima Mathematical Journal*
30. *Hokkaido Mathematical Journal*
31. *Jahrbuch Bayerische* – Akademie der Wissenschaften
32. *Jahrbuch der Akademie der Wissenschaften in Göttingen*
33. *Journal of the London Mathematical Society*
34. *Klapalekiana* – Czech Entomological Society
35. *Lecturas Matemáticas* - Colombia
36. *Mathematical Reports* – Romanian Academy
37. *Palæobiodiversity and Palæoenvironments* – Senckenberg Research Institute
38. *Proceedings of the London Mathematical Society*
39. *São Paulo Journal of Mathematical Sciences*
40. *SUT Journal of Mathematics* - Science University of Tokio

Colabora: